AUTOPHAGY ENHANCED BY RASSF1A SUPPRESSES DIETHYLNITROSAMINE (DEN)-INDUCED HEPATOCARCINOGENESIS

A Dissertation

by

WENJIAO LI

Submitted to the Office of Graduate and Professional Studies of
Texas A&M University
in partial fulfillment of the requirements for the degree of

DOCTOR OF PHILOSOPHY

Chair of Committee,	Leyuan Liu
Committee Members,	Fen Wang
	Roderick H. Dashwood
	Dekai Zhang
	Jason T Kimata
Head of Department,	Warren Zimmer

December 2017

Major Subject: Medical Sciences

ABSTRACT

Hepatocellular carcinoma (HCC) is the most common type of human liver cancer and it is now the second leading cause of cancer death worldwide. In the United States, its incidence has tripled since 1980 and the death rates are increasing. RASSF1A (Ras association domain family 1 isoform A) is a tumor suppressor and frequently inactivated in HCC by promoter hypermethylation. However, the exact role and detailed mechanism of RASSF1A in the development of HCC has not been investigated.

Autophagy is a catabolic pathway to degrade dysfunctional organelles and misfolded or aggregated proteins. Autophagy defects enhance oxidative stresses which trigger DNA damage and genome instability to promote tumorigenesis. The interaction of RASSF1A with microtubule-associated autophagy activator MAP1S triggered us to examine whether RASSF1A itself activates autophagy to suppress HCC through MAP1S. We show here first time that RASSF1A is essential to maintain autophagy activity and RASSF1A depletion causes decreased autophagy flux both in vitro and in vivo. RASSF1A-deletion-caused autophagy defects lead to an acceleration of diethylnitrosamine (DEN)-induced HCC and a 31% reduction in mouse survivals.

RASSF1A activates autophagy by enhancing both autophagy initiation and maturation. RASSF1A does not impact MAP1S-Bcl-2-p27 non-canonical autophagy initiation pathway but acts through the Hippo pathway-regulatory

protein Mst1 to promote autophagy initiation through PI3K-Akt-mTOR pathway, a major pathway suppressing autophagy initiation. Acetylated microtubules are required for the trafficking of autophagosomes to fuse with lysosomes. RASSF1A enhances microtubular acetylation and recruits LC3-II-associated autophagosomes onto RASSF1A-stabilized acetylated microtubules through MAP1S to promote autophagy maturation.

In sum, in addition to identify RASSF1A as a novel regulator of autophagy, we show here first time that the epigenetic inactivation of RASSF1A actually promotes HCC and shortens survivals by suppressing autophagy initiation and maturation, which may provide a novel paradigm of the prevention and therapy of HCC.

DEDICATION

I would like to dedicate this dissertation to my parents for their unconditional love, encouragement and support.

ACKNOWLEDGEMENTS

First of all, I would like to thank my mentor, Dr. Leyuan Liu, and my committee members, Dr. Fen Wang, Dr. Roderick H. Dashwood, Dr. Dekai Zhang, and Dr. Jason T Kimata, for their guidance and support throughout the course of this research. Dr. Liu offered me the precious opportunity to join his lab, and gave me the valuable guidance for my thesis study. More importantly, he always trained me think and work independently, which is essential for my future academic pursuit. Dr. Wang always gave me incisive questions to make me think deeper about my research. Dr. Dashwood always encouraged me to participate in public presentations to improve communication skills, and his questions broadened my perspective in cancer research area. Dr. Zhang always offered me precious suggestions to my presentation and research. Dr. Kimata always gave me insightful suggestions for my project and helped me improve my writing skills.

I would also like to thank all the faculties and staffs at Texas A&M University Institute of Bioscience and Technology. They create a relaxed and friendly atmosphere which makes my time here a great experience. Special gratitude goes to graduate student program for their support. Thanks to student program coordinator Ms. Cynthia Lewis, who is always patient to answer all of my questions and warmly help me solve all the administrative issues. My gratitude also goes to all the members in Dr. Liu's lab for their kindness. I am very thankful to Dr. Fei Yue in the lab, who always share experimental materials, good idea and new

techniques with me. Thanks to Dr. Stefan Siwko for his precious advice for my study and life. I am also grateful for my friends in IBT, Yanqing Huang, Yixiang Xu, Junchen Liu, Lei An, Lian He, Ji Jing, Li Zeng, Yifan Zhang, Yi Liang et al. Their company, friendship and kindness make my life in Houston full of fun and happiness.

Last but not least, thanks to my boyfriend Yuan Dai and my family for their love, encouragement and support.

CONTRIBUTORS AND FUNDING SOURCES

Contributors

This work was supervised by a dissertation committee consisting of Professors Leyuan Liu (advisor) and Fen Wang of the Center for Translational Cancer Research in Texas A&M Health Science Center IBT and Professor Roderick H. Dashwood of the Center for Epigenetics & Disease Prevention in Texas A&M Health Science Center IBT and Professor Dekai Zhang of the Center for Infectious and Inflammatory Diseases in Texas A&M Health Science Center IBT and Professor Jason T Kimata of the Department of Molecular Virology and Microbiology in Baylor College of Medicine.

All work conducted for the dissertation was completed by the student, under the advisement of Dr. Leyuan Liu.

Funding Sources

This work was funded by National Institutes of Health under Grant Number R01CA142862 to Leyuan Liu.

NOMENCLATURE

AMPK	AMP-activated protein kinase
ATGs	Autophagy-related genes
ATM	Ataxia telangiectasia mutated
BAF	Bafilomycin A1
Bax	Bcl-2-associated X protein
Bcl-xL	B-cell lymphoma-extra large
Bcl-2	B-cell lymphoma 2
BNIP3L/NIX	Bcl-2 interacting protein 3 like
BSA	Bovine Serum Albumin
C19ORF5	Chromosome 19 open reading frame 5
CQ	Chloroquine
DAB	3, 3'-Diaminobenzidine
DEN	Diethylnitrosamine
DHE	Dihydroethidium hydrochloride
DMEM	Dulbecco's Modified Eagle Medium
DSB	DNA double-strand breaks
EBSS	Earle's Balanced Salt Solution
ER	Endoplasmic reticulum
FBS	Fetal Bovine Serum
FL	Full length

GAP	GTPase-activating protein
HBD	HDAC4-binding domain
HBV	Hepatitis B
HBSS	Hanks' Balanced Salt Solution
HC	Heavy chain
HCC	Hepatocellular carcinoma
HCV	Hepatitis C
HDAC4	Histone deacetylase 4
HDAC6	Histone deacetylase 6
HEK	Human embryonic kidney
HRP	Horseradish peroxidase
HSC	Hepatic stellate cells
H&E	Hematoxylin and Eosin
ITS-G	Insulin-Transferrin-Selenium
LC	Light chain
LC3	Microtubule-associated protein 1 light chain 3
LKB1	Liver kinase B1
LRPPRC	Leucine-rich PPR motif-containing protein
MAP1S	Microtubule-Associated Protein 1 Small form
MDM2	Mouse double minute 2
MEF	Mouse embryonic fibroblast
MOAP-1	Modulator of apoptosis 1

Mst	Mammalian sterile 20-like kinase
mTOR	Mammalian target of rapamycin
PBS	Phosphate-buffered saline
PE	Phosphatidylethanolamine
PI3K	Phosphatidylinositol 3-phosphate kinase
PI3P	Phosphatidylinositol-3-P
PMSF	Phenylmethanesulfonyl fluoride
PVDF	Polyvinylidene difluoride
p27	Cyclin-dependent kinase inhibitor 1B
RASSF1A	Ras association domain family 1 isoform A
Rheb	Ras homolog enriched in brain
ROS	Reactive oxygen species
Sav1	Salvador homolog 1
SC	Short chain
SDS-PAGE	SDS-polyacrylamide gels
SQSTM1	Sequestosome 1
TBST	Tris-buffered Saline with Tween-20B/CS

TABLE OF CONTENTS

Page

ABSTRACT ii

DEDICATION iv

ACKNOWLEDGEMENTS v

CONTRIBUTORS AND FUNDING SOURCES vii

NOMENCLATURE viii

TABLE OF CONTENTS xi

LIST OF FIGURES xiii

LIST OF TABLES xv

CHAPTER I INTRODUCTION 1

CHAPTER II DEPLETION OF RASSF1A RESULTS IN DECREASED AUTOPHAGY FLUX 13

- Introduction 13
- Materials and Methods 15
- Results 22
- Discussion 27

CHAPTER III DELETION OF RASSF1A GENE IN MICE ACCELERATES DEN-INDUCED HEPATOCARCINOGENESIS 30

- Introduction 30
- Materials and Methods 36
- Results 40
- Discussion 48

CHAPTER IV RASSF1A PROMOTES AUTOPHAGY MATURATION BY RECRUITING AUTOPHAGOSOMES ONTO RASSF1A-STABILIZED ACETYLATED MICROTUBULES THROUGH MAP1S 50

Introduction 50
Materials and Methods 52
Results 59
Discussion 72

CHAPTER V RASSF1A PROMOTES AUTOPHAGY INITIATION BY SUPPRESSING PI3K-AKT-MTOR PATHWAY THROUGH HIPPO PATHWAY REGULATORY PROTEIN MST1 75

Introduction 75
Materials and Methods 78
Results 82
Discussion 92

CHAPTER VI CONCLUSIONS 97

REFERENCES 102

LIST OF FIGURES

Page

Figure 1 Overview of the dynamic process of autophagy 2

Figure 2 Map of RASSF1 gene and structure of RASSF1A protein 8

Figure 3 Knockdown of RASSF1A in HeLa cells causes reduced autophagy 23

Figure 4 Deletion of RASSF1A gene in mice causes reduced autophagy flux in MEFs 24

Figure 5 Deletion of RASSF1A gene causes reduced autophagy flux in mouse livers 26

Figure 6 Deletion of RASSF1A causes no abnormality in mouse livers under normal conditions 40

Figure 7 Deletion of RASSF1A gene in mice accelerates DEN-induced hepatocarcinogenesis 42

Figure 8 RASSF1A knockout mice have a shorter lifespan than wild-type mice with DEN treatment 43

Figure 9 Deletion of RASSF1A enhances oxidative stresses in mouse livers 45

Figure 10 Deletion of RASSF1A promotes DNA damage in mouse livers 47

Figure 11 RASSF1A deletion causes reduced levels of acetylated α-tubulin in mouse livers 60

Figure 12 RASSF1A enhances the acetylation of α-tubulin and associates with acetylated α-tubulin 61

Figure 13 RASSF1A interacts with HDAC6 62

Figure 14 RASSF1A interacts with LC3-II 64

Figure 15 RASSF1A interacts with MAP1S via the overlapping domain between heavy chain (HC) and short chain (SC) of MAP1S 66

Figure 16 RASSF1A interacts with MAP1S via the RA domain 67

Figure 17 The interaction of RASSF1A with LC3-II requires MAP1S 69

Figure 18 RASSF1A recruits autophagosomes onto RASSF1A-stabilized acetylated microtubules through MAP1S 71

Figure 19 RASSF1A has no impact on MAP1S-mediated autophagy initiation pathway in HeLa cells 83

Figure 20 RASSF1A has no impact on MAP1S-mediated autophagy initiation pathway in mouse livers 84

Figure 21 RASSF1A suppression causes the activation of PI3K-Akt-mTOR pathway in HeLa cells 86

Figure 22 RASSF1A deletion causes the activation of PI3K-Akt-mTOR pathway in mice 87

Figure 23 RASSF1A suppresses PI3K-Akt-mTOR pathway to promote autophagy initiation through Hippo pathway regulatory protein Mst1 89

Figure 24 RASSF1A deletion has no impact on the downstream effectors of Hippo pathway 91

Figure 25 A diagram showing the potential mechanism by which RASSF1A regulates autophagy and suppresses hepatocarcinogenesis 99

LIST OF TABLES

Page

Table 1 Primers used for mouse genotyping PCR 16

Table 2 Primers used for real-time PCR analyses of mouse RASSF1A mRNA levels 20

Table 3 Primers used for plasmid construction 54

CHAPTER I

INTRODUCTION

Cancer, the second leading cause of death worldwide, causes over 8 million deaths worldwide in every recent year (1). Hepatocellular carcinoma (HCC), a primary malignancy of the liver, is the second most common lethal cancer worldwide and its incidence has tripled in recent decades in the United States (2,3). There are many risk factors for liver cancer, mainly including chronic Hepatitis B (HBV) or Hepatitis C (HCV) infection, alcoholic liver disease and non-alcoholic fatty liver disease. Other risk factors, such as hereditary hemochromatosis, alpha-antitrypsin deficiency, autoimmune hepatitis, some porphyrias, and Wilson's disease, also contribute to the formation and progression of liver cancer. Most of these risk factors cause liver cirrhosis, and the long-term chronic injuries in liver finally promote the formation of HCC. Clinical statistic data showed that 80-90% patients with HCC also develop liver cirrhosis. Currently, it is very difficult to diagnose HCC at very early stage. Therefore, only a small portion of patients with early-stage HCC receive curative treatments including surgical resection or liver transplantation. Currently, there are no very effective treatments for most patients with late-stage HCC and the 5-year survival rate has remained below 12%. Considering the poor prognosis and high mortality, it is urgent to understand the exact molecular mechanisms underlying HCC development for developing novel therapeutic strategies.

Autophagy was first observed in the 1960s and it is a major catabolic pathway to degrade misfolded or aggregated proteins, dysfunctional organelles and other macromolecules (4,5). Autophagy is a dynamic process that begins with the formation of isolation membranes. The membranes then engulf substrates to form the compartment known as autophagosomes. Autophagosomes migrate along acetylated microtubules to finally fuse with lysosomes to generate autolysosomes in which substrates are degraded by lysosomal enzymes (Figure 1). Therefore, the autophagic process can be generally divided into two main steps: autophagy initiation and autophagy maturation.

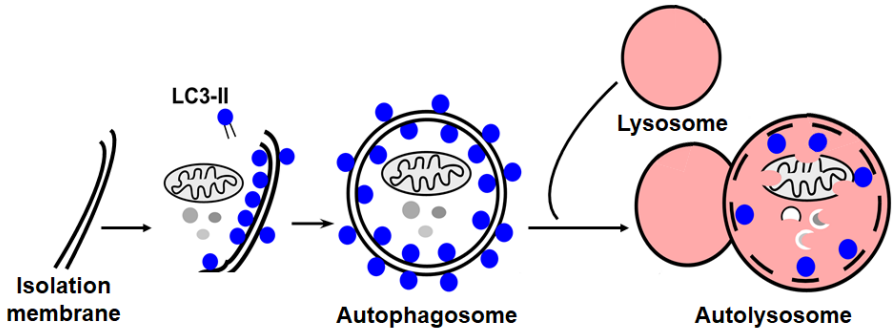

Figure 1. Overview of the dynamic process of autophagy (6)**.** Modified from Hansen TE, Johansen T: Following autophagy step by step. BMC Biology 2011, 9:39.

Although autophagy has been studied mainly in mammalian cells after being first reported in 1957 in mammalian cells (7), the groundbreaking experiments in the identification of its molecular regulators were conducted in yeast in the 1990s (8). One of the key regulators of autophagy is the mammalian target of rapamycin (mTOR) which negatively regulates autophagy initiation (9). In the presence of insulin and growth factors, the well-characterized class I phosphatidylinositol 3-phosphate kinase (PI3K)-protein kinase B (Akt)-mTOR signaling pathway is activated to inhibit autophagy induction. mTOR can also inhibit autophagy induction through the liver kinase B1 (LKB1)-AMP-activated protein kinase (AMPK)-mTOR pathway in response to nutrients and metabolites. Downstream of the mTOR, a number of autophagy-related genes (ATGs) encoding proteins that are essential for the execution of autophagy have been identified so far. According to the functions in distinct stages of autophagy process, ATG proteins can be classified into three main groups. The first one is the ATG1 complex (ATG1, ATG13, ATG17) that is commonly considered as the initiator of the autophagic cascade (8,10). Under nutrient-rich conditions, mTOR is activated and then directly phosphorylates and inactivates ATG13 to prevent the formation of ATG1 initiator complex. Meanwhile, ATG1 is also hyperphosphorylated by activated mTOR, resulting in a reduction in ATG1 kinase activity and the subsequent inhibition of autophagy initiation. Upon starvation, ATG1 and ATG13 are rapidly dephosphorylated and form a complex, which leads to the recruitment of other ATG proteins to promote autophagy induction. After

autophagy is initiated, class III phosphoatidylinositol-3-kinase (PI3K) complex (ATG6, ATG14, and VPS34) is responsible for the phagophore nucleation. As a core component of class III PI3K complex, ATG6 binds to VPS34 (class III PI3K) and modulates its lipid kinase activity. This lipid kinase complex then phosphorylates phosphoinositides to produce phosphatidylinositol-3-P (PI3P), which leads to the recruitment of important autophagy proteins involved in phagophore nucleation (11). Two ubiquitin-like conjugation systems are required for the expansion of phagophore and the completion of autophagosome formation. One is the ATG12 conjugation system (ATG5, ATG12, and ATG16). ATG12, an ubiquitin-like protein, is first activated by an ubiquitin-activating enzyme (E1)-like protein ATG7 and then transferred to ATG5 by ATG10, an ubiquitin carrier protein (E2)-like protein. ATG12 covalently conjugates with ATG5 and then recruits ATG16 to form the ATG12-ATG5-ATG16 complex which specifically targets to the membranes of early autophagosomes and functions as the E3-like enzyme for another ubiquitin-like conjugation system: LC3 (microtubule-associated protein 1 light chain 3, the mammalian homolog of ATG8) lipidation system (ATG3, ATG7, and LC3). Once autophagy is initiated, the 22-KD full-length LC3 precursor, an ubiquitin-like protein, is first cleaved by cysteine protease ATG4 to expose the conserved C-terminal Gly120 to produce the cytosolic LC3-I. Subsequently, LC3-I is activated by ATG7 and then transferred to ATG3, another ubiquitin carrier protein (E2)-like protein. ATG3-LC3-I conjugates target to the isolation membrane initiation sites and then the C-terminal glycine

covalently conjugates with the membrane lipid molecule phosphatidylethanolamine (PE) to generate PE-conjugated LC3 (called LC3-II) with the assistance of ATG12-ATG5-ATG16 complex. LC3-II is localized in both outer and inner membranes of phagophores and is considered to be important for the membrane extension and the eventual membrane closure (12). After mature autophagosomes form, the ATG12 complex disassociates, whereas LC3-II still associates with autophagosomal membrane and is eventually degraded in lysosomes.

LC3-II is now widely used as a key marker to monitor autophagy process (12,13). After lipidation, LC3-II tightly associates with autophagosomal membrane and plays an important role in the process of selective autophagy. Autophagic cargo receptors such as p62/SQSTM1 (sequestosome 1), NBR1 (neighbor of Brca1 gene), NDP52 (nuclear dot protein 52 kDa) and BNIP3L/NIX (Bcl-2 Interacting Protein 3 Like) can directly bind to the autophagosome-associated LC3-II through a LC3-interacting region (LIR) (14) so that the target cargo are enveloped by the phagophore membrane to form autophagosomes. Autophagosome-associated LC3-II also serves as a linker to bridge mature cargo-containing autophagosomes with microtubules for trafficking. Finally, autophagosomes fuse with lysosomes and LC3-II is degraded in lysosomes together with substrates. Therefore, the conversion of LC3-1 to LC3-II indicates autophagosomal biogenesis and the degradation of LC3-II indicates autophagosomal degradation. If the degradation of LC3-II is blocked by lysosomal

inhibitor, such as bafilomycin A1 (BAF), chloroquine (CQ) or ammonium chloride (NH4Cl), the amount of accumulated LC3-II can be used to quantify the autophagic activity. Western blot is one of the most popular assay to detect levels of LC3-I and LC3-II. Although the PE-conjugated LC3 (LC3-II) has a larger mass, it shows faster electrophoretic mobility in SDS-PAGE gels, probably due to its increased hydrophobicity. Therefore, LC3-I (approximately 16-18 KD) and LC3-II (approximately 14-16 KD) can be separated well on SDS-PAGE gels (13). A fluorescent protein tagged LC3, such as GFP-LC3 or RFP-LC3, is also widely used to monitor autophagic activity by fluorescent microscopy. Under nutrient-rich conditions, GFP-LC3 or RFP-LC3 diffuse in the cytoplasm. Upon autophagy is activated, GFP-LC3 or RFP-LC3 translocate to autophagosomal membranes and present as fluorescent punctate foci. Therefore, as a good fluorescent marker for autophagosomes, GFP-LC3 or RFP-LC3 punctate foci can be used for quantification of autophagic activity. Transgenic mice systemically expressing GFP-LC3 has been generated to monitor the autophagic activity in vivo (15).

Increasing evidences have showed that autophagy is a tumor suppressor pathway. The link between autophagy and tumorigenesis was first established in 1999, when the ATG gene Beclin1 (the homolog of ATG6 in yeast) was discovered to express at a decreased level in breast, ovarian and prostate cancers (16,17). Monoallelic deletion of Becclin1 in mice results in a significant reduction in autophagy flux and the development of spontaneous tumors (18,19). Subsequently, studies showed that mice lacking an autophagy-regulatory protein,

such as ATG4, ATG5, ATG7, Bif1 or MAP1S also exhibit a reduction in autophagy activity and an increase in tumorigenesis (20-22). Studies in these vivo models highlight the critical role of autophagy in tumor suppression. It has been demonstrated that autophagy defects promote tumorigenesis by destabilizing genome (23-25). Under normal conditions, autophagy occurs at a very low level to maintain cellular homeostasis. Under unfavorable conditions, autophagy can be rapidly activated to play a protective role by removing the damaged components, such like the damaged organelles and protein aggregates. Conversely, autophagy defects lead to the accumulation of damaging components which create a tumor-promoting environment by enhancing the production of reactive oxygen species (ROS). In addition to further damage cellular components, the enhanced ROS can trigger DNA double-strand breaks (DSB) and genome instability to promote tumorigenesis. Mice with either allelic loss of beclin1 or deletion of ATG5 or ATG7 exhibit increased DNA damage and genome instability.

Ras association domain family 1 isoform A (RASSF1A) is a tumor suppressor. Allelic loss of the 3p21.3 region of the human genome occurs frequently in lung cancer (26,27). In 2000, the gene located at this region was first cloned and named RASSF1, because the protein contains a putative Ras association domain (28). RASSF1 gene spans about 11,000 bp and contains eight exons, two CpG islands and two different promoters (Figure 2A). RASSF1 family has eight different isoforms (RASSF1A-RASSF1H) due to the alternative splicing

and the usage of the two different promoters. Among the eight isoforms, only RASSF1A has been subjected to the extensive studies. It is a 340-residue protein, containing four characterized domains: C1 domain, phorbol ester/diacylglycerol binding domain; ATM domain, ataxia-telangiectasia mutated domain; RA domain, Ras-association (RalGDS/AF-6) domain; SARAH (Salvador-RASSF-Hippo) domain, Mst and Sav1 binding domain (Figure 2B).

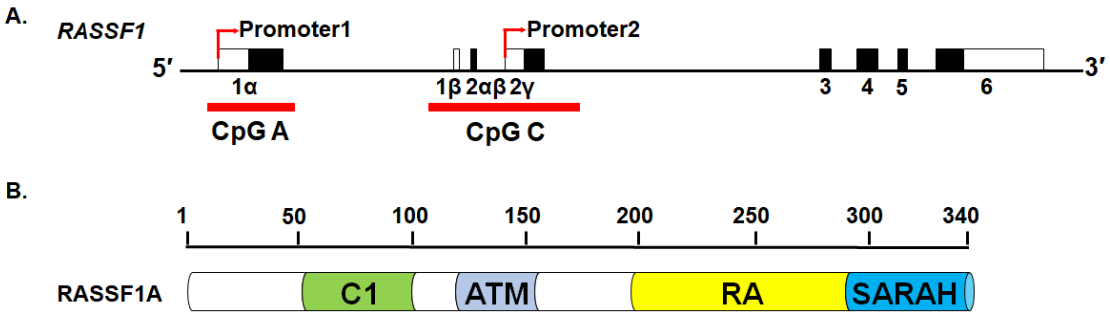

Figure 2. Map of RASSF1 gene and structure of RASSF1A protein. (**A**) A diagram showing the *RASSF1* gene locus. (**B**) A diagram showing the domain structure of RASSF1A protein.

RASSF1A is showed to have multiple different biological functions related to tumor suppression. RASSF1A localizes to and stabilizes microtubules. It is reported that RASSF1A inhibits cell mitosis by localizing to centrosomes, spindle microtubules, spindle poles, midzone and midbody (29,30). The ability to stabilize

microtubules also enables RASSF1A to inhibit cell migration (31,32). It is also reported that RASSF1A induces cell cycle arrest by directly interacting with cell division cycle protein 20 (Cdc20) to block its ability to activate the anaphase-promoting complex (APC) (33). In addition to inhibit cell mitotic progression, RASSF1A is also reported to promote cell apoptosis through modulator of apoptosis 1 (MOAP-1) and mammalian sterile 20-like kinase (Mst)/ protein salvador homolog 1 (Sav1) (34-36). RASSF1A directly interacts with MOAP-1 through its C1 domain, which relieves the inhibitory intramolecular interaction of MOAP-1 and promotes the association of MOAP-1 with Bcl-2-associated X protein (Bax). The increased association leads to the conformational change of Bax, mitochondrial membrane insertion, cytochrome c release and eventually apoptosis. RASSF1A is also reported to promote apoptosis by enhancing the transcription of some proapoptotic genes. RASSF1A directly interacts with Mst/Sav1 through its SARAH domain to activate Mst-mediated proapoptotic signaling pathway, which causes the translocation of transcriptional factor Yap in to nucleus. Yap associates with p73 (a homologue of tumor suppressor p53) to enhance the transcription of the proapoptotic genes. Studies showed that RASSF1A also promotes DNA damage response (37,38). Upon DNA damage, DNA damage checkpoint protein ataxia telangiectasia mutated (ATM) phosphorylates RASSF1A on Ser131 at its ATM domain, which leads to the Mst-mediated apoptosis. It also showed that RASSF1A directly interacts with mouse double minute 2 (MDM2, also known as E3 ubiquitin-protein ligase) through its C1

domain, which sequesters MDM2 away from p53 and inhibits MDM2-mediated ubiquitination and degradation of p53. The activated p53 induces cell-cycle arrest and apoptosis to maintain genome integrity.

RASSF1A is frequently inactivated by hypermethylation of CpG island in the promoter region in numerous human cancers, such as bladder, lung, kidney, breast and ovarian cancers (39-41). In human HCC, RASSF1A promoter methylation occurs at the highest frequency. Meta-analyses showed that RASSF1A gene has an aberrant promoter methylation in about 90% of human HCC tissues (42,43). However, the exact role of RASSF1A in the development of HCC has not been investigated. In order to improve the limited therapy and poor prognosis of HCC patients, it is imperative to understand the exact role and detailed mechanism of RASSF1A in this deadly disease.

Microtubule-associated protein 1 small form (MAP1S), originally named as C19ORF5 (chromosome 19 open reading frame 5), is a microtubule-associated autophagy activator. It was first identified in 2002 as an interactive partner of leucine-rich PPR motif-containing protein (LRPPRC). Similar to its homologue of neuronal-specific MAP1A and MAP1B, the full length MAP1S(FL) is post-translationally modified into multiple isoforms, including heavy chain (HC), short chain (SC) and light chain (LC) (44). Autophagy marker microtubule-associated protein 1 light chain 3 (LC3) was first discovered as an interactive partner of MAP1A and MAP1B (45,46). The interaction with MAP1A/B facilitates the microtubule association of LC3. In addition to MAP1A/B, we previously reported

that MAP1S-FL, HC, SC, but not LC, also interact with LC3, enabling MAP1S to bridge autophagosomes with microtubules to affect autophagosomal biogenesis and degradation (47). Moreover, we also found that MAP1S is able to promote autophagy initiation through the p27-mediated non-canonical autophagy pathway (47,48). MAP1S activates autophagy to suppress HCC. MAP1S-deleted mice have accelerated formation of liver tumor foci and develop more malignant hepatocellular carcinomas with diethylnitrosamine (DEN) treatment (25). MAP1S-deleted mice also have a significant 5.6-month reduction in lifespans compared with wild-type mice (49). In addition, our previous studies showed that MAP1S can be used as a novel marker for the prognosis of patients with prostate adenocarcinomas (PCA) and clear cell renal cell carcinoma (ccRCC) (50,51). Patients with low levels of MAP1S usually exhibit worse clinical features and have a shorter survival time than those with high levels of MAP1S.

MAP1S was identified as a major interactive protein of RASSF1A in the yeast two-hybrid analysis in a human liver and brain cDNA library (52,53). The interaction of RASSF1A with autophagy activator MAP1S triggered us to examine whether RASSF1A activates autophagy through MAP1S. Considering the frequent inactivation of RASSF1A gene in human liver cancer and the critical role of autophagy in tumor suppression, we were triggered to hypothesize that RASSF1A depletion may promote hepatocarcinogenesis by suppressing autophagy. Indeed, in this study we show that RASSF1A enhances the acetylation of microtubules, interacts with MAP1S and recruits LC3-II-associated

autophagosomes onto acetylated microtubules through MAP1S to promote autophagy maturation; and RASSF1A interacts with Hippo pathway-regulatory protein Mst1 and enhances Mst1 stability to inhibit PI3K-Akt-mTOR pathway to promote autophagy initiation. RASSF1A deletion in mice leads to reduced autophagy flux which promotes oxidative stresses, DNA damage and DEN-induced HCC and shortens mouse survivals.

CHAPTER II

DEPLETION OF RASSF1A RESULTS IN DECREASED AUTOPHAGY FLUX

Introduction

RASSF1A belongs to RASSF1 (Ras association domain family 1) family. RASSF1 gene locates in the 3p21.3 region of the human genome. The frequent allelic loss of this region in human lung cancers promotes people to try to identify the protein encoded by this region. The gene was successfully cloned and characterized to a human RAS effector homologue (RASSF1) in 2000 (28). Among the eight identified different isoforms of RASSF1 (RASSF1A-RSSF1H), only RASSF1A is subjected to extensive studies.

RASSF1A is found to be frequently inactivated by promoter hypermethylation in numerous human cancers. To elucidate the mechanism by which RASSF1A exerts its tumor suppressive activities, Dallol et al. performed a yeast two-hybrid analysis in 2004 to identify the direct binding partners of RASSF1A in a human brain cDNA library (52). Consistent with our previous reports that MAP1S interacts with RASSF1A in a yeast two-hybrid analysis in a human liver cDNA library (53), they found that microtubule-associated proteins, including MAP1B and MAP1S, are the major interactive partners of RASSF1A. Subsequent studies showed that RASSF1A can colocalize with MAP1S on microtubules and promote microtubule stabilization (52,54). It is also reported that MAP1S recruits RASSF1A to spindle poles to inhibit mitotic progression (30).

MAP1A/B, the homologues of MAP1S, was reported to facilitate the association of LC3 with microtubules by interacting with LC3 (12,46). In addition, MAP1B was found to be involved in the regulation of autophagosomal trafficking in neurons (55). In addition to the microtubule dynamics regulation, we previously reported that MAP1S also plays a significant role in autophagy regulation. MAP1S-deleted mice exhibit decreased autophagy flux (47). MAP1S recruits LC3 to microtubules to promote autophagosomal biogenesis and degradation. The interaction of RASSF1A with autophagy activator MAP1S triggered us to reason that RASSF1A may also play a role in autophagy regulation. Indeed, here we show that RASSF1A depletion leads to a reduction in autophagy flux both in vitro and in vivo.

Materials and Method

Animals

All animal protocols were approved by the Institutional Animal Care and Use Committee (IACUC), Institute of Biosciences and Technology, Texas A&M Health Science Center. All animals received humane care according to the criteria outlined in the “Guide for the Care and Use of Laboratory Animals” prepared by the National Academy of Sciences and published by the National Institutes of Health (NIH publication 86-23 revised 1985). C57BL/6 RASSF1A-/- mice were gifts from Dr. Pfeifer, the Center for Epigenetics, Van Andel Research Institute. C57BL/6 wild-type and RASSF1A-/- mice were bred and genotyped as described (56). Primers used for mouse genotyping PCR analyses are listed in Table 1. GFP-LC3 transgenic mice were gifts from Dr. Noboru Mizushima, the Department of Physiology and Cell Biology, Tokyo Medical and Dental University Graduate School and Faculty of Medicine. Chloroquine (CQ) (Sigma, #C6628) is a lysosomal inhibitor and was used to block autophagosomal degradation by raising the lysosomal pH. Mice were intraperitoneally injected with 50mg/kg body weight of CQ dissolved in saline per day for four days. Liver tissues were then harvested immediately after the animals were euthanized by CO2 asphyxiation.

Table 1. Primers used for mouse genotyping PCR.

Primer	Sequence
UMIOAI	5′-TTGTGCCGTGCCCCGCCCA-3′
LMIIAA	5′-TGACCAGCCCTCCACTGCCGC-3′
Neo48U	5′-GGGCCAGCTCATTCCTCCCAC-3′

Cell Culture

HeLa, HeLa cells stably expressing ERFP-LC3 (HeLa-RFP-LC3), and mouse embryonic fibroblast (MEF) cells were cultured in Dulbecco's Modified Eagle Medium (DMEM) (GenDEPOT, #CM001) containing 10% Fetal Bovine Serum (FBS) (GenDEPOT, #F0900) and antibiotics (Thermo Scientific, #SV30010). Primary mouse hepatocytes were cultured in William's E culture media (Sigma, #W4125) with 10% FBS, antibiotics, Insulin-Transferrin-Selenium (ITS-G) (Invitrogen, #51300-044) and 100 nM dexamethasone (Sigma, D4902). Phosphate-buffered saline (PBS) of pH 7.4 and 0.25% trypsin (GenDEPOT, #CA014) were used for subculture. All cells were cultured in a tissue culture incubator at 37°C with 5% CO2.

siRNA and Cell Transfection

The negative control siRNA (Invitrogen, #AM4635) was purchased from Invitrogen. The siRNAs specific to human RASSF1A (Santa Cruz, #sc-44070) was from Santa Cruz Biotechnology. HeLa cells or HeLa cells stably expressing ERFP-LC3 (HeLa-RFP-LC3) were transfected with random or RASSF1A-specific siRNAs by using Oligofectamine (Invitrogen, #12252-011) according to the manufacturer's recommended instruction. The total proteins were harvested at 48 hours after transfection.

Western Blotting

Cells or mouse tissues were lysed in lysis buffer (50 mM HEPES, pH 7.5, 150 mM NaCl, 1 mM EDTA, 2.5 mM EGTA, 0.1% Triton X-100, 10% Glycerol, 1 mM NaF) with 1 mM phenylmethanesulfonyl fluoride (PMSF) (Sigma, #P7626) and protease inhibitor cocktail (Sigma, #P8849) on ice. The total protein extracts were harvested by centrifugation. The protein concentration was determined by using BCA protein assay kit (Thermo Scientific, #23225). The lysates mixed with sodium dodecyl sulfate (SDS) loading buffer were then boiled for 10 minutes. Lysates containing the equal amounts of protein were separated by SDS-polyacrylamide gels (SDS-PAGE) and transferred onto polyvinylidene difluoride (PVDF) membranes (GE Health, #10600023). The membranes were blocked with 5% (w/v) non-fat milk dissolved in Tris-buffered Saline with Tween-20 (TBST) for 1 hour at room temperature and then incubated with primary antibodies overnight

at 4°C. The primary antibodies and the dilutions are: anti-RASSF1A (Abcam, #ab23950), 1:1000; anti-LC3 (Novus Biologicals, #NB100-2331), 1:1000; anti-β-Actin, (Santa Cruz, #47778), 1:2000; and anti-GAPDH, (Santa Cruz, #25778), 1:2000. After being washed with TBST buffer to remove nonspecific antibodies, the membranes were then incubated with horseradish peroxidase (HRP)-conjugated secondary antibodies (Bio-Rad, #172-1011, #170-6515, dilution 1:10000) for 1 hours at room temperature. After being washed with TBST buffer to remove the unbound antibodies, the specifically bound antibodies were detected by using ECL Prime Western Blotting Detection Reagents (GE Health, #RPN2232). The membranes were imaged by exposing to X-ray films (Pheonix, #F-BX57). Finally, the relative intensity of a band to the internal control was measured by using the ImageJ software (NIH).

Fluorescent Confocal Microscopy

HeLa-RFP-LC3 cells or primary hepatocytes derived from GFP-LC3 transgenic mice were treated with 10 nM lysosomal inhibitor balifomycin A1 (BAF) (Sigma, #11707) for 6 hours. Cells were then fixed with 4% (w/v) paraformaldehyde (Sigma, #P6148) in PBS for 30 minutes at room temperature. Images were captured with a Zeiss LSM 510 Meta Confocal Microscope. The number of RFP-LC3 or GFP-LC3 punctate foci on each image was calculated by using ImageJ software.

Establishment of Mouse Embryonic Fibroblasts (MEFs)

Mouse embryonic fibroblasts (MEFs) were prepared from wild-type (RASSF1A+/+) and RASSF1A knockout mice (RASSF1A-/-) as described (47). Briefly, embryos collected at E12.5-14.5 were minced in Dulbecco's modified Eagle's medium (DMEM), incubated with 0.25% trypsin at 37 °C for 10 min and then filtered through 70 μm cell strainer (Corning, # 352350). The separated cells were then harvested and cultured in DMEM containing 10% Fetal Bovine Serum (FBS) (GenDEPOT, #F0900) and antibiotics (Thermo Scientific, #SV30010).

Real-time Reverse Transcription (RT)-PCR

Total RNA was isolated from wild-type or RASSF1A-/- MEFs with Trizol reagent (Invitrogen, #15596-026) according to the manufacturer's instructions. Reverse transcription was performed using the Invitrogen SuperScript III reverse transcriptase with random primers. Real-time PCR reactions were performed using SYBR Premix ExTaq (TaKaRa, #RR820A). Primers used for real-time PCR analyses of mouse RASSF1A mRNA levels are listed in the Table 2. The abundance of mRNA was calculated by using the comparative threshold (CT) cycle method. Relative quantification of mRNA was achieved by normalization to the amount of β-actin.

Table 2. Primers used for real-time PCR analyses of mouse RASSF1A mRNA levels

Primer	Sequence
RASSF1A Forward	5′-GTACAACACGCAATCCGTC-3′
RASSF1A Reverse	5′-GCAGACGAGCGCGCGAC-3′
β-actin Forward	5′-GCACCAGGGTGTGATGGTG-3′
β-actin Reverse	5′-TGGATGGCTACGTACATGGC-3′

Isolation of Primary Mouse Hepatocytes

Mouse primary hepatocytes were isolated from 12-week-old male wild-type (RASSF1A+/+) and RASSF1A knockout mice (RASSF1A-/-) by the two-steps liver perfusion method as previously described (57). Briefly, mice were anesthetized and the portal vein was catheterized after cutting open the abdomen. The liver was then first perfused in situ with Earle's Balanced Salt Solution (EBSS) (Invitrogen, #14115-063) containing 0.5 mM EGTA (Sigma, #E4378) for 8-10 min with the inferior vena cava cut and then perfused for 5 min with Hanks' Balanced Salt Solution (HBSS) (Invitrogen, #14170-112) supplemented with 0.3mg/ml type IV collagenase (Roche, #11088874103). After perfusion, the liver was extirpated, transferred into plates filled with DMEM, removed of gallbladder and gently squeezed to help hepatocytes detach. Then cell suspension was filtered through sterile 70 μm cell strainers, washed by centrifugation at 600 rpm for 2 min at RT,

resuspended in Percoll (GE Health, #17-0891-02)/10XHBSS (Invitrogen, #14185-052) (9:1) mixture and centrifuged at 600 rpm for 15 min at RT. Cell viability was examined by Trypan Blue staining. After centrifugation, pellet was washed and seeded at dish.

Statistical Analysis

Statistically significant effects were examined using Student's t-test. A P value of less than 0.05 was considered significant and significance were set to *, $p \leq 0.05$; **, $P \leq 0.01$; and ***, $P \leq 0.001$. Error bars represent standard deviation.

Results

Knockdown of RASSF1A in HeLa Cells Leads to Decreased Autophagy Flux

Due to the hypermethylation of CpG island in promoter region, RASSF1A is epigenetically inactivated in numerous cancer cell lines. However, HeLa cells retain the expression of RASSF1A. Therefore, to examine whether RASSF1A regulates autophagy, RASSF1A-specific siRNA was first utilized to suppress the expression of RASSF1A in HeLa cells and levels of the key autophagy marker LC3-II was measured to represent autophagy flux. With lysosomal inhibitor bafilomycin A1 (BAF) treatment, RASSF1A-suppressed HeLa cells had less accumulated LC3-II than the control cells (Figure 3A, B), indicating that RASSF1A knockdown caused a reduction in autophagy flux. To confirm this result, we then suppressed the expression of RASSF1A in HeLa cells stably expressing RFP-LC3 to observe the amounts of RFP-LC3 punctate foci representing autophagosomes. Expectedly, RASSF1A-suppressed cells exhibited a significant reduction in the number of RFP-LC3 punctate foci (Figure 3C, D) and the intensity of RFP-LC3 band and endogenous LC3-II band (Figure 3E, F) in the presence of BAF. Therefore, knockdown of RASSF1A in HeLa cells results in a reduction in autophagy flux.

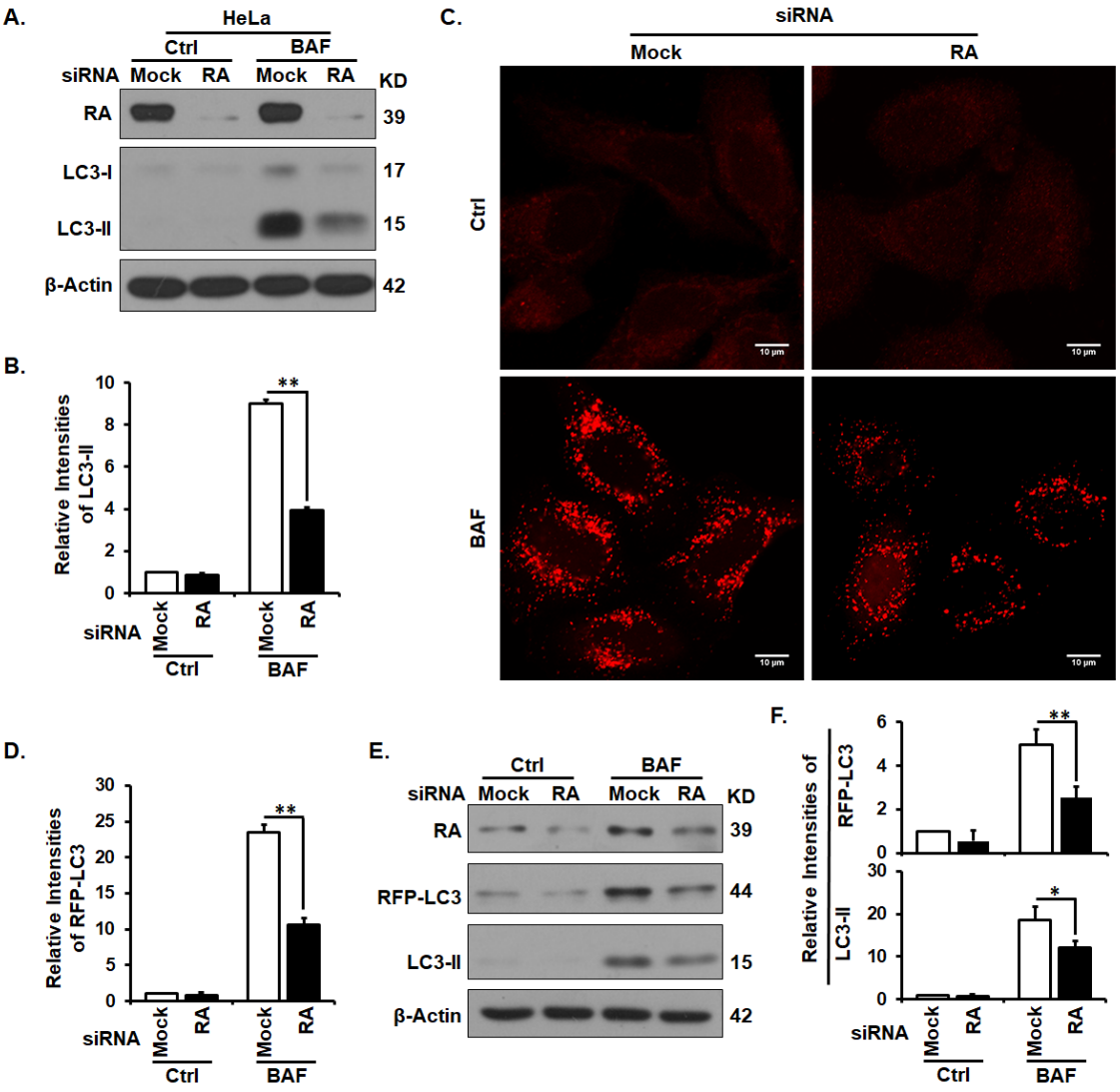

Figure 3. Knockdown of RASSF1A in HeLa cells causes reduced autophagy flux. (**A**, **B**) Immunoblot analysis (**A**) and quantification (**B**) of LC3-II levels in HeLa cells treated with random (Mock) or RASSF1A-specific siRNAs (RA) in the absence (Ctrl) or presence of lysosomal inhibitor BAF (10 μM overnight before harvest). (**C**, **D**) Representative fluorescent images (**C**) and quantification (**D**) of RFP-LC3 punctate foci in HeLa cells stably expressing RFP-LC3 treated with random (Mock) or RASSF1A-specific siRNAs in the absence (Ctrl) or presence of BAF. Scale bar, 10μM. (**E**, **F**) Immunoblot analysis (**E**) and quantification (**F**) of levels of RFP-LC3 and endogenous LC3-II in similar cells as shown in (**C**). *, P ≤ 0.05; **, P ≤ 0.01.

Deletion of RASSF1A Gene Leads to Decreased Autophagy Flux in Mouse Embryonic Fibroblasts (MEFs)

To examine whether RASSF1A depletion also results in decreased autophagy flux in mice, we first isolated MEFs from wild-type and RASSF1A-/- mice and measured levels of autophagy flux. The genotyping results (Figure 4A) and the quantitative real-time PCR analyses (Figure 4B) confirmed the deletion of RASSF1A gene in RASSF1A-/- mice. As expected, RASSF1A deletion led to a reduced accumulation of LC3-II in the presence of BAF (Figure 4C, D). Therefore, RASSF1A deletion causes reduced autophagy flux in MEFs.

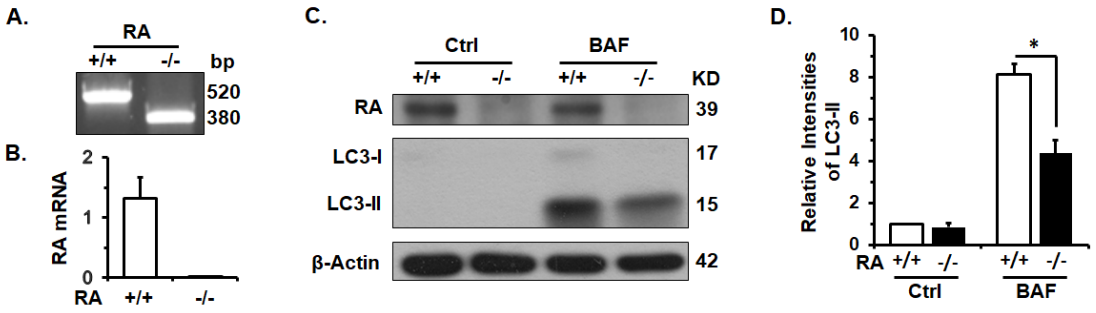

Figure 4. Deletion of RASSF1A gene in mice causes reduced autophagy flux in MEFs. (**A**) PCR analysis of DNA samples from MEFs to genotype wild-type and RASSF1A$^{-/-}$ MEFs. (**B**) Quantitative real-time PCR analysis of levels of RASSF1A mRNA in MEFs derived from wild-type and RASSF1A$^{-/-}$ mice. (**C**, **D**) Immunoblot analysis (**C**) and quantification (**D**) of LC3-II levels in wild-type and RASSF1A$^{-/-}$ MEFs in the absence (Ctrl) or presence of BAF. *, $P \leq 0.05$.

Deletion of RASSF1A Gene Leads to Decreased Autophagy Flux in Mouse Livers

We then examined the impact of RASSF1A on autophagy flux in mouse livers which are highly depend on autophagy to maintain their functions (58). In the presence of BAF, RASSF1A deletion resulted in a reduction of LC3-II levels in mouse primary hepatocytes, indicating a decreased autophagy flux (Figure 5A, B). Such reduction in autophagy flux was confirmed by a significant reduction in the number of GFP-LC3 punctate foci in BAF-treated hepatocytes isolated from GFP-LC3 transgenic RASSF1A-/- mice (Figure 5C, D). To further confirm this result, levels of autophagy flux were examined in three pairs of male littermates of wild-type and RASSF1A-/- mice intraperitoneally injected with lysosomal inhibitor chloroquine (CQ) (50mg/kg per day) for four days. CQ accumulates in lysosomes and raises lysosomal pH to inhibit lysosomal enzymes that require an acidic pH. Immunoblot analysis showed that in the presence of CQ, liver tissues from RASSF1A-/- mice had decreased levels of LC3-II compare to the wild-type mice (Figure 5E, F). Therefore, deletion of RASSF1A gene causes reduced autophagy flux in mouse livers.

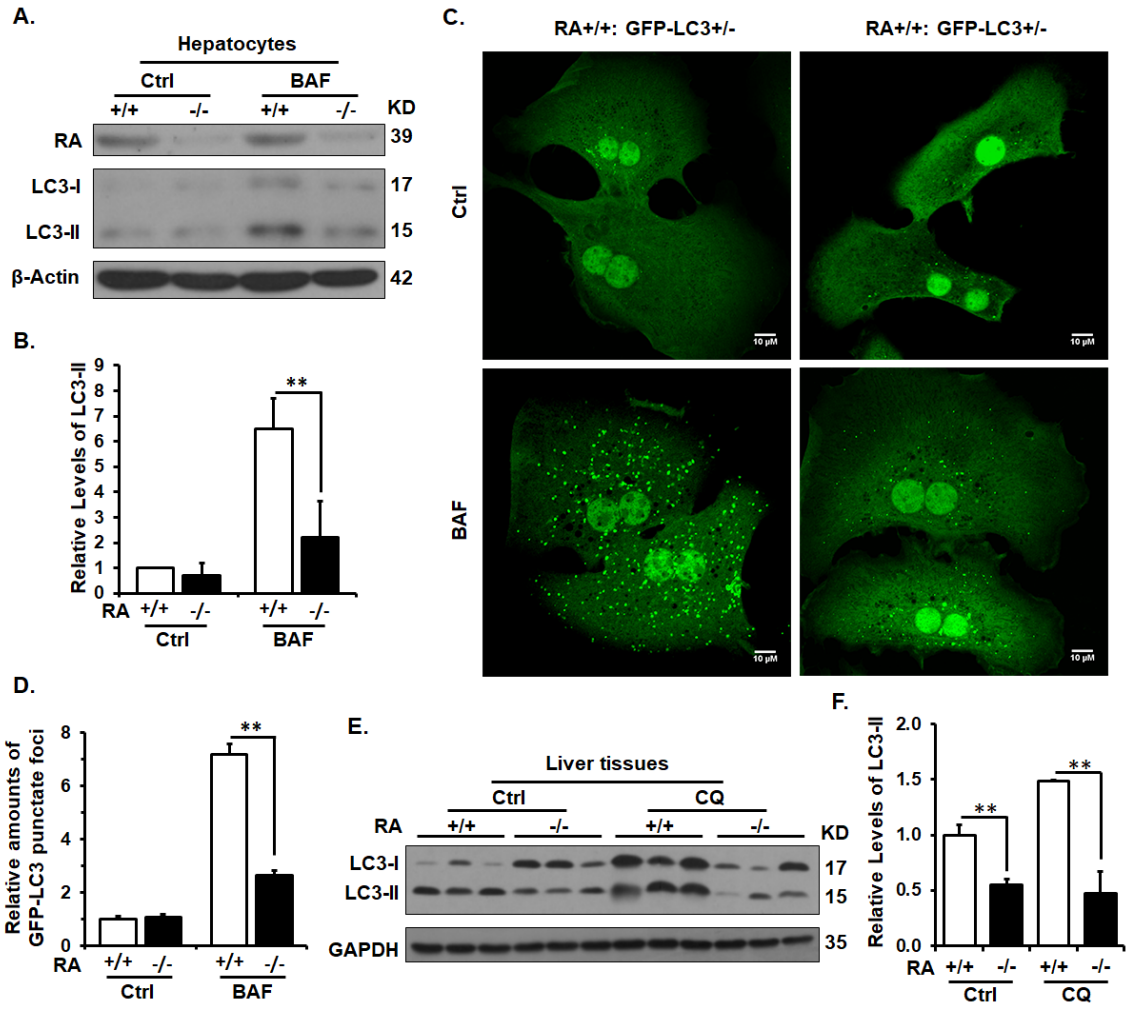

Figure 5. Deletion of RASSF1A gene causes reduced autophagy flux in mouse livers. (**A**, **B**) Immunoblot analysis (**A**) and quantification (**B**) of LC3-II levels in wild-type and RASSF1A$^{-/-}$ hepatocytes in the absence (Ctrl) or presence of BAF. (**C**, **D**) Representative fluorescent images (**C**) and quantification (**D**) of GFP-LC3 punctate foci in hepatocytes isolated from GFP-LC3 transgenic wild-type and RASSF1A$^{-/-}$ mice. Scale bar, 10μM. (**E**, **F**) Immunoblot analysis (**E**) and quantification (**F**) of LC3-II levels in liver tissues from wild-type and RASSF1A$^{-/-}$ mice injected with saline (Ctrl) or lysosomal inhibitor CQ. **, P ≤ 0.01.

Discussion

Autophagy is a highly conserved self-digestion process. As a house keeper, autophagy maintains cellular homeostasis by degrading aged or dysfunctional organelles and protein aggregates. Autophagy also has a key role in promoting cellular survival during starvation by providing nutrients, and protecting cells from stresses-induced damage by degrading damaged cellular components.

Among all the autophagy-related proteins, LC3 is most widely used to monitor and quantify autophagy activity (13). LC3 was first identified in 1994 as a co-purified protein with MAP1A/B in rat brain and proposed to regulate the microtubule binding activity of MAP1A/B (46). In 2000, LC3 was identified as the first mammalian protein associated with autophagosomal membrane (12). Upon autophagy is initiated, the full length LC3 precursor is first truncated into cytosolic LC3-I which then conjugates with autophagosomal membrane component phosphatidylethanolamine (PE) to be anchored to autophagosomal membrane. Finally, PE-associated LC3, also known as LC3-II, is degraded in lysosomes along with substrates. Therefore, the amount of LC3-II represents the number of autophagosomes. Due to the generated LC3-II is constantly degraded by lysosomes, the increased levels of LC3-II may indicate the enhanced conversion of LC3-I to LC3-II or the impaired autophagosomal degradation by lysosomes. Therefore, to correctly monitor autophagy activity, we usually measure the total amounts of LC3-II after the autophagosomal degradation is blocked by a

lysosomal inhibitor, such like bafilomycin A1 (BAF), chloroquine (CQ) or ammonium chloride (NH4Cl). In this chapter, by using western blots and GFP or RFP-LC3 punctate foci forming assay, we show first time that in the presence of lysosomal inhibitor, RASSF1A depletion causes reductions in levels of LC3-II and number of GFP or RPF-LC3 punctate foci both in vitro and in vivo, indicating that RASSF1A depletion leads to a reduction in autophagy activity.

Microscopic anatomy study shows that liver is formed by two major types of cells, including parenchymal hepatocytes (hereafter hepatocytes) and non-parenchymal cells. In this study, we mainly examined the impact of RASSF1A on autophagy flux in hepatocytes. Hepatocytes that constitute 60% of the total number of liver cells perform the majority of hepatic functions, such as carbohydrate metabolism, bile production, protein synthesis and storage, excretion of exogenous and endogenous substances. Hepatocytes have more lysosomes and lysosomal enzymes such as cathepsin than other cell types, indicating that hepatocytes have a higher autophagy activity (59). Studies showed that hepatocytes are highly dependent on autophagy to execute their metabolic functions. Alteration in hepatic autophagy significantly impacts the hepatic physiology and causes liver diseases (58).

The other 40% of liver cells are non-parenchymal cells, such like hepatic stellate cells (HSC), sinusoidal endothelial cells, phagocytic Kupffer cells and lymphocytes. Whether RASSF1A deletion also causes a reduced autophagy flux in these non-parenchymal liver cells or not is not investigated in this study.

Although the role of autophagy in these non-parenchymal cells is poorly understood, it is reported that autophagy plays a significant role in HSC activation (60). Activated HSC are the key cellular source of extracellular matrix synthesis in the process of liver fibrosis (61). Therefore, determining the role of RASSF1A-regulated autophagy in HSC activation may provide a novel paradigm in the prevention of liver fibrosis.

CHAPTER III

DELETION OF RASSF1A GENE IN MICE ACCELERATES DEN-INDUCED HEPATOCARCINOGENESIS

Introduction

Hepatocellular carcinoma (HCC) is the second leading cause of cancer mortality worldwide. In 2016, more than 35,000 people were diagnosed with liver cancer in the United States and more than 25,000 people died (3). The death rates caused by HCC are increasing. Although HBV vaccination and antiviral treatment against HBV or HCV infection can reduce the risk of HCC, very effective treatments for HCC are not available currently (2). For the patients with very early stage HCC, the surgical resection is one of the most appropriate treatment. However, the already existed chronic injuries in livers continue to promote the formation of new HCC. Therefore, there is as high as 70% recurrence risk of HCC in 5 years after surgery. Another most appropriate treatment for very early stage HCC patients is liver transplantation. The 5-year survival rate can reach up to as high as 75% after transplantation. However, currently, it is very difficult to diagnose the very early stage HCC which is defined as a single, asymptomatic lesion with less than 2 cm in diameter and no vascular or distant metastases. Only 13% of patients with HCC in the United States are diagnosed early enough to receive surgical resection or liver transplantation, but the prognosis of HCC patients is very poor and the 5-year survival rate is less than 12% (62). Therefore,

there is an urgent need to define the exact molecular mechanisms underlying HCC development for developing novel therapeutic strategies.

Autophagy, a cellular self-degradation process, plays an important role in maintaining diverse functions of livers. First, liver is particular dependent on autophagy to maintain the balance of energy and nutrients (58). In response to starvation, autophagy in livers is significantly activated to supply hepatocytes with the necessary nutrients for survival by degrading intracellular materials. Studies showed that mice starved for 48 hours can lose up to 40% of total liver proteins per hour, while mice in normal conditions just lose 1.5% of total liver proteins (63,64). Hepatocytes have a large number of mitochondria which are particular rich in proteins and lipids. In addition to protein degradation during starvation, selective mitochondria degradation by autophagy (also known as mitophagy) also occurs, which accounts for approximately 85% of autophagy events in the cultured hepatocytes (65,66). Hepatocytes from ATG5, ATG7 or Beclin1-deficient mice are characterized by the accumulation of protein aggregates as well as damaged mitochondria (21,23). In addition, during starvation, the blood glucose levels of liver-specific ATG7 deletion mice declined within a larger range than wild-type mice, suggesting that autophagy also plays an important role in maintaining hepatic glucose levels (67). It is also found that liver mediates the degradation of hepatocellular triglycerides (TGs) and lipid droplets (LDs), which is known as lipophagy (68). Lipophagy provides hepatocytes with free fatty acids (FFAs) to promote cellular ATG production, which balances cellular metabolism and energy

generation. Autophagy was also found to be implicated in the immune response of livers. Liver, the largest immune organ in the body, faces the continuous challenge of orally-ingested antigens and intestinal bacteria released products such as lipopolysaccharide (LPS). Liver is also the major target of a number of liver viruses, such like HBV, HCV and dengue virus (DENV). Studies showed that autophagy can sense microbial infection and then stimulate the toll-like receptor (TLR) signaling. The activated TLR in turn promotes autophagy induction (69,70). Studies also showed that autophagy functions in the degradation of microbes (known as xenophagy) and the process of antigen for MHC presentation (71-76). Taken together, in liver, autophagy has an essential role in the turnover of protein aggregates, dysfunctional or damaged organelles, and other macromolecules to maintain its basic functions.

Autophagy defects promote tumorigenesis, including liver tumors. The evidence first came from a study in 1999 which shows that the induced autophagy activity by the essential autophagy protein Beclin1 is associated with the decreased tumorigenesis ability of human MCF7 breast carcinoma cells (16). Subsequently, the inverse relationship between autophagy and tumorigenesis was well established by the examination of mice with loss of autophagy-related genes. Mice with allelic loss of Beclin1 are partially defective for autophagy and develop spontaneous hepatocellular carcinomas as well as other cancers, such as lung cancer and lymphomas (18,19). Mice with deficiency in an autophagy-related gene such as ATG7, Beclin1-interactive protein Bif1 (also known as

Endophilin B1), or ATG5, also exhibit a reduction in autophagy activity and an increase in spontaneous tumor incidence at advanced age (21,22). In addition, mice with ATG4C (one of the four mammalian ATG4 homologues) deficiency are more prone to develop fibrosarcomas with chemical carcinogens treatment (20). We previously found that mice with the novel autophagy activator MAP1S deficiency also showed an increased susceptibility to develop DEN-induced hepatocarcinomas (25). Natural component spermidine prevents DEN-induced HCC and prolongs mouse lifespans by activating MAP1S-mediated autophagy (57). Taken together, autophagy plays a critical role in suppressing tumorigenesis.

Defective autophagy enhances oxidative stresses which trigger DNA double strand break (DSB) and genome instability to promote tumorigenesis (5,23,25,77). Autophagy defects lead to the excessive accumulation of damaged organelles and protein aggregates that enhance the production of oxidative stress. The aged or damaged mitochondria are the major source of reactive oxygen species (ROS) (78,79). Oxidative protein folding is another source of oxidative stress (80). Studies showed that the accumulation of damaged or misfolded proteins in cytosol increase the burden on endoplasmic reticulum (ER) protein folding machinery (24). The generated ROS in turn further damages the surrounding cellular components to enhance ROS production. Enhanced ROS causes telomere attrition and DNA double-strand breaks (DSB) and simultaneously subverts mitotic checkpoints (81-84). Therefore, instead of oxidative stress-triggered cell death, some cells with DNA damage can survive

from the weakened mitotic checkpoint. The broken chromosomal fragment tends to randomly fuse with another chromosomal fragment, which potentially results in the formation of a new chromosome with two centromeres (85). During mitotic metaphase, chromosomal bridge forms. After telophase, chromosomal bridge breaks and generates new broken ends. If cells with DSB escape from the weakened mitotic checkpoint, they will produce aneuploidy daughter cells. Survived aneuploidy cells potentially initiate a cascade of autocatalytic karyotypic evolution through the continuous chromosomal breakage-fusion-bridge cycles (86). Eventually the genome is destabilized to promote tumorigenesis. Liver is particular dependent on autophagy to maintain its diverse functions (58). The critical role of autophagy in suppressing hepatocarcinogenesis has been well demonstrated by the studies in vivo models. Mice with loss of an autophagy-related gene such as Beclin1, ATG5, ATG7 or MAP1S, exhibit a reduced autophagy activity and an increased incidence of liver tumors (21,23). Studies also showed that autophagy-deficient tumor cells have accumulated swelling mitochondria, ubiquitinated protein aggregates, oxidative stress, DNA damage and genome instability.

RASSF1A, a tumor suppressor, is epigenetically silenced by promoter hypomethylation in over 90% of human HCC tissues. However, the exact role and detailed mechanism of RASSF1A in the development of HCC has not been investigated. In chapter II, we have demonstrated that RASSF1A deletion causes reduced autophagy flux in mouse livers. Considering the critical role of autophagy

in suppressing HCC formation, we reasoned that RASSF1A deletion may accelerate the formation of HCC by suppressing autophagy flux. Indeed, here we show that RASSF1A-deletion-caused autophagy defects in mouse livers enhance oxidative stresses and genome instability to promote DEN-induced HCC and shorten survival times of mice suffering from HCC.

Materials and Methods

Animals

All animal protocols were approved by the Institutional Animal Care and Use Committee (IACUC), Institute of Biosciences and Technology, Texas A&M Health Science Center. All animals received humane care according to the criteria outlined in the “Guide for the Care and Use of Laboratory Animals” prepared by the National Academy of Sciences and published by the National Institutes of Health (NIH publication 86-23 revised 1985). Diethylnitrosamine (DEN) (Sigma, #0756) was used as a carcinogenic reagent to induce liver tumors as previously described (25,87). 15-day-old wild-type and RASSF1A-/- male littermates were intraperitoneally injected with a single dose of DEN of 10 μg/g body weight dissolved in saline. Mice were euthanized by CO2 asphyxiation at 6, 7, 9, 12 months after DEN injection. Immediately after euthanasia, mice were weighted and livers were excised, weighed, and photographed. Ratio of liver weight to body weight (LW/BW) at each time point were recorded. Grossly visible surface tumors of each liver were scored. Liver tissues were frozen or fixed for further analyses. For the survival analysis, mice with DEN injection at 15 days after birth were observed to record their survival times when they were found dead or when they were found to be moribund.

Cell Culture

HeLa cells were cultured in DMEM medium containing 10% FBS and

antibiotics. PBS of pH 7.4 and 0.25% trypsin were used for subculture. Cells were cultured in a tissue culture incubator at 37°C with 5% CO2.

siRNA and Cell Transfection

HeLa cells were transfected with random or RASSF1A-specific siRNAs by using Oligofectamine according to the manufacturer's recommended instruction. The total proteins were harvested at 48 hours after transfection.

Western Blotting

Cells or mouse tissues were lysed in lysis buffer with 1 mM PMSF and protease inhibitor cocktail on ice. The protein concentration was determined by using BCA protein assay kit. The lysates mixed with SDS loading buffer were then boiled for 10 minutes. Lysates containing the equal amounts of protein were separated by SDS-PAGE gels and transferred onto PVDF membranes. The membranes were blocked with 5% (w/v) non-fat milk in TBST for 1 hour at room temperature and then incubated with primary antibodies overnight at 4°C. The primary antibodies and the dilutions are: anti-RASSF1A (Abcam, #ab23950), 1:1000; anti- γ-H2AX (Cell Signaling, #9718S), 1:1000; and anti-β-Actin, (Santa Cruz, #47778), 1:2000. After being washed with the TBST buffer to remove nonspecific antibodies, the membranes were then incubated with HRP-conjugated secondary antibodies for 1 hours at room temperature. After being washed with the TBST buffer to remove the unbound antibodies, the specifically

bound antibodies were detected by using ECL Prime Western Blotting Detection Reagents. Then, the membranes were imaged by exposing to X-ray films. Finally, the relative intensity of a band to the internal control was measured by using the ImageJ software (NIH).

Dihydroethidium (DHE) Staining

A part of frozen samples was cryosectioned and used for measurement of oxidative stress. The cryosections were stained with 2 mM dihydroethidium hydrochloride (DHE) (Invitrogen, #D-1168) for 30 minutes at 37 °C as previously described (49). DHE is able to permeate into cells and be oxidized by cytosolic ROS. The oxidized DHE then intercalates into genomic DNA to labels nuclei with red fluorescent signals which represent levels of oxidative stress in cells. The fluorescent signals were monitored by fluorescent microscopy and the intensities of signals were quantified by ImageJ software.

Histology

Liver tissues were fixed with 4% paraformaldehyde-PBS solution for 24 hours. The fixed liver tissues were then serially dehydrated, embedded in paraffin and sectioned. For general histology, liver tissue sections were re-hydrated and stained with hematoxylin (Fisher Scientific, #SH26) and Eosin (H&E) (Sigma, #HT110116). The occupied area of liver tumor foci was quantified by ImageJ software. For immunohistochemistry staining, liver sections were first re-hydrated

and boiled in citrate buffer (10 mM sodium citrate, 0.05% Tween-20), pH 8.0 for 20 minutes to retrieve antigen. Sections were then stained with γ-H2AX (Cell Signaling, #9718, dilution 1:500) using HRP/ 3, 3'-Diaminobenzidine (DAB) detection IHC kit (Abcam, #64261) according to the manufacturer's instruction. The sections were finally counterstained with hematoxylin to label nuclei.

Statistical Analysis

Statistically significant effects were examined using Student's t-test. A P value of less than 0.05 was considered significant and significance were set to *, $p \leq 0.05$; **, $P \leq 0.01$; and ***, $P \leq 0.001$. Error bars represent standard deviation. The overall survival and median survival times of mice were analyzed by the Kaplan-Meier method. The significance of difference between wild-type and RASSF1A-/- mice was estimated by log-rank test.

Results

Deletion of RASSF1A Gene Causes No Abnormality in Mouse Livers under Normal Conditions

RASSF1A gene is frequently inactivated by promoter hypermethylation in human HCC tissues. To investigate the function of RASSF1A in HCC, we first maintained 3 pairs of male littermates of wild-type and RASSF1A-/- mice under normal conditions for months to observe HCC formation. We were unbale to detect any tumor foci on the liver surfaces up to 12 months (Figure 6A). As displayed by hematoxylin and eosin (H&E) staining, no abnormality associated with the onset of neoplasia was detected in liver tissues from wild-type and RASSF1A-/- mice (Figure 6B).

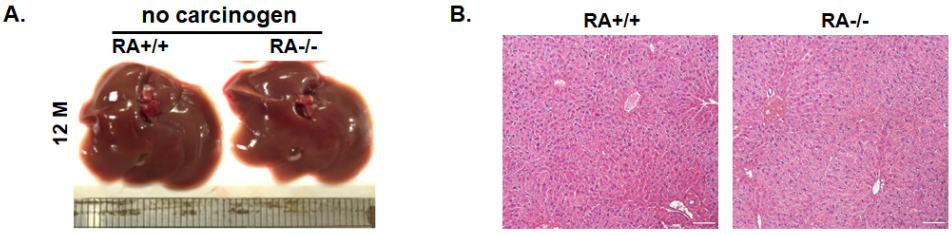

Figure 6. Deletion of RASSF1A causes no abnormality in mouse livers under normal conditions. (**A**) The morphology of livers from 12-month-old wild-type and RASSF1A$^{-/-}$ mice. (**B**) A comparative H&E staining of livers as shown in (**A**). Scale bar, 20μM.

Deletion of RASSF1A Gene in Mice Accelerates DEN-induced Hepatocarcinogenesis

Although deletion of RASSF1A gene may not be sufficient to induce liver cancer under normal conditions, we reasoned that RASSF1A deletion may accelerate liver cancer formation under certain types of stresses. DEN is widely used as a carcinogenic reagent to induce liver cancer in mice (87). We started to intraperitoneally inject 15 days-old male littermates of wild-type and RASSF1A-/- mice with a single dose of DEN (10 μg/g body weight) to induce HCC. We started to observe small liver surface tumors in RASSF1A-/- mice at 6 months and wild-type mice at 7 months after DEN treatment (Figure 7A). At this stage, although the body weights and liver weights were not significantly different (Figure 7B, C), RASSF1A-/- mice developed more liver surface tumors (Figure 7A, E) and larger tumor foci (Figure 7F, G). When mice became older, the large tumor foci occupied almost the entire liver surfaces of DEN-treated 12 months-old RASSF1A-/- mice, and RASSF1A-/- mice exhibited higher liver weights (Figure 7C) and liver/body weight ratios (Figure 7D) than wild-type mice. Histologically, at 12 months after DEN treatment, wild-type mice had about 40% area with normal liver structures, 10% with encircled tumor foci and 50% area with typical HCC trabecular structure, while RASSF1A-/- mice had only 10% area with encircled tumor foci, 65% typical HCC trabecular structure and 25% highly distorted liver structures (Figure 7H). Therefore, RASSF1A deletion promotes DEN-induced hepatocarcinogenesis.

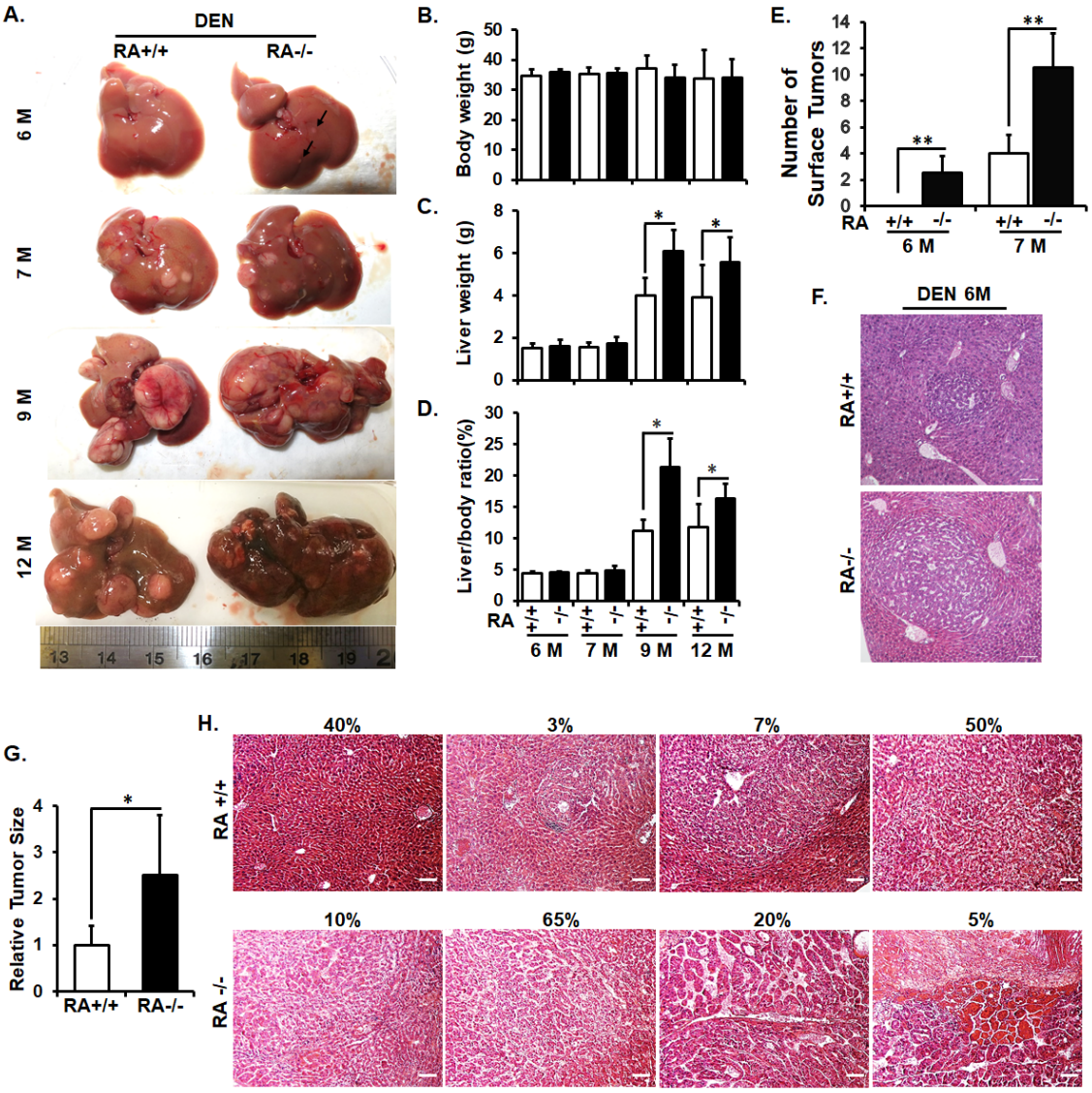

Figure 7. Deletion of RASSF1A gene in mice accelerates DEN-induced hepatocarcinogenesis. (**A**) Representative images of liver tissues from DEN-treated wild-type and RASSF1A$^{-/-}$ mice at different ages. Black arrows indicate liver surface tumors. (**B**-**E**) Plots of body weights (**B**), liver weights (**C**), ratios of body weight to liver weight (**D**), and the number of surface tumors (**E**) to ages of DEN-treated wild-type and RASSF1A$^{-/-}$ mice as shown in (**A**). (**F**) A comparative H&E staining of liver tissues from DEN-treated 6-month-old mice as shown in (**A**). Scale bar, 20μM. (**G**) Relative size of tumor foci as shown in (**F**). (**H**) A comparative H&E staining of liver tissues from DEN-treated 12-month-old mice as shown in (**A**). Scale bar, 20μM. *, P ≤ 0.05; **, P ≤ 0.01.

Deletion of RASSF1A Gene Causes Reduced Lifespan of DEN-treated Mice

Due to the accelerated hepatocarcinogenesis, RASSF1A-/- mice had a significant 174 days reduction in lifespan (or 31% reduction in median survival times, hazard ratio of 12.85) compared with wild-type mice in the presence of DEN (Figure 8).

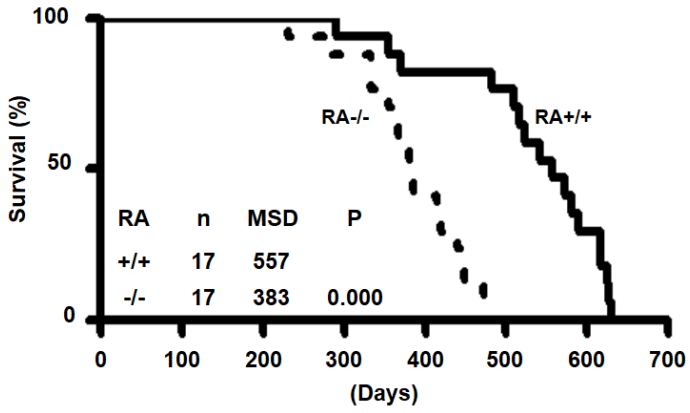

Figure 8. RASSF1A knockout mice have a shorter lifespan than wild-type mice with DEN treatment. The Kaplan-Meier survival curves showing the survival times of DEN-treated wild-type and RASSF1A$^{-/-}$ mice. n, number of mice; MSD, median survival days. The significance of difference between two groups was estimated by log-rank test, and *P* value for each plot was the probability larger than the chi-square value.

Deletion of RASSF1A Gene Enhances Oxidative Stress in Mouse Livers

Autophagy defects enhance oxidative stresses which further trigger DNA double-strand breaks (DSB) and genome instability to promote tumorigenesis (5,23,25,77). In chapter II, we have shown that RASSF1A deletion leads to a reduced autophagy flux in mouse livers. To examine whether RASSF1A-deletion-caused autophagy defects contribute to the accelerated hepatocarcinogenesis, we first measured levels of oxidative stresses in mouse livers by performing dihydroethidium (DHE) fluorescence assay. Cytosolic ROS oxidize DHE after DHE permeates into cells. The oxidized DHE then intercalates into genomic DNA and labels nuclei with red fluorescent signals. We intraperitoneally injected 3 pairs of male littermates of wild-type and RASSF1A-/- mice at 15-day-old with a single dose of either vehicle or DEN (10 μg/g body weight). Two days later, liver tissues were collected, immediately cryosectioned and stained with 2 mM DHE for 30 min at 37°C. There was no significant difference in levels of oxidative stress in liver tissues between wild-type and RASSF1A-/- mice under normal conditions. However, at two days after DEN treatment, RASSF1A-/- mice exhibited high levels of oxidative stress as indicated by the elevated intensity of red fluorescent signals (Figure 9A, B). Therefore, RASSF1A deletion enhances oxidative stress in mouse livers.

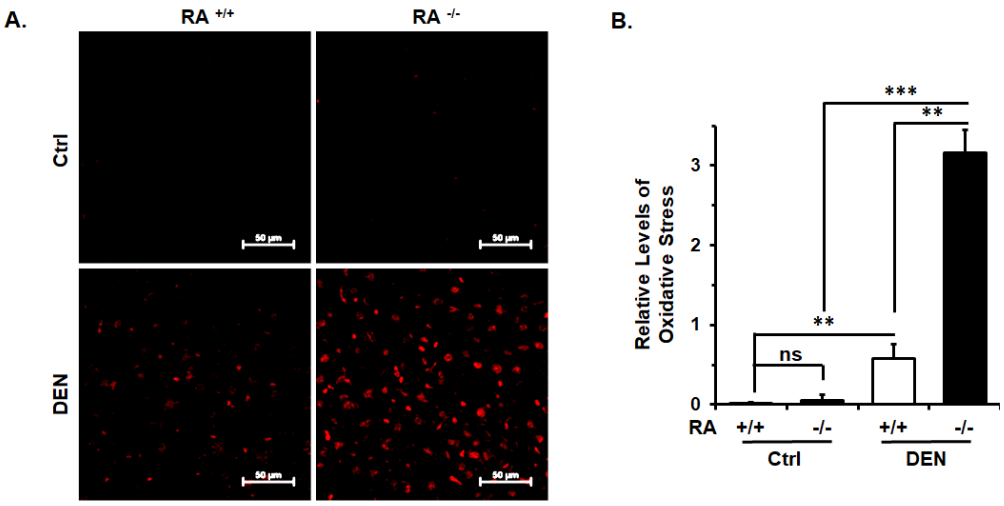

Figure 9. Deletion of RASSF1A enhances oxidative stresses in mouse livers. (**A**) Comparative analyses of levels of oxidative stress revealed by dihydroethidine hydrochloride (DHE) staining among liver tissues from wild-type and RASSF1A$^{-/-}$ mice treated with vehicle (Ctrl) or DEN for two days. Scale bar, 50μM. (**B**) Quantification of the relative levels of oxidative stress as shown in (**A**) by ImageJ software. **, $P \leq 0.01$; ***, $P \leq 0.001$; ns, nonsignificant, $P > 0.05$.

Deletion of RASSF1A Gene Promotes DNA Damage in Mouse Livers

Oxidative stress resulted from autophagy defects trigger DNA double strand break (DSB) and genome instability to promote tumorigenesis. We then examined whether the elevated oxidative stresses in RASSF1A-/- mice lead to increased DNA damage. Knockdown of RASSF1A in HeLa cells caused a significant increase in γ-H2AX levels (Figure 10A, B), the marker of DNA double strand breakage (88). Consistently, RASSF1A deletion also caused elevated levels of γ-H2AX in mouse liver tissues collected at 6 months after DEN treatment compared to wild-type mice (Figure 10C, D). The immunohistochemistry staining further showed that with DEN treatment, liver tissues from RASSF1A-/- mice had a dramatically increased number of cells positively stained with γ-H2AX compared with wild-type mice (Figure 10E, F). Therefore, RASSF1A deletion promotes DNA damage in mouse livers.

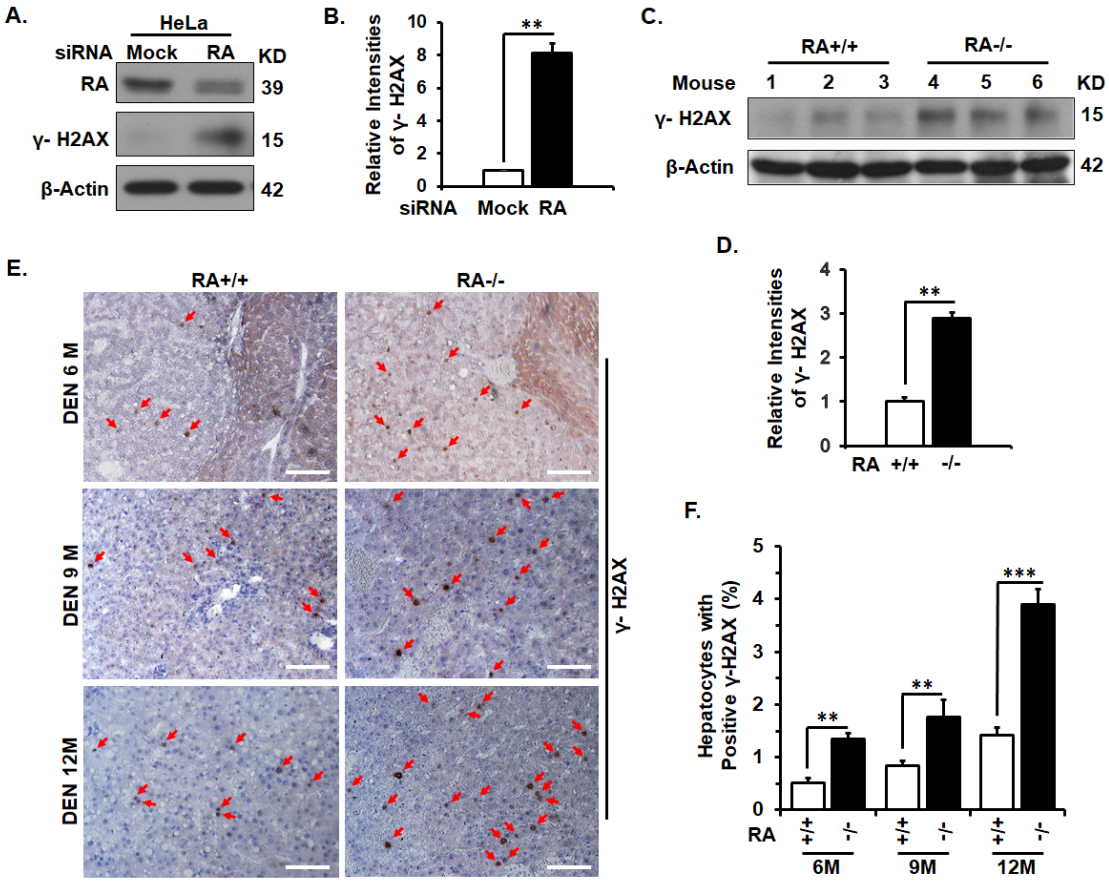

Figure 10. Deletion of RASSF1A promotes DNA damage in mouse livers. (**A**, **B**) Immunoblot analysis (**A**) and quantification (**B**) of γ-H2AX levels in HeLa cells treated with random (Mock) or RASSF1A-specific siRNAs. (**C**, **D**) Immunoblot analysis (**C**) and quantification (**D**) of γ-H2AX levels in liver tissues from DEN-treated 6-month-old wild-type and RASSF1A$^{-/-}$ mice as shown in Figure 7A. (**E**) Representative immunostaining of γ-H2AX in liver tissue sections of DEN-treated wild-type and RASSF1A$^{-/-}$ mice at different ages as shown in Figure 7A. Red arrows indicate γ-H2AX positive cells. Scale bar, 20 μm. (**F**) Quantification of the percentage of γ-H2AX positive cells in total cells of liver tissue sections as shown in (**E**). **, P ≤ 0.01; ***, P ≤ 0.001.

Discussion

Autophagy-lysosome pathway plays a critical role in maintaining cellular homeostasis by degrading misfolded or aggregated proteins, dysfunctional organelles and other macromolecules. Autophagy defects enhance oxidative stresses (5,77). Reactive oxygen species (ROS) destabilize genome by causing telomere attrition and DNA double strand breakage (DSB) and simultaneously subverting mitotic checkpoints (81-84). If cell with a destabilized genome escapes from the weak mitotic checkpoints, it potentially initiates a cascade of autocatalytic karyotypic evolution through continuous cycles of chromosomal breakage-fusion-bridge and eventually destabilizes genome to promote tumorigenesis (77,86).

In addition to promote cancer initiation, autophagy defects also promote cancer development. Although it is believed that the established tumor cells utilize autophagy to survive metabolic stresses, such like low nutrient and hypoxia, studies showed that autophagy defects in established tumor cells can promote tumor progression (23,25). Autophagy defects lead to different types of cell death including apoptosis, necrosis, and pyroptosis (89,90). Oxidative stress or lysosomal rupture resulted from autophagy defects activate NLRP3 inflammasomes, which leads to the activation of caspase-1 to induce a type of cell death referred to as pyroptosis (91-93). Pyroptosis is an inflammatory form of cell death and characterized by the release of proinflammatory cytokines that can fuel pro-inflammatory cascades to cause the death of other cells in the environment (94-96). Furthermore, in established tumor cells, autophagy defects further

promote DNA damage due to the inability of tumor cells to remove oxidative stress. The subverted cell cycle checkpoints and apoptosis resistance in tumor cells may allow further manifestation of genome damage. A destabilized genome leads to increased mutation rate in the remaining viable tumor cells, which facilitates tumor progression. Therefore, autophagy defects promote both initiation and development of cancer.

Although RASSF1A-/- mice with decreased autophagy activity did not develop spontaneous HCC under normal conditions, they exhibited an accelerated initiation and development of HCC with chemical carcinogen DEN treatment, which is consist with the suppressive role of autophagy in tumorigenesis. In addition, reduction in autophagy activity led to elevated levels of oxidative stress and DNA damage both of which accelerate DEN-induced initiation and progression of HCC. Autophagy prolongs mouse lifespans (49,57). DEN-treated RASSF1A-/- mice lived much shortened lifespans than the DEN-treated wild-type mice possibly also due to the reduced autophagy activity.

Taken together, we show here first time that epigenetic inactivation of tumor suppressor RASSF1A actually promotes HCC by suppressing autophagy flux, which may provide a novel paradigm of the prevention and therapy of human liver cancer.

CHAPTER IV

RASSF1A PROMOTES AUTOPHAGY MATURATION BY RECRUITING AUTOPHAGOSOMES ONTO RASSF1A-STABILIZED ACETYLATED MICROTUBULES THROUGH MAP1S

Introduction

Autophagy, an evolutionarily conserved catabolic process, functions in the turnover of protein aggregates and damaged organelles through the lysosomal degradation pathway. After autophagy is initiated, the target substrates are captured by the phagophore to form autophagosomes which then fuse with lysosomes for degradation. Once autophagy is initiated, the cytosolic LC3 undergoes lipidation by conjugating with membrane component phosphatidylethanolamine (PE) (12). The PE-conjugated LC3 (LC3-II) directs phagophore membrane to sequester target cargo by directly binding with the cargo receptors, such as p62/SQSTM1, NBR1, NDP52 and BNIP3L/NIX (14,97-101). These cargo receptors specifically recognize and bind to the substrates. Meanwhile, the LC3-interacting region (LIR) in these cargo receptors mediates their interaction with autophagosome-associated LC3-II. Thus, the three-way interactions of cargo receptors with LC3-II and substrates enable the substrates to be targeted and packaged by phagophore to form autophagosomes. Autophagosome-anchored LC3-II bridges the mature autophagosomes with microtubules for trafficking. There are regular non-acetylated and stable

acetylated microtubules in cells and acetylated microtubules have been demonstrated to serve as the tracks for movement of mature autophagosomes and bring autophagosomes and lysosomes together for fusion to form autolysosomes (102). Finally, LC3-II as well as captured substrates are degraded in lysosomes.

Our previous studies showed that MAP1S, a microtubule-associated protein, interacts with LC3-II to facilitate its association with microtubules (47), so that LC3-II-associated mature autophagosomes are recruited onto microtubules for migration (103,104). Stabilized acetylated microtubules are required for the trafficking and fusion of autophagosomes with lysosomes (102). It is well documented that RASSF1A associates with and stabilizes microtubules and RASSF1A was reported to stabilize microtubules by enhancing the acetylation of α-tubulin (31,52,54). In addition, we previously reported that MAP1S associates with microtubules stabilized by RASSF1A (54). Based on these reports, we reasoned that RASSF1A may enhance the acetylation of microtubules and recruit LC3-II-associated autophagosomes onto RASSF1A-stablized acetylated microtubules through its interactive protein MAP1S to promote autophagy maturation. Indeed, here we show that RASSF1A promotes the acetylation of microtubules by inhibiting the deacetylase activity of RASSF1A-interactive HDAC6, and recruits LC3-II- associated autophagosomes onto RASSF1A-stablized acetylated microtubules through its interactive protein MAP1S.

Materials and Methods

Animals

All animal protocols were approved by the Institutional Animal Care and Use Committee (IACUC), Institute of Biosciences and Technology, Texas A&M Health Science Center. All animals received humane care according to the criteria outlined in the “Guide for the Care and Use of Laboratory Animals” prepared by the National Academy of Sciences and published by the National Institutes of Health (NIH publication 86-23 revised 1985). C57BL/6 wild-type and RASSF1A-/- mice were bred and genotyped as described (56). Liver tissues were frozen immediately after mice were euthanized by CO2 asphyxiation for further analyses.

Cell Culture

HeLa, human embryonic kidney (HEK)-293T and mouse embryonic fibroblast (MEF) cells were cultured in DMEM medium containing 10% FBS and antibiotics. Primary mouse hepatocytes were cultured in William’s E culture medium with 10% FBS, antibiotics, Insulin-Transferrin-Selenium (ITS-G) and dexamethasone. PBS of pH 7.4 and 0.25% trypsin were used for subculture. All cells were cultured in a tissue culture incubator at 37°C with 5% CO2.

Plasmid Construction

HA-RASSF1A in pcDNA3.1 was kindly supplied by Dr. John Minna. RFP-LC3 and GFP-LC3 were kindly supplied by Dr. Mizushima. The construction of

GFP-RASSF1A, HA-MAP1S isoforms (HA-FL, HA-HC, HA-SC and HA-LC), GFP-MAP1S full length, R653-Q855 fragment of MAP1S in HA-PCMV plasmid (HA-HBD), HA-MAP1S with R653-Q855 fragment deleted (HA-FLΔ) were described previously (53,54,105). Plasmid encoding Myc-LC3 (Addgene, #24919) and HDAC6 (Addgene, #30482) were purchased from Addgene. Four fragments of RASSF1A (F1, F2, F3 and F4) were PCR-amplified by using HA-RASSF1A as a template, digested with XhoI and BamHI, and ligated with pEGFP-C3 vector (Addgene, #6082-1) digested with XhoI and BamHI similarly as we previously described (53). The primers used for amplifying F1 (fragment from amino acid 1-151), F2 (fragment from amino acid 152-186), F3 (fragment from amino acid 187-287) and F4 (fragment from amino acid 288-340) were listed in Table 3. Sequence verification was performed by GENEWIZ. To construct the plasmid HA-RAΔ encoding RASSF1A with the RA domain (from187aa-287aa) deleted, a pair of primers listed in Table 3 were first phosphorylated with T4 polynucleotide kinase. HA-RASSF1A plasmid was then used as a template to PCR-amplify the HA-RAΔ by using the KOD hot start DNA polymerase from TOYOBO. After amplification, HA-RASSF1A template was digested by the restriction enzyme DpnI. Finally, the PCR product was ligated by T4 DNA Ligase (New England Biolabs, #M0202) to become a circular plasmid which was verified by DNA sequencing.

Table 3. Primers used for plasmid construction.

Primer	Sequence
F1 Forward	5′-CCGCTCGAGATGTCGGGGGAGCCTGAGCTCATT-3′
F1 Reverse	5′-CGCGGATCCTCAGAAGAGGTTGCTTTGATCTGGGC-3′
F2 Forward	5′-CCGCTCGAGATGAGCTTGAACAAGGACGGTTC-3′
F2 Reverse	5′-CGCGGA TCCTCACTGCAAGGAGGGTGGCTTCTT-3′
F3 Forward	5′-CCGCTCGAGGATGCCCGGCGGGGCCCA GGA-3′
F3 Reverse	5′-CGCGGATCCTCAGTCATTTTCCTTCAGGACAAA GCTC-3′
F4 Forward	5′-CCGCTCGAGTCTGGGGAGGTGAACTGGGA-3′
F4 Reverse	5′-CGCGGAT CCTCACCCAAGGGGGCAGGCGT-3′
HA-RAΔ Forward	5′-CCGCTCGAGTCTGGGGAGGTGAACTGGGA-3′
HA-RAΔ Reverse	5′-CGCGGAT CCTCACCCAAGGGGGCAGGCGT-3′

Cell Transfection

HeLa, HEK-293T and MEF cells were used for transient transfection. HeLa and MEF cells were transfected with control vectors or plasmids encoding specific genes by Lipofectamine 2000 according to the manufacturer's instruction. HEK-293T cells were transfected with control vectors or plasmids encoding specific genes by using calcium phosphate mammalian transfection kit (Clontech, #631312) according to the manufacturer's instruction. The total proteins were harvested at 24 hours after transfection.

Western Blotting

Cells or mouse tissues were lysed in lysis buffer with 1 mM PMSF and protease inhibitor cocktail on ice. The protein concentration was determined by

using BCA protein assay kit. The lysates mixed with SDS loading buffer were then boiled for 10 minutes. Lysates containing the equal amounts of protein were separated by SDS-PAGE gels and transferred onto PVDF membranes. The membranes were blocked with 5% (w/v) non-fat milk in TBST for 1 hour at room temperature and then incubated with primary antibodies overnight at 4°C. The primary antibodies and the dilutions are: anti-RASSF1A (Abcam, #ab23950), 1:1000; anti-HA (Covance, #MMS-101P), 1:1000; anti-Acetylated-α-tubulin (Santa Cruz, #23950), 1:1000; anti-HDAC6 (Santa Cruz, #11420), 1:1000; anti-Flag (Sigma, #F3165), 1:2000; anti-Myc-Tag (Cell Signaling, #2276), 1:1000; and anti-GFP (Santa Cruz, #8334), 1:1000; anti-β-Actin, (Santa Cruz, #47778), 1:2000; anti-GAPDH (Santa Cruz, #25778), 1:2000; anti-MAP1S mouse monoclonal antibody 4G1 was kindly supplied by Dr. Joe Corvera (A&G Pharmaceuticals, Inc., Columbia, MD). After being washed with the TBST buffer to remove nonspecific antibodies, the membranes were then incubated with HRP-conjugated secondary antibodies for 1 hours at room temperature. After being washed with the TBST buffer to remove the unbound antibodies, the specifically bound antibodies were detected by using ECL Prime Western Blotting Detection Reagents. The membranes were then imaged by exposing to X-ray films. Finally, the relative intensity of a band to the internal control was measured by using the ImageJ software (NIH).

Co-immunoprecipitation (IP)

To study the interaction between two proteins, the plasmids expressing specific proteins were co-transfected into HEK-293T or MEF cells. Cells were then lysed in NP-40 buffer (50 mM Tris-Hcl, pH 7.4, 150 mM NaCl, 5 mM EDTA, pH 7.4, 1% NP-40) with 1 mM PMSF and protease inhibitor cocktails at 24 hours after transfection. The supernatants were collected after centrifugation and incubated with 1.5 µg correspondent antibodies or control IgG at 4 °C for 1.5 hours. The antibodies and control IgG are: anti-RASSF1A (eBioscience, #14-6888-82); anti-LC3 (Novus Biologicals, #NB100-2331); normal mouse control IgG (Santa Cruz, #2025); normal rabbit control IgG (Santa Cruz, #2027) and anti-MAP1S mouse monoclonal antibody 4G1 was kindly supplied by Dr. Joe Corvera. After incubation, 20 µl Protein G-Sepharose beads (GE Health, #17-0618-01) were added and incubated at 4 °C for another 1.5 hours. After incubation, the beads were extensively washed with NP-40 buffer for five times. Finally, the precipitates were mixed with 100 µl lysis buffer containing SDS loading buffer, boiled in water for 10 minutes and analyzed by Western blotting.

Fluorescent Confocal Microscopy

HeLa cells were transfected with plasmids encoding specific genes, and then fixed with 4% (w/v) paraformaldehyde in PBS (prewarmed to 37 °C) for 30 minutes at 24 hours after transfection, and blocked with 1% Bovine Serum Albumin (BSA) (EMD Millipore, #2960) in PBS for 20 minutes. Cells were then

incubated with primary antibodies for 1 hour at room temperature. The primary antibodies and the dilutions are: anti-HA (Cell Signaling, #3724), 1:1000; anti-Acetylated-α-tubulin (Santa Cruze, #23950), 1:200. After extensive washing with PBS, cells were then incubated with corresponding secondary antibodies (Invitrogen, #A21202, #R-6394, dilution 1:400) for 1 hour at room temperature for fluorescence microscopy analysis. Images were captured with a Zeiss LSM 510 Meta Confocal Microscope.

Isolation of Primary Mouse Hepatocytes

Mouse primary hepatocytes were isolated from 12-week-old male wild-type mice (RASSF1A+/+) and RASSF1A knockout mice (RASSF1A-/-) by the two-steps liver perfusion method as previously described (57). Briefly, mice were anesthetized and the portal vein was catheterized after cutting open the abdomen. Then the liver was first perfused in situ with Earle's Balanced Salt Solution (EBSS) containing 0.5 mM EGTA for 8-10 min with the inferior vena cava cut and then perfused for 5 min with Hanks' Balanced Salt Solution (HBSS) supplemented with 0.3mg/ml type IV collagenase. After perfusion, the liver was extirpated, transferred into plates filled with DMEM, removed of gallbladder and gently squeezed to help hepatocytes detach. Then cell suspension was filtered through sterile 70 μm cell strainers, washed by centrifugation at 600 rpm for 2 min at RT, resuspended in Percoll/10XHBSS (9:1) mixture and centrifuged at 600 rpm for 15 min at RT. Cell

viability was examined by Trypan Blue staining. After centrifugation, pellet was washed and seeded at dish.

Statistical Analysis

Statistically significant effects were examined using Student's t-test. A P value of less than 0.05 was considered significant and significance were set to *, $p \leq 0.05$; **, $P \leq 0.01$; and ***, $P \leq 0.001$. Error bars represent standard deviation.

Results

RASSF1A Deletion Causes Reduced Levels of Acetylated Microtubules in Mouse Livers

RASSF1A associates with and stabilizes microtubules (29,52,54). It is reported that RASSF1A stabilizes microtubules by promoting the acetylation of α-tubulin (31). Stabilized acetylated microtubules are required for the trafficking and fusion of autophagosomes with lysosomes (102). To understand the molecular mechanism by which RASSF1A regulates autophagy activity, we first examined the impact of RASSF1A on the acetylation of microtubules in mouse livers. We found that RASSF1A deletion caused a reduction in levels of acetylated α-tubulin in mouse liver tissues (Figure 11A, B). The result was then confirmed in isolated primary hepatocytes from wild-type and RASSF1A-/- mice (Figure 11C, D). Therefore, RASSF1A deletion suppresses microtubular acetylation in mouse liver tissues.

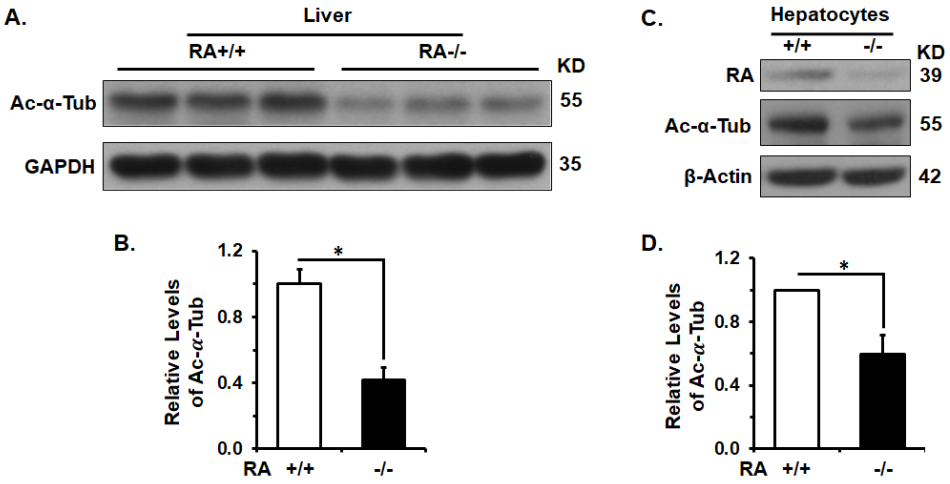

Figure 11. RASSF1A deletion causes reduced levels of acetylated α-tubulin in mouse livers. (**A**, **B**) Immunoblot analysis (**A**) and quantification (**B**) of levels of acetylated α-tubulin in liver tissues from 4-month-old wild-type and RASSF1A$^{-/-}$ mice. (**C**, **D**) Immunoblot analysis (**C**) and quantification (**D**) of levels of acetylated α-tubulin in primary hepatocytes isolated from wild-type and RASSF1A$^{-/-}$ mice. *, P ≤ 0.05.

RASSF1A Associates with Acetylated Microtubules

Then we examined the subcellular distribution of RASSF1A and acetylated microtubules. Consistent with previous report, overexpressed RASSF1A did greatly enhance the acetylation of α-tubulin (Figure 12A, B) (31). In addition, as shown in the fluorescent images, RASSF1A colocalized with acetylated α-tubulin (Figure 12C, D). Therefore, RASSF1A not only enhances acetylation of microtubules but also associates with acetylated microtubules.

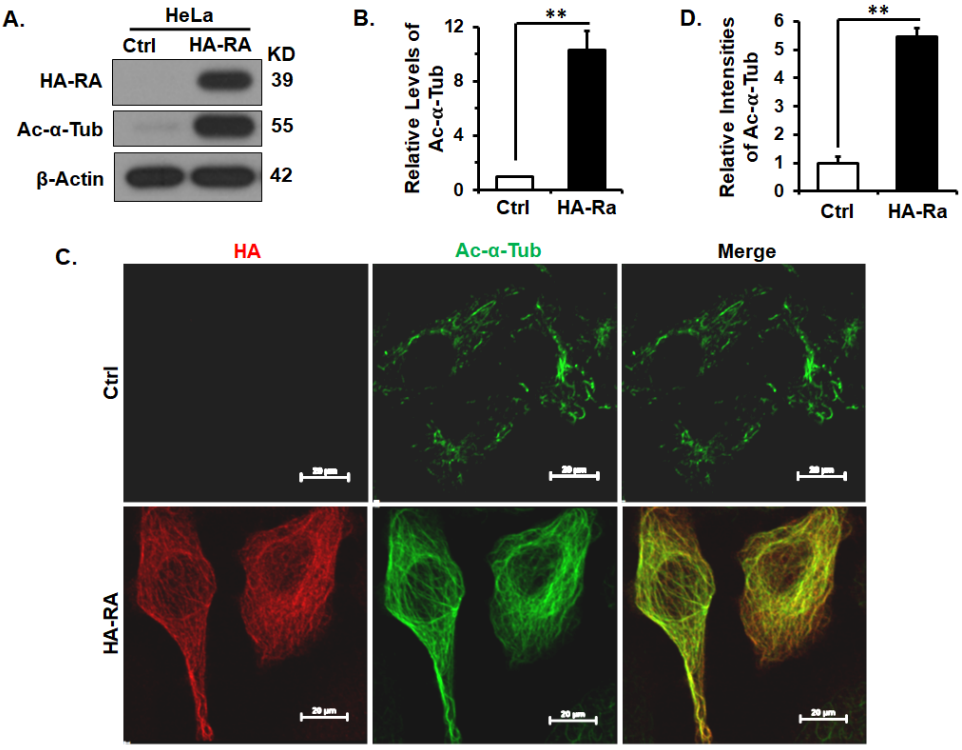

Figure 12. RASSF1A enhances the acetylation of α-tubulin and associates with acetylated α-tubulin. (**A**, **B**) Immunoblot analysis (**A**) and quantification (**B**) of levels of acetylated α-tubulin in HeLa cells transiently transfected with control plasmid (Ctrl) or plasmid expressing HA-RASSF1A (HA-RA). (**C**) Representative fluorescent images showing the colocalization (yellow) of RASSF1A (red) with acetylated microtubules (green) in cells similar to those in (**A**). Scale bar, 20μM. (**D**) Quantification of the immunostaining intensities of acetylated α-tubulin as shown in (**C**). **, $P \leq 0.01$.

RASSF1A Interacts with Histone Deacetylase 6 (HDAC6)

Histone deacetylase 6 (HDAC6), a member of the histone deacetylase family, is localized primarily in the cytoplasm and associates with microtubules to

function as the tubulin deacetylase (106). RASSF1A is reported to impair HDAC6 deacetylase activity on α-tubulin, but the underneath mechanism is unknown (31). We showed here that RASSF1A did have no effect on protein levels of HDAC6 as reported (Figure 13A) (31). However, we found that RASSF1A-specific antibody could pull down the exogenous or endogenous RASSF1A together with overexpressed HDAC6 (Figure 13B, C). The RASSF1A-HDAC6 interaction may result in an impairment of HDAC6 deacetylase activity on α-tubulin. Therefore, RASSF1A interacts with HDAC6 to inhibit its deacetylase activity to enhance microtubular acetylation.

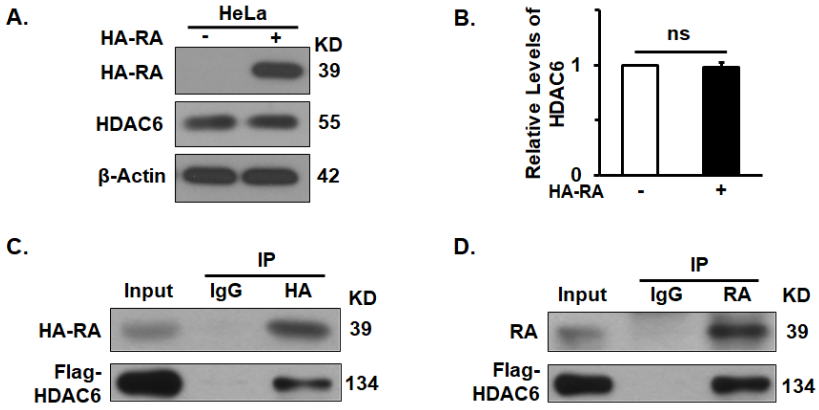

Figure 13. RASSF1A interacts with HDAC6. (**A**, **B**) Immunoblot analysis (**A**) and quantification (**B**) of HDAC6 levels in cells transiently transfected with control plasmid (Ctrl) or plasmid expressing HA-RASSF1A (HA-RA). (**C**, **D**) RASSF1A interacts with HDAC6. Lysates from 293T cells transiently overexpressing HA-RASSF1A and Flag-HDAC6 were precipitated with a HA-specific antibody or IgG control antibody (**C**). Lysates from HeLa cells transiently overexpressing Flag-HDAC6 were precipitated with RASSF1A-specific antibody or IgG control antibody (**D**).

RASSF1A Interacts with LC3-II

Autophagosome-associated LC3-II serves as a linker to bridge cargo-containing autophagosomes with microtubules for trafficking. Mass spectrometry analysis showed that RASSF1 associates with LC3 (107), which triggers us to hypothesize that RASSF1A interacts with LC3-II and helps recruit LC3-II-associated autophagosomes onto acetylated microtubules to promote autophagy maturation. Expectedly, as shown by the immunoprecipitation analysis, RASSF1A-specific antibody co-precipitated the overexpressed RASSF1A with the overexpressed Myc-LC3-II in HEK-293T cells (Figure 14B). Further studies showed that the RA domain in RASSF1A mediated its interaction with LC3-II (Figure 14A, C). Therefore, RASSF1A interacts with LC3-II, which further indicates that RASSF1A may recruit autophagosomes onto acetylated microtubules to promote autophagy maturation.

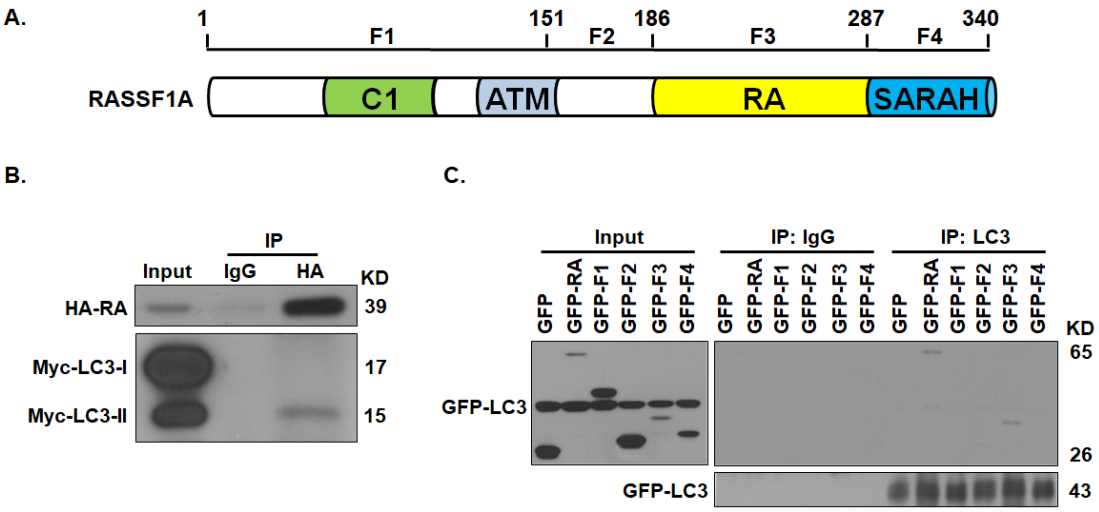

Figure 14. RASSF1A interacts with LC3-II. (**A**) A diagram showing the domain structure of RASSF1A protein and its mutant constructs. RASSF1A contains four characterized domains: C1, phorbol ester/diacylglycerol binding domain; ATM, ataxia-telangiectasia mutated domain; RA*, Ras-association (RalGDS/AF-6) domain; SARAH, Mst and Sav1 binding domain. Four fragments of RASSF1A (F1, F2, F3 and F4) were fused with GFP, respectively. (**B**) Immunoblot analysis showing the interaction between RASSF1A and LC3-II in MEFs transiently expressing HA-RASSF1A and Myc-LC3. Cell lysates were precipitated with a HA-specific antibody or IgG control antibody. (**C**) LC3-II interacts with RA domain in RASSF1A. Lysates from 293T cells transiently expressing GFP-LC3 and GFP fused RASSF1A constructs were precipitated with LC3-specific antibody or IgG control antibody.

RASSF1A Interacts with Microtubule-associated Protein 1s (MAP1S)

Autophagy activator MAP1S interacts with autophagosome-associated LC3 and bridges autophagosomes with microtubules for trafficking (47). We reported that RASSF1A stabilizes microtubules and recruits MAP1S onto the stabilized microtubules, and RASSF1A recruits LC3 on RASSF1A-stabilized microtubules only in cells transiently expressing MAP1S-SC (47,54). The previous studies triggered us to hypothesize that RASSF1A recruits LC3-II-associated autophagosomes onto RASSF1A-stabilized acetylated microtubules through MAP1S. To test this hypothesis, we first examined whether RASSF1A interacts with MAP1S by performing immunoprecipitation analysis. Results showed that RASSF1A interacted with full length (FL), heavy chain (HC) and short chain (SC) but not light chain (LC) of MAP1S (Figure 15B, C, D and E), suggesting that the overlapping region between HC and SC (from R653 to Q855) in MAP1S is the potential binding domain for RASSF1A. This region has been identified as the HDAC4-binding domain (HBD) (105). Expectedly, RASSF1A pulled down the HA-fused R653 to Q855 fragment of MAP1S (HA-HBD), and in turn HA-HBD also pulled down RASSF1A (Figure 15F, G). Deletion of HBD domain from MAP1S (HA-FLΔ) abolished the interaction between MAP1S and RASSF1A (Figure 15H). Therefore, RASSF1A interacts with MAP1S.

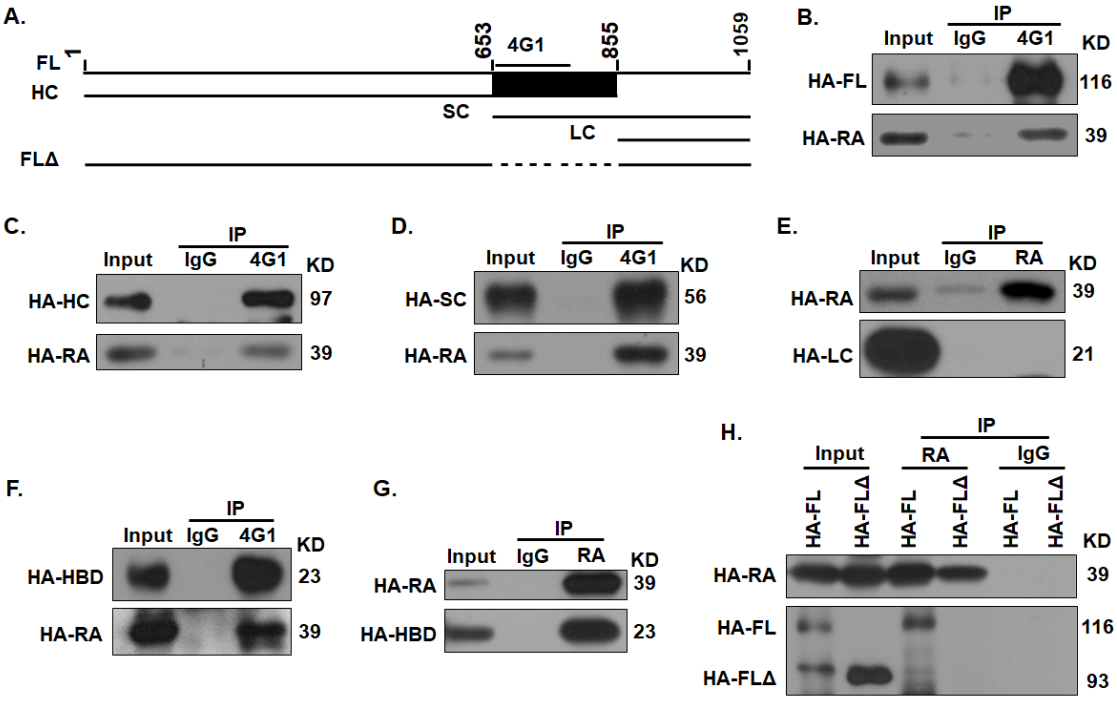

Figure 15. RASSF1A interacts with MAP1S via the overlapping domain between heavy chain (HC) and short chain (SC) of MAP1S. (**A**) A diagram showing the domain structure of MAP1S protein. FL (full length), HC (heavy chain), SC (short chain), LC (light chain). 4G1, region recognized by MAP1S monoclonal antibody 4G1; HBD, HDAC4-binding domain (the overlapping domain (R653-Q855) between HC and SC). (**B-E**) RASSF1A interacts with MAP1S isoforms FL (**B**), HC (**C**) and SC (**D**) but not LC (**E**). Lysates from 293T cells transiently expressing HA-RASSF1A and HA-fused MAP1S isoforms were precipitated with MAP1S-specific 4G1 antibody, or RASSF1A-specific antibody, or IgG control. (**F**, **G**) RASSF1A interacts with the HBD domain of MAP1S. Lysates from 293T cells transiently expressing HA-RASSF1A and HA-fused HBD domain of MAP1S (HA-HBD) were precipitated with RASSF1A-specific antibody, or MAP1S-specific 4G1 antibody, or IgG control. (**H**) MAP1S-FL with the HBD domain deleted (FLΔ) does not interact with RASSF1A. Lysates from 293T cells transiently expressing HA-RASSF1A and HA-fused MAP1S FL (HA-FL) or HA-fused FLΔ (HA- FLΔ) were precipitated with RASSF1A-specific antibody or IgG control.

RASSF1A Interacts with MAP1S via The RA Domain

Next, we examined which domain in RASSF1A mediates its interaction with MAP1S. Immunoprecipitation analysis showed that MAP1S-specific antibody co-precipitated the endogenous MAP1S with the overexpressed RA domain of RASSF1A (Figure 16A). Deletion of RA domain from RASSF1A resulted in the abolishment of its interaction with MAP1S (Figure 16B). Therefore, RA domain in RASSF1A mediates its interaction with MAP1S.

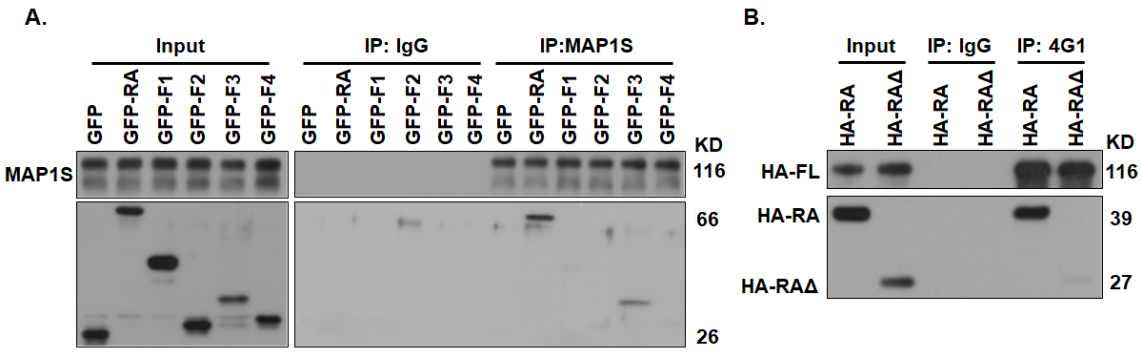

Figure 16. RASSF1A interacts with MAP1S via the RA domain. (**A**) MAP1S interacts with the RA domain in RASSF1A. Lysates from 293T cells transiently expressing GFP, or GFP fused RASSF1A fragments were precipitated with MAP1S-specific 4G1 antibody or IgG control. (**B**) RASSF1A with RA domain deleted (RAΔ) does not interact with MAP1S. Lysates from 293T cells transiently expressing HA-FL and HA-RASSF1A or HA-fused RAΔ (HA-RAΔ) were precipitated with MAP1S-specific 4G1 antibody or IgG control.

The Interaction between RASSF1A and LC3-II Requires MAP1S

To further test our hypothesis that RASSF1A recruits LC3-II-associated autophagosomes onto RASSF1A-stabilized acetylated microtubules through MAP1S, we then examined whether the interaction of RASSF1A with LC3-II requires MAP1S. The immunoprecipitation analysis showed that in wild-type MEFs cells, but not in MAP1S knockout MEFs cells, RASSF1A-specific antibody co-precipitated the overexpressed RASSF1A with the overexpressed Myc-LC3-II and endogenous MAP1S (Figure 17A), indicating that RASSF1A interacts with LC3-II in a MAP1S-dependent manner. To confirm it, HA-RASSF1A, Myc-LC3 and HA-FL were transiently co-transfected into HEK-293T cells and the immunoprecipitation analysis were performed. We found that RASSF1A pulled down more LC3-II in cells transiently expressing HA-FL, but not HA-FLΔ which has no interaction with RASSF1A (Figure 17A). Therefore, RASSF1A, MAP1S and LC3-II form a complex, and the association between RASSF1A and LC3-II requires MAP1S.

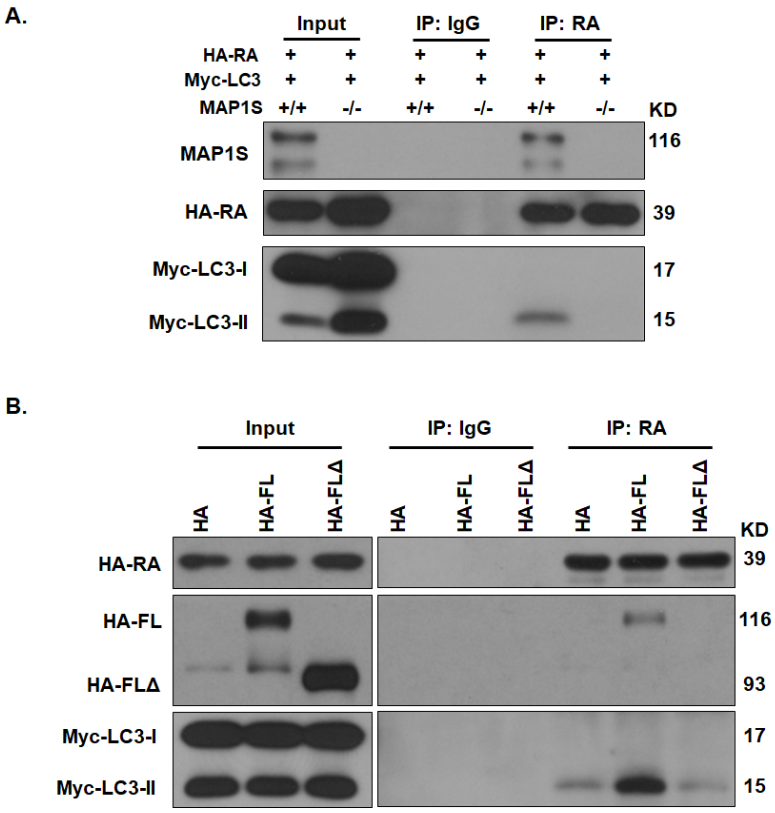

Figure 17. The interaction of RASSF1A with LC3-II requires MAP1S. (**A**) The interaction between RASSF1A and LC3-II requires MAP1S. Lysates from wild-type and MAP1S-deleted MEFs transiently expressing HA-RASSF1A and Myc-LC3 were precipitated with RASSF1A-specific antibody or IgG control. (**B**) MAP1S, but not HBD domain deleted MAP1S, promotes the association between RASSF1A and LC3-II. Lysates from 293T cells transiently expressing HA-RASSF1A, Myc-LC3 and HA, or HA-FL, or HA- FLΔ were precipitated with RASSF1A-specific antibody or IgG control.

RASSF1A Recruits Autophagosomes onto Acetylated Microtubules through MAP1S

To examine whether RASSF1A recruits LC3-II-associated autophagosomes onto acetylated microtubules through MAP1S, we then performed the immunofluorescent staining analysis. The images showed that without RASSF1A, overexpressed MAP1S was detected diffusely in the cytoplasm. However, overexpressed RASSF1A not only enhanced the acetylation of microtubules, but also recruited MAP1S onto acetylated microtubules (Figure 18A). Further analysis showed that overexpressed RASSF1A recruited MAP1S and then LC3 onto acetylated microtubules (Figure 18B). Taken together, RASSF1A enhances microtubular acetylation and then recruits LC3-II-associated autophagosomes onto acetylated microtubules through LC3-II-interactive MAP1S to promote autophagy maturation (Figure 18C).

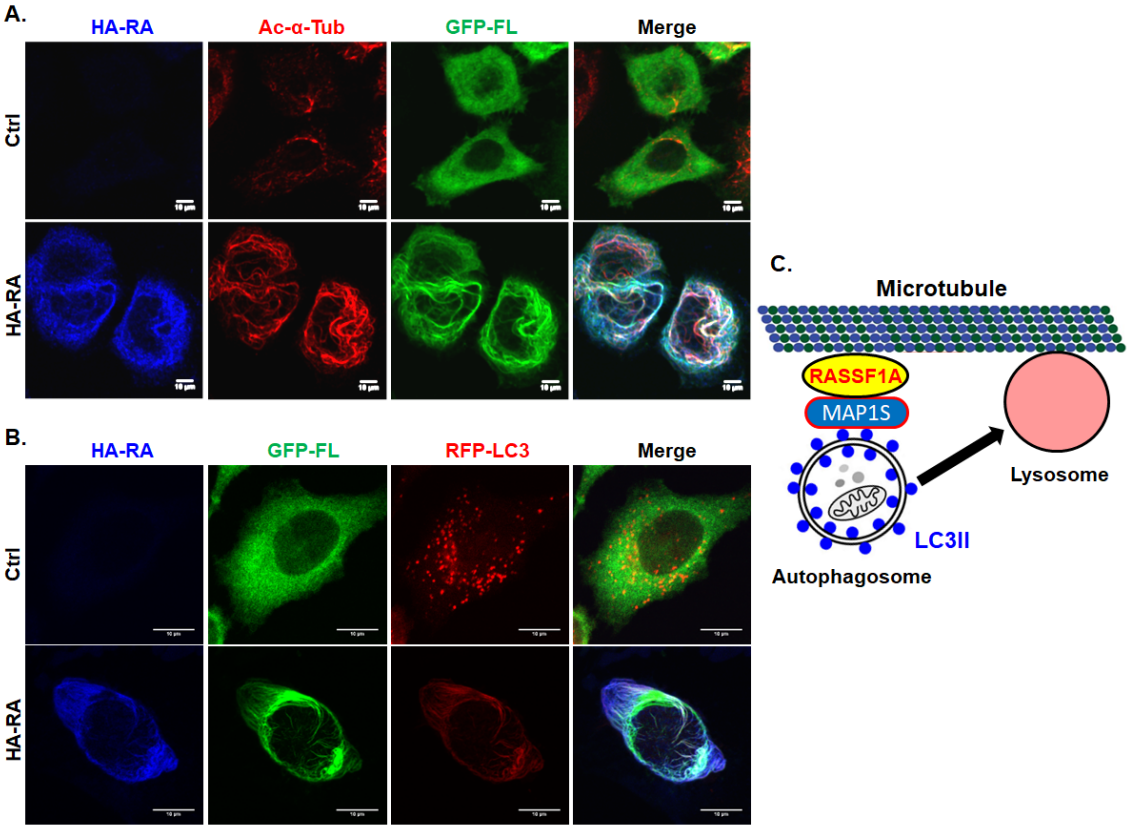

Figure 18. RASSF1A recruits autophagosomes onto RASSF1A-stabilized acetylated microtubules through MAP1S. (**A**) Representative fluorescent images show that RASSF1A recruits MAP1S onto RASSF1A-stabilized acetylated microtubules. Scale bar, 10 μM. (**B**) Representative fluorescent images show that RASSF1A greatly promotes the co-localization of MAP1S and LC3 on acetylated microtubules. Scale bar, 10 μM. (**C**) A diagram showing the mechanism by which RASSF1A promotes autophagy maturation. RASSF1A enhances microtubular acetylation and associates with acetylated microtubules. Meanwhile, RASSF1A interacts with MAP1S and thereby recruits LC3-II-associated autophagosomes onto acetylated microtubules to promote autophagy maturation.

Discussion

In previous chapters, we show that RASSF1A deletion leads to autophagy defects in mouse livers which promote hepatocarcinogenesis induced by chemical carcinogen DEN. However, the underlying mechanism by which RASSF1A regulates autophagy is unknown. In this chapter, we found that RASSF1A promotes autophagy maturation by recruiting LC3-II-associated autophagosomes onto RASSF1A-stabilized acetylated microtubules through MAP1S.

In 2000, LC3 was identified as the first mammalian protein that is specifically localized in autophagosomal membranes (12). The autophagosomal-anchored LC3 (LC3-II) functions in autophagosomal trafficking by linking autophagosomes to microtubules. MAP1S, a microtubule-associated autophagy activator, promotes autophagosomal trafficking on microtubules by directly interacting with LC3 (47). Because RASSF1A interacts with MAP1S, we expected that RASSF1A would regulate autophagy maturation through MAP1S. As expected, RASSF1A interacts autophagosome-associated LC3-II in a MAP1S-dependent manner and RASSF1A recruits MAP1S and LC3-II onto RASSF1A-stabilized acetylated microtubules, indicating that RASSF1A promotes MAP1S-mediated autophagosomal trafficking.

Microtubules, filamentous intracellular structures, are formed by the polymerization of α-tubulin and β-tubulin heterodimers. The constant polymerization and depolymerization of microtubules are regulated by microtubule-associated proteins (108,109). Microtubule dynamics play an

essential role in the movement of intracellular vesicles, organelles and macromolecular assemblies (110). In the past decade, studies have demonstrated that microtubules are also implicated in several steps of the dynamic autophagy process, including autophagosomal initiation, maturation and fusion with lysosomes (102-104). Regular non-acetylated microtubules are involved in, but not essential for autophagosomal formation, as evidenced by the still existence but a significantly decreased ratio of autophagosomal biogenesis or the LC3-I to LC3-II conversion in the absence of the intact regular microtubules. Regular non-acetylated microtubules are not involved in the process of fusion of autophagosomes with lysosomes, because there is no accumulation of LC3-II with their interruption (103,104). Acetylated microtubules are required for trafficking and fusion of mature autophagosomes with lysosomes which also move along microtubules to distribute throughout the cytoplasm (102,111,112). Disruption of both non-acetylated and acetylated microtubules impairs the conversion of LC3-I to LC3-II and the autophagosomal degradation (102). RASSF1A enhances microtubular acetylation and recruits autophagosomes onto the acetylated microtubules where autophagosomes are delivered to fuse with lysosomes and the captured substrates as well as LC3-II are degraded. Therefore, without RASSF1A, cargo-containing autophagosomes are not recruited onto microtubules for trafficking and fusion with lysosomes, which causes the accumulation of protein aggregates and dysfunctional organelles such as mitochondria to enhance oxidative stresses and genome instability. In addition to

serve as tracks for autophagosomal trafficking, microtubules also play an essential role in regulating the progress of cell cycle and cellular migration. High level of RASSF1A maintains microtubules in stabilized state so that during mitosis, RASSF1A localizes to centrosomes, spindle microtubules and spindle poles to arrest mitosis and promote cell death (113). The ability to stabilize microtubules also allows RASSF1A to suppress cellular migration (31). Therefore, level of RASSF1A in cells plays an essential role in mediating the decision to promote autophagy or cell death.

Although RASSF1A enhances acetylation of α-tubulin, the underlying mechanism is unclear. The acetylation of α-tubulin at K40 is a hallmark of stable microtubules. α-tubulin acetyl-transferase (α-TAT) is known to transfer an acetyl group from acetyl-CoA to K40 of α-tubulin and histone deacetylase (HDAC6) functions as the α-tubulin deacetylase (106,114). Although RASSF1A has no impact on protein levels of HDAC6, we show here that RASSF1A interacts with HDAC6. We predict that RASSF1A may bind to HDAC6 enzymatic domain and block its deacetylase activity, or RASSF1A may compete with HDAC6 in binding to microtubules, which needs to be further investigated. In addition, examining whether RASSF1A acts on α-TAT may also help to uncover the underlying mechanism.

CHAPTER V

RASSF1A PROMOTES AUTOPHAGY INITIATION BY SUPPRESSING PI3K-AKT-MTOR PATHWAY THROUGH HIPPO PATHWAY REGULATORY PROTEIN MST1

Introduction

Autophagy, a lysosome-mediated degradation pathway, can be rapidly enhanced during starvation to sustain cell metabolism by supplying necessary nutrients. Autophagy can also be activated during stresses to protect cells through eliminating damaged organelles and proteins that accumulate in the cytoplasm. It is well established that mTOR is a major negative regulator of autophagy initiation (115,116). In the presence of growth factors, mTOR, a serine/threonine kinase, can be activated by the receptor tyrosine kinase (RTK)-class I PI3K-Akt signaling pathway. Specifically, the activated Akt first directly phosphorylates the tuberous sclerosis (TSC) tumor suppressor complex (TSC1/TSC2) which is the most important upstream negative regulator of mTOR (117,118). The phosphorylated TSC1/2 then rapidly dissociate from lysosomal surface (119). TSC1/2 is a GTPase-activating protein (GAP) for the Ras homolog enriched in brain (Rheb) GTPase (120). Therefore, the Rheb localized on lysosome is subsequently turned on. GTP-bound Rheb, an essential mTOR activator, then activates mTOR (121). The activated mTOR phosphorylates the downstream effector autophagy-initiating kinase Ulk1 (a homologue of yeast ATG1) to suppress autophagy

initiation. The relationship between mTOR and ATG1 complex has been well studied in yeast. mTOR can directly phosphorylate ATG13, a critical component of the ATG1 complex, and thereby prevent ATG13 from forming the complex with ATG1 (122-124). It is reported that, in mammalian cells, the activated mTOR can inhibit Ulk1 activation by phosphorylating Ulk1 at Ser 757 (125).

Microtubule-associated protein 1 small form (MAP1S), a homologue of neuron-specific MAP1A/B, is demonstrated to regulate autophagy initiation through Bcl-2/xL enhanced p27-mediated non-canonical autophagy pathway (47). In addition to anti-apoptotic roles, B-cell lymphoma 2 (Bcl-2) and B-cell lymphoma-extra large (Bcl-xL) exhibit the opposite roles in autophagy initiation. Under normal conditions, Bcl-2/Xl can bind to Beclin1 and prevent Beclin1 (a homologue of yeast ATG6) from interacting with class III PI3K to form class III PI3K complex which is responsible for the phagophore nucleation. Thus, the Beclin-1 dependent autophagy initiation is inhibited. Bcl-2/xL can also activate autophagy initiation by increasing the levels of cyclin-dependent kinase inhibitor 1B (p27) which elevates ATG5 levels to activate autophagy through a Beclin1-independent autophagy pathway (48,126,127). Our previous studies showed that MAP1S deletion in mice causes a reduced autophagy flux along with the decreased levels of Bcl-2/xL and p27, but no alteration in Akt-mTOR activity, suggesting that MAP1S sustains Bcl-2/xL and p27 levels to enhance autophagy initiation (47).

In chapter I, we show that RASSF1A depletion results in a significant reduction in levels of LC3-II in the presence of lysosomal inhibitor, indicating a

reduction in autophagy initiation due to RASSF1A depletion. However, the underlying mechanism by which RASSF1A regulates autophagy initiation has not been elucidated. The direct interaction of RASSF1A with autophagy activator MAP1S triggered us to reason that RASSF1A may regulate autophagy initiation through MAP1S. However, here we show that RASSF1A does not regulate autophagy initiation in the same way as MAP1S does. RASSF1A interacts with Hippo pathway regulator Mst1 and stabilizes Mst1 to suppress PI3K-Akt-mTOR pathway to promote autophagy initiation.

Materials and Methods

Animals

All animal protocols were approved by the Institutional Animal Care and Use Committee (IACUC), Institute of Biosciences and Technology, Texas A&M Health Science Center. All animals received humane care according to the criteria outlined in the “Guide for the Care and Use of Laboratory Animals” prepared by the National Academy of Sciences and published by the National Institutes of Health (NIH publication 86-23 revised 1985). C57BL/6 wild-type and RASSF1A-/- mice were bred and genotyped as described (56). Liver tissues were frozen immediately after mice were euthanized by CO2 asphyxiation for further analyses.

Cell Culture

HeLa and MEFs cells were cultured in DMEM medium containing 10% FBS and antibiotics. PBS of pH 7.4 and 0.25% trypsin were used for subculture. All cells were cultured in a tissue culture incubator at 37°C with 5% CO2.

siRNA and Cell Transfection

HeLa cells were transfected with random or RASSF1A-specific siRNA molecules by using Oligofectamine according to the manufacturer’s recommended instruction. The total proteins were harvested at 48 hours after transfection. HeLa cells were transfected with control vector or plasmid encoding p27 gene (Addgene, #14049) by Lipofectamine 2000 according to the

manufacturer's instruction. The total proteins were harvested at 24 hours after transfection.

Western Blotting

Cells or mouse tissues were lysed in lysis buffer with 1 mM PMSF and protease inhibitor cocktail on ice. The protein concentration was determined by using BCA protein assay kit. The lysates mixed with SDS loading buffer were then boiled for 10 minutes. Lysates containing the equal amounts of protein were separated by SDS-PAGE gels and transferred onto PVDF membranes. The membranes were blocked with 5% (w/v) non-fat milk in TBST for 1 hour at room temperature and then incubated with primary antibodies overnight at 4°C. The primary antibodies and the dilutions are: anti-RASSF1A (Abcam, #ab23950), 1:1000; anti-HDAC4 (Cell Signaling, #7628S), 1:1000; anti-Bcl-2 (Santa Cruz, #7382), 1:1000; anti-p27 (Santa Cruz, #528), 1:1000; anti-Acetyl-lysine (EMD Millipore, #05515), 1:1000; anti-Flag (Sigma, #F3165), 1:1000; anti-p-Akt (Cell Signaling, #2965S), 1:1000; anti-Akt (Santa Cruz,, #5298), 1:1000; anti-p-MST1 (Cell Signaling, #3681S), 1:1000; anti-MST1 (Proteintech, #22245-1-AP), 1:1000; anti-p-S6K (Cell Signaling, #9205S), 1:1000; anti-LC3 (Novus Biologicals, #NB100-2331), 1:1000; anti-Yap (Cell Signaling, #4912S), 1:1000; anti-p-Yap (Cell Signaling, #4911S), 1:1000; anti-CTGF (Abcam, #ab6992), 1:1000; anti-GAPDH (Santa Cruz, #25778), 1:1000; anti-β-Actin (Santa Cruz, #47778), 1:2000; anti-MAP1S mouse monoclonal antibody 4G1 was kindly supplied by Dr.

Joe Corvera (A&G Pharmaceuticals, Inc., Columbia, MD). After being washed with the TBST buffer to remove nonspecific antibodies, the membranes were then incubated with HRP-conjugated secondary antibodies for 1 hours at room temperature. After being washed with the TBST buffer to remove the unbound antibodies, the specifically bound antibodies were detected by using ECL Prime Western Blotting Detection Reagents. The membranes were then imaged by exposing to X-ray films. Finally, the relative intensity of a band to the internal control was measured by using the ImageJ software (NIH).

Co-immunoprecipitation (IP)

To study the interaction between two proteins or the acetylation levels of one protein, cells or liver tissues were first lysed in NP-40 buffer with 1 mM PMSF and protease inhibitor cocktails. The supernatants were collected after centrifugation and incubated with 1.5 μg correspondent antibodies or control IgG at 4 °C for 1.5 hours. The antibodies and control IgG are: anti-Acetyl-lysine (EMD Millipore, #05515); anti-RASSF1A (eBioscience, #14-6888-82); anti-Akt (Santa Cruz, #5298); normal mouse control IgG (Santa Cruz, #2025); and anti-MAP1S mouse monoclonal antibody 4G1 was kindly supplied by Dr. Joe Corvera. After incubation, 20 μl protein G-Sepharose beads (GE Health, #17-0618-01) were added and incubated at 4 °C for another 1.5 hours. After incubation, the beads were extensively washed with NP-40 buffer for five times. Finally, the precipitates

were mixed with 100 µl lysis buffer containing SDS loading buffer, boiled in water for 10 minutes and analyzed by Western blotting.

Establishment of Mouse Embryonic Fibroblasts (MEFs)

Mouse embryonic fibroblasts were prepared from wild-type (RASSF1A+/+) and RASSF1A knockout mice (RASSF1A-/-) as described (47). Briefly, embryos collected at E12.5-14.5 were minced in DMEM medium, incubated with 0.25% trypsin at 37 °C for 10 min and then filtered through 70 µm cell strainer. The separated cells were then harvested and cultured in DMEM containing 10% FBS and antibiotics.

Statistical Analysis

Statistically significant effects were examined using Student's t-test. A P value of less than 0.05 was considered significant and significance were set to *, $p \leq 0.05$; **, $P \leq 0.01$; and ***, $P \leq 0.001$. Error bars represent standard deviation.

Results

RASSF1A Does Not Regulate Autophagy Initiation through MAP1S in HeLa Cells

Reduced LC3-II levels in RASSF1A-suppressed HeLa cells, RASSF1A-deleted MEFs, mouse hepatocytes and mouse liver tissues (Figure 3, 4, 5) indicate that RASSF1A depletion causes a reduction in autophagy initiation. The interaction between RASSF1A and autophagy activator MAP1S triggered us to examine whether RASSF1A directly regulates MAP1S to affect MAP1S-mediated autophagy initiation. Our lab previously reported that MAP1S sustains levels of Bcl-2/xL which increase p27 levels to enhance p27-mediated autophagy initiation (47,48). Acetylated MAP1S plays an essential role in promoting autophagy. Mammalian histone deacetylase 4 (HDAC4) has been demonstrated to deacetylate and destabilize MAP1S to suppress MAP1S-mediated autophagy (105). Here we found that although levels of HDAC4, Bcl-2 and p27 reduced in RASSFA-suppressed HeLa cells, levels of MAP1S remained constant (Figure 19A, B and C). Moreover, levels of acetylated MAP1S were not altered in HeLa cells transiently expressing RASSF1A without or with HDAC4 inhibitor apicidin treatment (Figure 19D and E). Forced expression of p27 in RASSF1A-suppressed HeLa cells did not restore the reduced autophagy flux (Figure 19F, G). Taken together, knockdown of RASSF1A in HeLa cells results in reduced autophagy initiation not through MAP1S-Bcl-2-p27 non-canonical pathway.

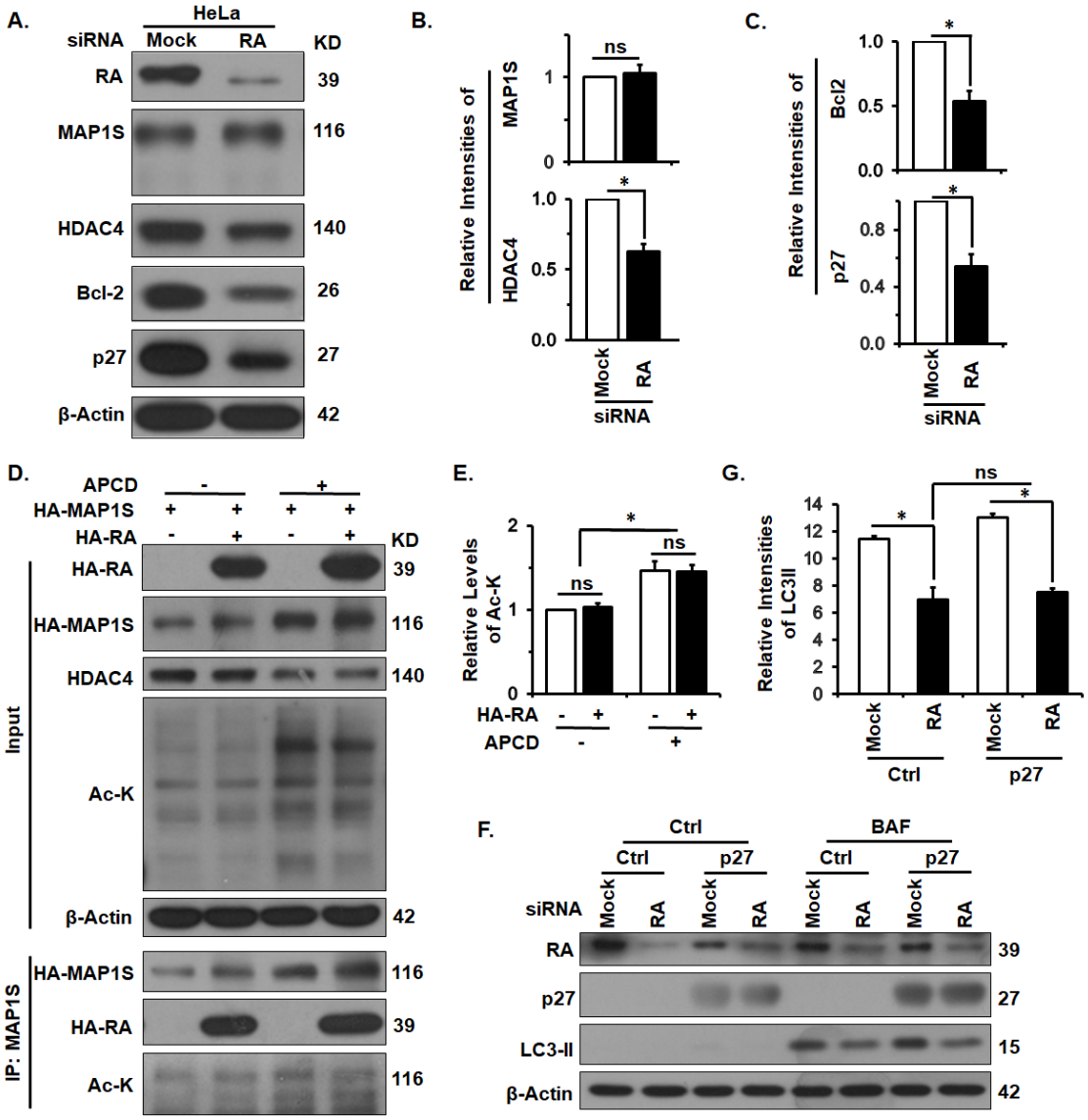

Figure 19. RASSF1A has no impact on MAP1S-mediated autophagy initiation pathway in HeLa cells. (A-C) Immunoblot analysis (**A**) and quantification (**B**, **C**) of levels of MAP1S, HDAC4, Bcl-2 and p27 in wild-type and RASSF1A-suppressed HeLa cells. (**D**) Overexpressed RASSF1A has no impact on levels of acetylated MAP1S. Lysates from 293T cells transiently expressing HA-MAP1S and HA or HA-RASSF1A were precipitated with MAP1S-specific antibody and blotted with Ac-K antibody. APCD, Histone deacetylase inhibitor. (**E**) Quantification of levels of acetylated MAP1S as shown in (**D**). (**F**, **G**) Immunoblot analysis (**F**) and quantification (**J**) of LC3-II levels in wild-type and RASSF1A-suppressed HeLa cells transiently transfected with control vector or vector encoding p27 in the absence or presence of BAF. *, $P \leq 0.05$; ns, nonsignificant, $P > 0.05$.

RASSF1A Does Not Regulate Autophagy Initiation through MAP1S in Mouse Livers

Next, we examined whether RASSF1A deletion alters MAP1S-mediated autophagy initiation pathway in mouse livers. The immunoblot results showed that RASSF1A deletion had no impact on protein levels of MAP1S, HDAC4, Bcl-2 and p27 in mouse livers (Figure 20A, B and C). Moreover, RASSF1A deletion also did not alter levels of acetylated MAP1S in liver tissues from wild-type and RASSF1A-/- mice (Figure 20D, E). Taken together, RASSF1A deletion results in reduced autophagy initiation in mouse livers not through MAP1S-Bcl-2-p27 non-canonical pathway.

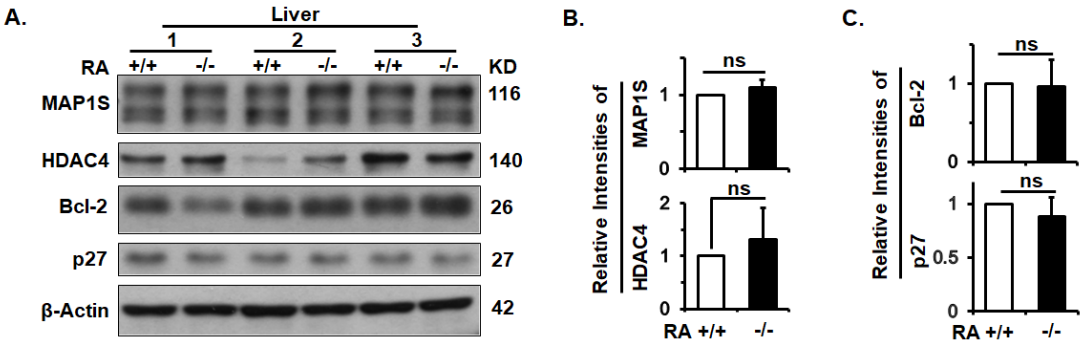

Figure 20. RASSF1A has no impact on MAP1S-mediated autophagy initiation pathway in mouse livers. (**A**-**C**) Immunoblot analysis (**A**) and quantification (**B**, **C**) of levels of MAP1S, HDAC4, Bcl-2 and p27 in liver tissues from wild-type and RASSF1A$^{-/-}$ mice. (**D**) RASSF1A deletion causes no change of levels of acetylated MAP1S. Liver tissue lysates from wild-type and RASSF1A$^{-/-}$ mice were precipitated with Ac-K-specific antibody. (**E**) Quantification of levels of acetylated MAP1S as shown in (**D**). ns, nonsignificant, $P > 0.05$.

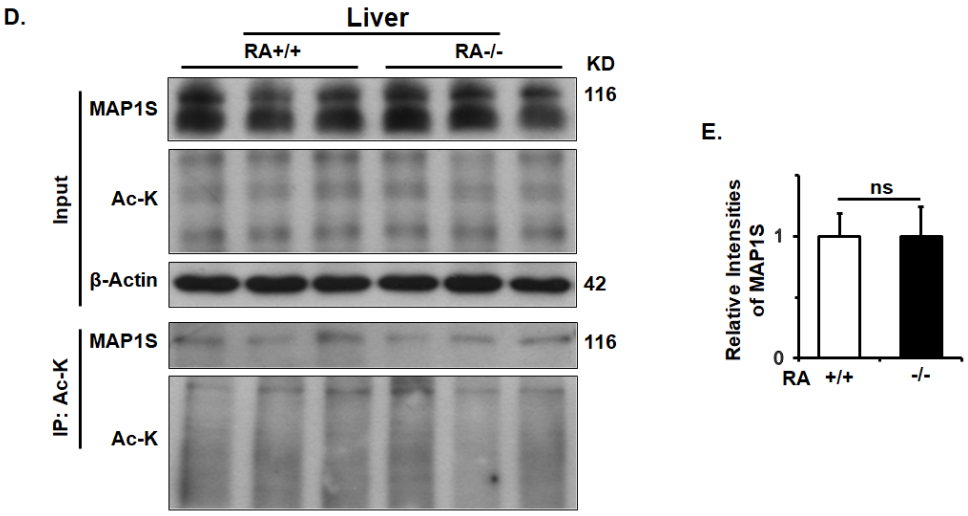

Figure 20. Continued.

RASSF1A Suppresses PI3K-Akt-mTOR Pathway to Promote Autophagy Initiation in HeLa Cells

PI3K-Akt-mTOR pathway is a well-known pathway that acts as a major negative regulator of autophagy initiation (116,124). We found that knockdown of RASSF1A in HeLa cells caused increases in levels of phosphorylated Akt and phosphorylated S6K, a downstream effector of mTOR (Figure 21A, B, C). Therefore, RASSF1A suppresses PI3K-Akt-mTOR pathway in HeLa cells to promote autophagy initiation.

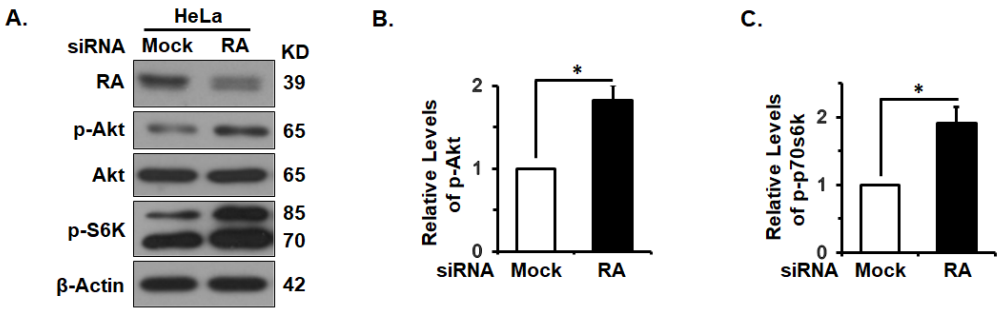

Figure 21. RASSF1A suppression causes the activation of PI3K-Akt-mTOR pathway in HeLa cells. (**A**-**C**) Immunoblot analysis (**A**) and quantification (**B, C**) of levels of p-Akt and p-S6K in HeLa cells treated with random (Mock) or RASSF1A-specific siRNAs (RA).

RASSF1A Suppresses PI3K-Akt-mTOR Pathway to Promote Autophagy Initiation in Mouse Livers

Next, we examined whether RASSF1A deletion in mice also causes the activation of PI3K-Akt-mTOR pathway. Immunoblot results showed that RASSF1A deletion also caused increases in levels of phosphorylated Akt and phosphorylated S6K in MEFs and mouse liver tissues (Figure 22A, B, C, D, E, F). PI3K-Akt-mTOR pathway was also activated in DEN-treated 6-month-old liver tissues from RASSF1A-/- mice (Figure 22G, H, I). Therefore, RASSF1A suppresses PI3K-Akt-mTOR pathway in mouse livers to promote autophagy initiation.

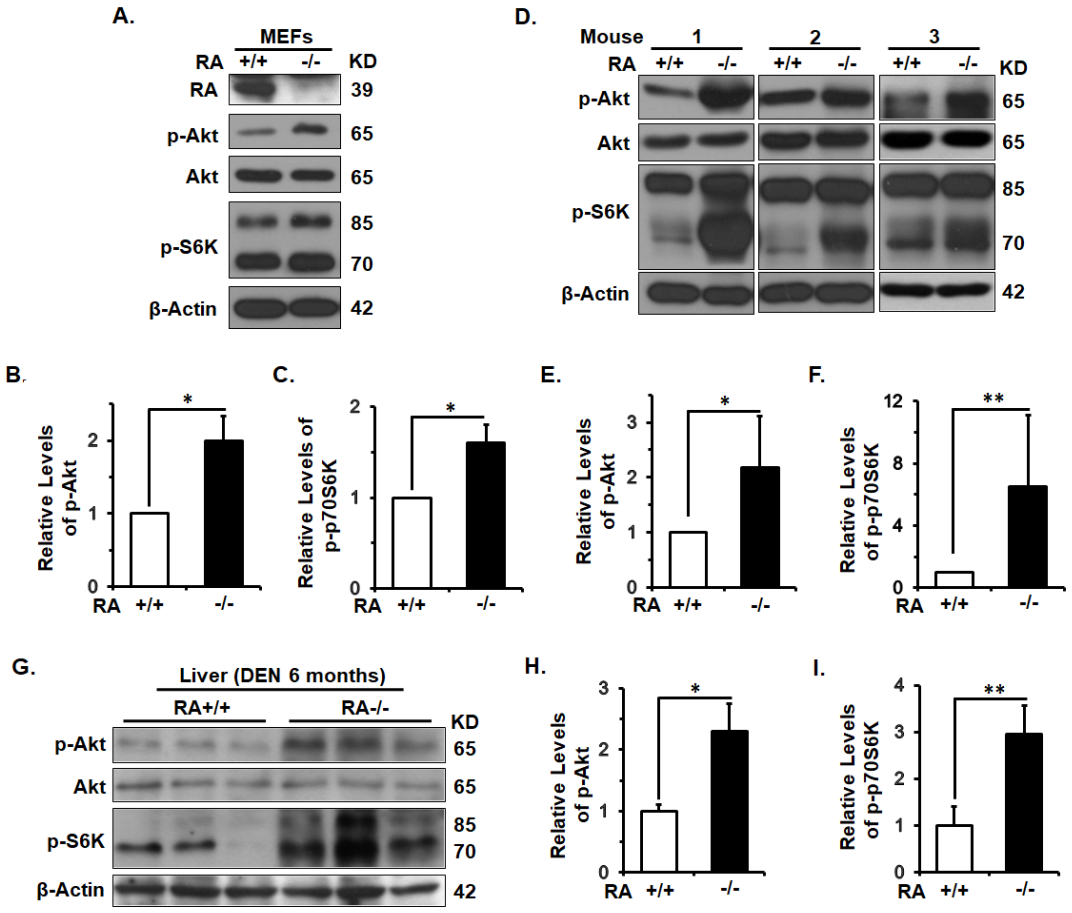

Figure 22. RASSF1A deletion causes the activation of PI3K-Akt-mTOR pathway in mice. (**A**-**C**) Immunoblot analysis (**A**) and quantification (**B, C**) of levels of p-Akt and p-S6K in MEFs from wild-type and RASSF1A$^{-/-}$ mice. (**D**-**F**) Immunoblot analysis (**D**) and quantification (**E, F**) of levels of p-Akt and p-S6K in liver tissues from wild-type and RASSF1A$^{-/-}$ mice. (**G**-**I**) Immunoblot analysis (**G**) and quantification (**H, I**) of levels of p-Akt and p-S6K in liver tissues from DEN-treated 6-month-old wild-type and RASSF1A$^{-/-}$ mice.

RASSF1A Suppresses PI3K-Akt-mTOR Pathway to Promote Autophagy Initiation through Hippo Pathway Regulatory Protein Mst1

We then examined the mechanism by which RASSF1A suppresses PI3K-Akt-mTOR pathway. It was reported that RASSF1A maintains the stability and activity of Mst1 (mammalian STE20-like kinase 1) by directly interacting with Mst1 and preventing it from dephosphorylation by PP2A (128). It was also reported that Mst1 acts as a direct inhibitor of Akt through directly binding to Akt (129). Therefore, we reasoned that RASSF1A depletion may lead to the dephosphorylation and instability of Mst1, resulting in a reduction in Mst1-Akt interaction and thereby an increase in Akt activity. We first reconfirmed that endogenous RASSF1A was able to pull down endogenous Mst1 as well as Akt (Figure 23A), and endogenous Akt was able to pull down endogenous Mst1 as well as RASSF1A (Figure 23B), indicating that RASSF1A, Akt and Mst1 form a protein complex. As expected, RASSF1A deletion did lead to decreased levels of phosphorylated Mst1 and total Mst1 in mouse liver tissues (Figure 23C, D and E). RASSF1A depletion in HeLa cells also led to a reduced level of total Mst1 so that the levels of Mst1 co-immunoprecipitated with Akt were dramatically decreased in RASSF1A-suppressed HeLa cells (Figure 23F, G). Therefore, RASSF1A depletion leads to the dephosphorylation and instability of Mst1, which results in a reduction in Mst1-Akt interaction and thereby the activation of PI3K-Akt-mTOR pathway to suppress autophagy initiation (Figure 23H).

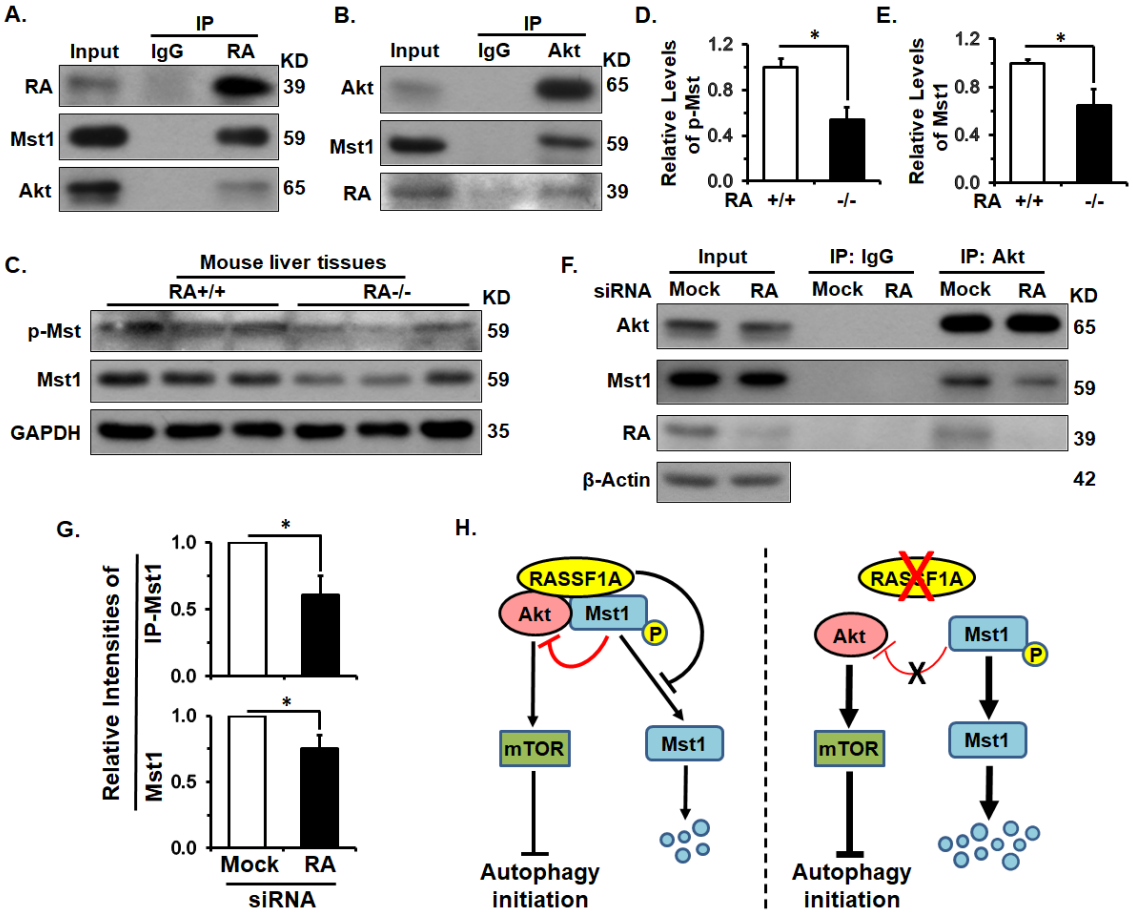

Figure 23. RASSF1A suppresses PI3K-Akt-mTOR pathway to promote autophagy initiation through Hippo pathway regulatory protein Mst1. (**A**) Endogenous RASSF1A interacts with endogenous MST1 and Akt. Lysates from HeLa cells were precipitated with RASSF1A-specific antibody or IgG control. (**B**) Endogenous Akt interacts with endogenous Mst1 and RASSF1A. Lysates from HeLa cells were precipitated with Akt-specific antibody or IgG control. (**C**-**E**) Immunoblot analysis (**C**) and quantification (**D, E**) of levels of p-Mst1 and total Mst1 in liver tissues from wild-type and RASSF1A$^{-/-}$ mice. (**F**) RASSF1A knockdown weakens the Akt-Mst1 interaction. Lysates from HeLa cells treated with mock or RASSF1A-specific siRNA were precipitated with Akt-specific antibody or IgG control. (**G**) Quantification of levels of total Mst1 and coprecipitated Mst1 as shown in (**F**). (**H**) A diagram showing the mechanism by which RASSF1A regulates autophagy initiation. RASSF1A interacts with and stabilizes Mst1 by preventing it from dephosphorylation. Stabilized Mst1 inhibits Akt activity by directly interacting with Akt. Without RASSF1A, Mst1 is dephosphorylated and then degraded. Thus, the Akt-Mst1 interaction is disrupted and Akt is activated to suppress autophagy initiation.

RASSF1A has No Impact on Hippo Pathway in Mouse Livers

Hippo pathway, an evolutionarily conserved pathway, controls organ size and tissue homeostasis by regulating cell proliferation, apoptosis, and stemness (130). Dysregulation of Hippo pathway leads to tumorigenesis (131,132). Since RASSF1A maintains the stability and activity of MST1 (Figure 23), RASSF1A was suggested to be an important regulator of Hippo pathway and suppress tumorigenesis through Hippo pathway. We then examined the impact of RASSF1A on the components of the Hippo pathway in mouse livers. However, we found that RASSF1A deletion did not alter levels of phosphorylated Yap, total Yap and CTGF, a direct Yap target gene (Figure 24 A, B). Therefore, at least in mouse liver tissues, RASSF1A deletion does not impact much the downstream effectors of the Hippo pathway.

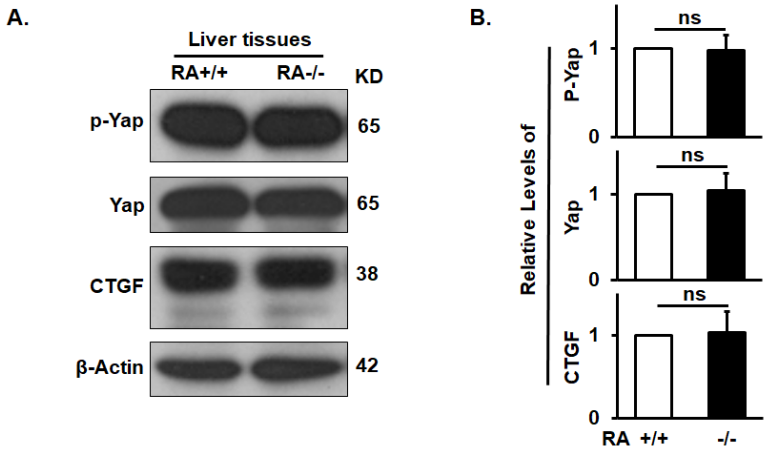

Figure 24. RASSF1A deletion has no impact on the downstream effectors of Hippo pathway. (A, **B)** Immunoblot analysis (**A**) and quantification (**B**) of levels of p-Yap, total Yap and CTGF in liver tissues from wild-type and RASSF1A$^{-/-}$ mice.

Discussion

Autophagy activator MAP1S regulates both autophagy initiation and maturation (47). In chapter IV, we showed that RASSF1A promotes autophagy maturation by recruiting LC3-II-associated autophagosomes onto RASSF1A-stabilized acetylated microtubules through MAP1S. This result triggered us to reason that RASSF1A may regulate autophagy initiation also through MAP1S.

Autophagy initiation is regulated through the well-known canonical PI3K-Akt-mTOR pathway or the non-canonical LKB1-AMPK-mTOR pathway (48). In addition to act as a cell cycle inhibitor, p27 is able to enhance autophagy initiation through the LKB1-AMPK-mTOR pathway (48). MAP1S sustains the levels of Bcl-2/xL which enhance p27 to promote autophagy initiation through LKB1-AMPK-mTOR pathway (47,126). However, here we found that RASSF1A has no impact on MAP1S-Bcl-2-p27 autophagy pathway. First, RASSF1A deletion did not alter levels of MAP1S, Bcl-2 and p27 in mouse liver tissues. Acetylation is one of the important post-translational modification of MAP1S. We previously reported that HDAC4 directly binds to, deacetylates and destabilizes MAP1S to suppress autophagy flux (105) and lysine 520 of MAP1S is critical for MAP1S to enhance autophagosomal degradation (57), indicating that acetylated MAP1S, but not the non-acetylated MAP1S, is essential in autophagy regulation. However, we found that RASSF1A also had no impact on levels of acetylated MAP1S both in vitro or in vivo. Second, although RASSF1A suppression resulted in decreased levels of Bcl-2 and p27 in HeLa cells, overexpressing p27 did not restore the decreased

autophagy flux caused by RASSF1A suppression. RASSF1A was reported to regulate cell cycle and apoptosis and the changes of Bcl-2 and p27 here caused by RASSF1A suppression may be involved in cell cycle and apoptosis regulation, which needs to be further investigated (30,33-36). Taken together, RASSF1A does not regulate autophagy initiation in the same way as its interactive protein MAP1S does.

It is well documented that RASSF1A interacts with Mst1, one of the key regulators of the Hippo pathway that regulates organ size and tissue homeostasis (130,133). The interaction suggests that RASSF1A may suppress tumorigenesis through Hippo pathway. Central to Hippo pathway is a kinase cascade. Conventionally, phosphorylated Mst1 kinase leads to the phosphorylation of its downstream effector Yap, a transcriptional factor. 14-3-3 protein binds to the phosphorylated Yap and retains Yap in the cytoplasm so that Yap cannot translocate into nuclear to promote the transcription of its target genes involved in cell proliferation, survival, and apoptosis. Studies of in vivo models generally support an oncogenic role of Yap and a tumor-suppressive function of Hippo pathway (130). Accumulating evidence also shows that dysfunction of Hippo pathway occurs in many human cancers (134,135). RASSF1A was reported to directly bind with and stabilize Mst1 through preventing its dephosphorylation by PP2A (128). Consistent with this report, we found that RASSF1A deletion leads to a significant reduction in levels of phosphorylated Mst1 and total Mst1 in mouse liver tissues. However, RASSF1A deletion does not alter levels of phosphorylated

Yap, total Yap and CTGF. Therefore, at least in mouse liver tissues, RASSF1A does not regulate autophagy flux and exert its tumor-suppressive role through conventional Hippo pathway.

It was reported that Mst1 interacts with Beclin1 and enhances its binding to Bcl-2/xL to inhibit autophagy flux in cardiomyocytes (136). In this chapter, we showed that RASSF1A deletion leads to decreased levels of total and phosphorylated Mst1 in mouse liver tissues, which suggests autophagy would be activated. However, our results show that autophagy was not activated but actually suppressed. In addition, RASSF1A deletion did not alter levels of Bcl-2 and Beclin1 (data not shown) in mouse liver tissues. Although RASSF1A-suppressed HeLa cells had a reduced level of Mst1, the interaction between Bcl-2 and Beclin1 were not altered in RASSF1A-suppressed HeLa cells (data not shown). Therefore, at least in mouse liver tissues, RASSF1A does not regulate autophagy initiation through Mst1-Beclin1-Bcl-2 pathway.

It was also reported that Mst1 directly interacts with the hydrophobic domain of Akt and the interaction is sufficient to inhibit Akt activity and the downstream signaling events (129). We reasoned that RASSF1A may promote autophagy initiation through suppressing PI3K-Akt-mTOR pathway, a well-known canonical autophagy-suppressive pathway. As expected, RASSF1A depletion causes a reduction in Mst1-Akt interaction and thereby activation of PI3K-Akt-mTOR pathway to inhibit autophagy initiation. Therefore, here we discover an alternative mechanism by which Mst1 regulates autophagy initiation through

directly binding with and inhibiting Akt activity. Mst1 is a serine-threonine kinase but not a dephosphorylase, so here it is impossible for Mst1 itself to directly dephosphorylate Akt. Studies showed that Mst1 inhibits Akt activity in a manner that depends on its direct binding to Akt, not its phosphotransferase activity (129). The hydrophobic domain of Akt that Mst1 binds to is a binding domain for several positive and negative regulators of Akt, so it is predicted that Mst1 may be competitive with the positive regulators to bind to Akt, or Mst1 may recruit the negative regulators to the Mst1-Akt complex to inhibit Akt activity. Understanding of the detailed mechanism by which Mst1 inhibits Akt activity needs further studies.

Although RASSF1A promotes autophagy maturation through its interactive protein MAP1S, we show here that RASSF1A does not regulate autophagy initiation through MAP1S. We previously reported that RASSF1A has a mitochondrial location in the absence of intact microtubules (54). Mitochondria as well as Golgi complex, endosomes, ER (endoplasmic reticulum) are the potential source for the phagophore (also called the isolation membrane) (137). It is widely accepted that a phagophore assembly site (PAS) first forms on the membrane of above organelles, and then some autophagy machinery docks at, or is delivered to the assembly site to be responsible for the formation of the isolation membrane. We predict that at the initial stages of autophagy, RASSF1A may locate to the phagophore assembly site on mitochondrial membrane and help autophagy machinery to assemble phagophore. After autophagy is initiated, cargo-containing

autophagosomes need to migrate along microtubules to fuse with lysosomes in different subcellular location. At this stage, RASSF1A recruits MAP1S which distribute in other subcellular locations onto RASSF1A-stabilized acetylated microtubules and bridges LC3-II-associated autophagosomes with microtubules through LC3-II interactive MAP1S. Therefore, RASSF1A and MAP1S distribute in different subcellular locations and may regulate autophagy initiation by their respective mechanisms. After mature autophagosomes form, RASSF1A and MAP1S meet with each other on RASSF1A-stabilized acetylated microtubules to promote autophagy maturation.

CHAPTER VI

CONCLUSIONS

Hepatocellular carcinomas (HCC) is the second leading cause of cancer death worldwide. Its incidence has more than tripled in the United States since1980 and the death rates have increased by almost 3% per year since 2000 (3). The very early stage of HCC is very hard to be diagnosed, while there are no very effective treatments for patients with the late stage of HCC (2). Therefore, it is very urgent to understand the underlying mechanism of HCC formation for developing novel therapeutic strategies. RASSF1A is a tumor suppressor and inactivated by promoter hypermethylation in over 90% of HCC patients (42,138). Therefore, in this report, we sought out to focus on characterizing the role and mechanism of RASSF1A in the development of HCC.

RASSF1A was suggested to suppress tumorigenesis through multiple different mechanisms including cell cycle arrest, apoptosis promotion, microtubular stabilization and migration inhibition. Because the interaction of RASSF1A with Mst1, RASSF1A was also suggested to suppress tumorigenesis through Hippo pathway. However, how RASSF1A causes tumor suppression is still debatable. Autophagy activity is inversely correlated with tumor formation (16,18,20-22). Autophagy defects enhance oxidative stress and genome instability to promote tumorigenesis (23-25). Liver is highly dependent on autophagy to maintain its basic functions and autophagy defects promote the

malignant transformation of liver cells (58,139). The interaction of RASSF1A with autophagy activator MAP1S triggered us to hypothesize that RASSF1A suppresses HCC by activating autophagy through MAP1S. We show here first time that RASSF1A does not impact the Hippo pathway but acts through Mst1, a Hippo pathway-regulatory protein, to promote autophagy initiation through the PI3K-Akt-mTOR pathway, a regulatory cascade different from MAP1S-Bcl-2-p27 noncanonical autophagy pathway; and RASSF1A enhances microtubular acetylation and recruits autophagosomes onto acetylated microtubules through MAP1S to promote autophagy maturation. RASSF1A deletion leads to autophagy defects which induce oxidative stress and DNA damage to accelerate DEN-induced HCC and shorten mouse survivals. Therefore, we provide here a novel mechanism for RASSF1A to activate autophagy and suppress HCC.

Overall, we show here first time with solid evidences that RASSF1A is a novel autophagy activator; and epigenetically inactivated RASSF1A actually promotes HCC by suppressing the initiation and maturation of autophagy process (Figure 25). This work not only advances our understanding of the biological functions of RASSF1A but also provides a novel paradigm of the prevention and therapy of human HCC.

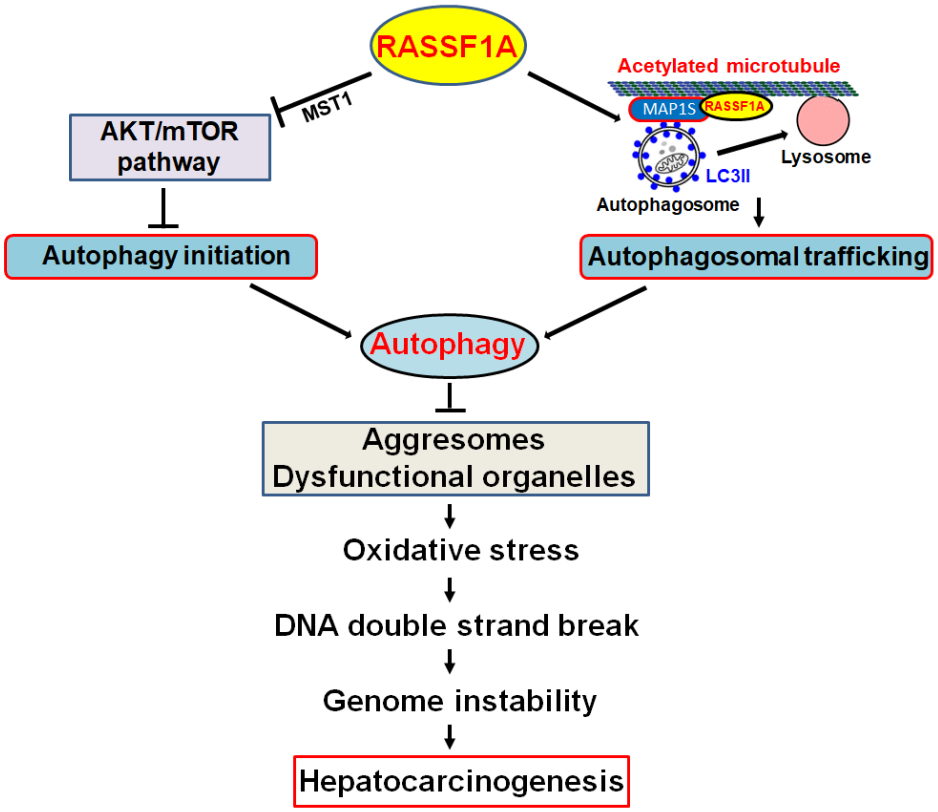

Figure 25. A diagram showing the potential mechanism by which RASSFA regulates autophagy and suppresses hepatocarcinogenesis.

While this dissertation has demonstrated that RASSF1A deletion promotes HCC by suppressing autophagy, there are still some interesting directions for future work to extend the scope of this dissertation. First, we can investigate whether overexpression of RASSF1A in mice is able to suppress DEN-induced HCC. Specifically, we can generate RASSF1A transgenic mice to examine whether RASSF1A overexpression suppresses DEN-induced

hepatocarcinogenesis. We can also generate RASSF1A inducible transgenic mice and induce RASSF1A expression after mice develop HCC to examine whether it can suppress the growth of established HCC. If RASSF1A overexpression in mice suppresses HCC, it will further show that RASSF1A is a potential target for HCC therapy. RASSF1A is epigenetically inactivated in about 90% of HCC, so exploring how RASSF1A is regulated and how to reactivate RASSF1A expression may provide a novel approach to HCC therapy. Second, our study shows that RASSF1A deletion in mice leads to autophagy defects by activating PI3K-Akt-mTOR pathway, so we can treat RASSF1A-/- mice with mTOR inhibitor, such like rapamycin, to examine whether suppression of mTOR prevents HCC development. Third, examining how RASSF1A regulates the acetylation of microtubules will help to better understand its basic functions. It is known that RASSF1A stabilizes microtubules, but the underlying mechanism is unclear. In this study we show that RASSF1A stabilizes microtubules by promoting microtubular acetylation; RASSF1A inhibits HDAC6 deacetylase activity on microtubules possibly due to its interaction with HDAC6. Future work can focus on investigating how the interaction inhibits HDAC6 activity. If RASSF1A regulates microtubular acetylation through HDAC6, we can treat mice with HDAC6 inhibitor to see whether it can suppress HCC development. We can also examine the impact of RASSF1A on α-TAT (α-tubulin acetyl-transferase), which may also help to uncover the underlying mechanism. Finally, this study mainly focuses on examining the role of RASSF1A in parenchymal hepatocytes

which perform the majority of hepatic functions. We can extend our studies in other non-parenchymal hepatocytes, such like hepatic stellate cells (HSC), sinusoidal endothelial cells, phagocytic Kupffer cells and lymphocytes. It is reported that autophagy plays an important role in HSC activation, sinusoidal endothelial cells-regulated liver ischemia-reperfusion injury, lymphocytes development and survival (60, 140). Investigating the role of RASSF1A-regulated autophagy in these non-parenchymal hepatocytes may provide novel therapy approaches in other liver diseases.

REFERENCES

1. Global Burden of Disease Cancer, C., Fitzmaurice, C., Dicker, D., Pain, A., Hamavid, H., Moradi-Lakeh, M., MacIntyre, M. F., Allen, C., Hansen, G., Woodbrook, R., Wolfe, C., Hamadeh, R. R., Moore, A., Werdecker, A., Gessner, B. D., Te Ao, B., McMahon, B., Karimkhani, C., Yu, C., Cooke, G. S., Schwebel, D. C., Carpenter, D. O., Pereira, D. M., Nash, D., Kazi, D. S., De Leo, D., Plass, D., Ukwaja, K. N., Thurston, G. D., Yun Jin, K., Simard, E. P., Mills, E., Park, E. K., Catala-Lopez, F., deVeber, G., Gotay, C., Khan, G., Hosgood, H. D., 3rd, Santos, I. S., Leasher, J. L., Singh, J., Leigh, J., Jonas, J. B., Sanabria, J., Beardsley, J., Jacobsen, K. H., Takahashi, K., Franklin, R. C., Ronfani, L., Montico, M., Naldi, L., Tonelli, M., Geleijnse, J., Petzold, M., Shrime, M. G., Younis, M., Yonemoto, N., Breitborde, N., Yip, P., Pourmalek, F., Lotufo, P. A., Esteghamati, A., Hankey, G. J., Ali, R., Lunevicius, R., Malekzadeh, R., Dellavalle, R., Weintraub, R., Lucas, R., Hay, R., Rojas-Rueda, D., Westerman, R., Sepanlou, S. G., Nolte, S., Patten, S., Weichenthal, S., Abera, S. F., Fereshtehnejad, S. M., Shiue, I., Driscoll, T., Vasankari, T., Alsharif, U., Rahimi-Movaghar, V., Vlassov, V. V., Marcenes, W. S., Mekonnen, W., Melaku, Y. A., Yano, Y., Artaman, A., Campos, I., MacLachlan, J., Mueller, U., Kim, D., Trillini, M., Eshrati, B., Williams, H. C., Shibuya, K., Dandona, R., Murthy, K., Cowie, B., Amare, A. T., Antonio, C. A., Castaneda-Orjuela, C., van Gool, C. H., Violante, F., Oh, I. H., Deribe, K., Soreide, K., Knibbs,

L., Kereselidze, M., Green, M., Cardenas, R., Roy, N., Tillmann, T., Li, Y., Krueger, H., Monasta, L., Dey, S., Sheikhbahaei, S., Hafezi-Nejad, N., Kumar, G. A., Sreeramareddy, C. T., Dandona, L., Wang, H., Vollset, S. E., Mokdad, A., Salomon, J. A., Lozano, R., Vos, T., Forouzanfar, M., Lopez, A., Murray, C., and Naghavi, M. (2015) The Global Burden of Cancer 2013. *JAMA Oncol* 1, 505-527

2. El-Serag, H. B. (2011) Hepatocellular carcinoma. *N Engl J Med* 365, 1118-1127
3. Siegel, R. L., Miller, K. D., and Jemal, A. (2016) Cancer statistics, 2016. *CA Cancer J Clin* 66, 7-30
4. De Duve, C., and Wattiaux, R. (1966) Functions of lysosomes. *Annu Rev Physiol* 28, 435-492
5. Mizushima, N., Noda, T., Yoshimori, T., Tanaka, Y., Ishii, T., George, M. D., Klionsky, D. J., Ohsumi, M., and Ohsumi, Y. (1998) A protein conjugation system essential for autophagy. *Nature* 395, 395-398
6. Hansen, T. E., Johansen, T. (2011) Following autophagy step by step. *BMC Biol* 9, 39
7. Clark, S. L., Jr. (1957) Cellular differentiation in the kidneys of newborn mice studies with the electron microscope. *J Biophys Biochem Cytol* 3, 349-362
8. Tsukada, M., and Ohsumi, Y. (1993) Isolation and characterization of autophagy-defective mutants of Saccharomyces cerevisiae. *FEBS Lett*

333, 169-174

9. Noda, T., and Ohsumi, Y. (1998) Tor, a phosphatidylinositol kinase homologue, controls autophagy in yeast. *J Biol Chem* 273, 3963-3966

10. Wong, P. M., Puente, C., Ganley, I. G., and Jiang, X. (2013) The ULK1 complex: sensing nutrient signals for autophagy activation. *Autophagy* 9, 124-137

11. Kihara, A., Noda, T., Ishihara, N., and Ohsumi, Y. (2001) Two distinct Vps34 phosphatidylinositol 3-kinase complexes function in autophagy and carboxypeptidase Y sorting in Saccharomyces cerevisiae. *J Cell Biol* 152, 519-530

12. Kabeya, Y., Mizushima, N., Ueno, T., Yamamoto, A., Kirisako, T., Noda, T., Kominami, E., Ohsumi, Y., and Yoshimori, T. (2000) LC3, a mammalian homologue of yeast Apg8p, is localized in autophagosome membranes after processing. *EMBO J* 19, 5720-5728

13. Klionsky, D. J., Abdelmohsen, K., Abe, A., Abedin, M. J., Abeliovich, H., Acevedo Arozena, A., et al. (2016) Guidelines for the use and interpretation of assays for monitoring autophagy (3rd edition). *Autophagy* 12, 1-222

14. Johansen, T., and Lamark, T. (2011) Selective autophagy mediated by autophagic adapter proteins. *Autophagy* 7, 279-296

15. Mizushima, N., Yamamoto, A., Matsui, M., Yoshimori, T., and Ohsumi, Y. (2004) In vivo analysis of autophagy in response to nutrient starvation using transgenic mice expressing a fluorescent autophagosome marker.

Mol Biol Cell 15, 1101-1111

16. Liang, X. H., Jackson, S., Seaman, M., Brown, K., Kempkes, B., Hibshoosh, H., and Levine, B. (1999) Induction of autophagy and inhibition of tumorigenesis by beclin 1. *Nature* 402, 672-676
17. Aita, V. M., Liang, X. H., Murty, V. V., Pincus, D. L., Yu, W., Cayanis, E., Kalachikov, S., Gilliam, T. C., and Levine, B. (1999) Cloning and genomic organization of beclin 1, a candidate tumor suppressor gene on chromosome 17q21. *Genomics* 59, 59-65
18. Qu, X., Yu, J., Bhagat, G., Furuya, N., Hibshoosh, H., Troxel, A., Rosen, J., Eskelinen, E. L., Mizushima, N., Ohsumi, Y., Cattoretti, G., and Levine, B. (2003) Promotion of tumorigenesis by heterozygous disruption of the beclin 1 autophagy gene. *J Clin Invest* 112, 1809-1820
19. Yue, Z., Jin, S., Yang, C., Levine, A. J., and Heintz, N. (2003) Beclin 1, an autophagy gene essential for early embryonic development, is a haploinsufficient tumor suppressor. *Proc Natl Acad Sci U S A* 100, 15077-15082
20. Marino, G., Salvador-Montoliu, N., Fueyo, A., Knecht, E., Mizushima, N., and Lopez-Otin, C. (2007) Tissue-specific autophagy alterations and increased tumorigenesis in mice deficient in Atg4C/autophagin-3. *J Biol Chem* 282, 18573-18583
21. Takamura, A., Komatsu, M., Hara, T., Sakamoto, A., Kishi, C., Waguri, S., Eishi, Y., Hino, O., Tanaka, K., and Mizushima, N. (2011) Autophagy-

deficient mice develop multiple liver tumors. *Genes Dev* 25, 795-800

22. Takahashi, Y., Coppola, D., Matsushita, N., Cualing, H. D., Sun, M., Sato, Y., Liang, C., Jung, J. U., Cheng, J. Q., Mule, J. J., Pledger, W. J., and Wang, H. G. (2007) Bif-1 interacts with Beclin 1 through UVRAG and regulates autophagy and tumorigenesis. *Nat Cell Biol* 9, 1142-1151

23. Mathew, R., Kongara, S., Beaudoin, B., Karp, C. M., Bray, K., Degenhardt, K., Chen, G., Jin, S., and White, E. (2007) Autophagy suppresses tumor progression by limiting chromosomal instability. *Genes Dev* 21, 1367-1381

24. Mathew, R., Karp, C. M., Beaudoin, B., Vuong, N., Chen, G., Chen, H. Y., Bray, K., Reddy, A., Bhanot, G., Gelinas, C., Dipaola, R. S., Karantza-Wadsworth, V., and White, E. (2009) Autophagy suppresses tumorigenesis through elimination of p62. *Cell* 137, 1062-1075

25. Xie, R., Wang, F., McKeehan, W. L., and Liu, L. (2011) Autophagy enhanced by microtubule- and mitochondrion-associated MAP1S suppresses genome instability and hepatocarcinogenesis. *Cancer Res* 71, 7537-7546

26. Whang-Peng, J., Kao-Shan, C. S., Lee, E. C., Bunn, P. A., Carney, D. N., Gazdar, A. F., and Minna, J. D. (1982) Specific chromosome defect associated with human small-cell lung cancer; deletion 3p(14-23). *Science* 215, 181-182

27. Hung, J., Kishimoto, Y., Sugio, K., Virmani, A., McIntire, D. D., Minna, J. D., and Gazdar, A. F. (1995) Allele-specific chromosome 3p deletions

occur at an early stage in the pathogenesis of lung carcinoma. *JAMA* 273, 558-563

28. Dammann, R., Li, C., Yoon, J. H., Chin, P. L., Bates, S., and Pfeifer, G. P. (2000) Epigenetic inactivation of a RAS association domain family protein from the lung tumour suppressor locus 3p21.3. *Nat Genet* 25, 315-319

29. Liu, L., Tommasi, S., Lee, D. H., Dammann, R., and Pfeifer, G. P. (2003) Control of microtubule stability by the RASSF1A tumor suppressor. *Oncogene* 22, 8125-8136

30. Song, M. S., Chang, J. S., Song, S. J., Yang, T. H., Lee, H., and Lim, D. S. (2005) The centrosomal protein RAS association domain family protein 1A (RASSF1A)-binding protein 1 regulates mitotic progression by recruiting RASSF1A to spindle poles. *J Biol Chem* 280, 3920-3927

31. Jung, H. Y., Jung, J. S., Whang, Y. M., and Kim, Y. H. (2013) RASSF1A Suppresses Cell Migration through Inactivation of HDAC6 and Increase of Acetylated alpha-Tubulin. *Cancer Res Treat* 45, 134-144

32. Dallol, A., Agathanggelou, A., Tommasi, S., Pfeifer, G. P., Maher, E. R., and Latif, F. (2005) Involvement of the RASSF1A tumor suppressor gene in controlling cell migration. *Cancer Res* 65, 7653-7659

33. Song, M. S., Song, S. J., Ayad, N. G., Chang, J. S., Lee, J. H., Hong, H. K., Lee, H., Choi, N., Kim, J., Kim, H., Kim, J. W., Choi, E. J., Kirschner, M. W., and Lim, D. S. (2004) The tumour suppressor RASSF1A regulates mitosis by inhibiting the APC-Cdc20 complex. *Nat Cell Biol* 6, 129-137

34. Baksh, S., Tommasi, S., Fenton, S., Yu, V. C., Martins, L. M., Pfeifer, G. P., Latif, F., Downward, J., and Neel, B. G. (2005) The tumor suppressor RASSF1A and MAP-1 link death receptor signaling to Bax conformational change and cell death. *Mol Cell* 18, 637-650

35. Matallanas, D., Romano, D., Yee, K., Meissl, K., Kucerova, L., Piazzolla, D., Baccarini, M., Vass, J. K., Kolch, W., and O'Neill, E. (2007) RASSF1A elicits apoptosis through an MST2 pathway directing proapoptotic transcription by the p73 tumor suppressor protein. *Mol Cell* 27, 962-975

36. Vos, M. D., Dallol, A., Eckfeld, K., Allen, N. P., Donninger, H., Hesson, L. B., Calvisi, D., Latif, F., and Clark, G. J. (2006) The RASSF1A tumor suppressor activates Bax via MOAP-1. *J Biol Chem* 281, 4557-4563

37. Hamilton, G., Yee, K. S., Scrace, S., and O'Neill, E. (2009) ATM regulates a RASSF1A-dependent DNA damage response. *Curr Biol* 19, 2020-2025

38. Yee, K. S., Grochola, L., Hamilton, G., Grawenda, A., Bond, E. E., Taubert, H., Wurl, P., Bond, G. L., and O'Neill, E. (2012) A RASSF1A polymorphism restricts p53/p73 activation and associates with poor survival and accelerated age of onset of soft tissue sarcoma. *Cancer Res* 72, 2206-2217

39. Chan, M. W., Chan, L. W., Tang, N. L., Lo, K. W., Tong, J. H., Chan, A. W., Cheung, H. Y., Wong, W. S., Chan, P. S., Lai, F. M., and To, K. F. (2003) Frequent hypermethylation of promoter region of RASSF1A in tumor tissues and voided urine of urinary bladder cancer patients. *Int J Cancer*

104, 611-616

40. Lee, M. G., Kim, H. Y., Byun, D. S., Lee, S. J., Lee, C. H., Kim, J. I., Chang, S. G., and Chi, S. G. (2001) Frequent epigenetic inactivation of RASSF1A in human bladder carcinoma. *Cancer Res* 61, 6688-6692

41. Agathanggelou, A., Honorio, S., Macartney, D. P., Martinez, A., Dallol, A., Rader, J., Fullwood, P., Chauhan, A., Walker, R., Shaw, J. A., Hosoe, S., Lerman, M. I., Minna, J. D., Maher, E. R., and Latif, F. (2001) Methylation associated inactivation of RASSF1A from region 3p21.3 in lung, breast and ovarian tumours. *Oncogene* 20, 1509-1518

42. Schagdarsurengin, U., Wilkens, L., Steinemann, D., Flemming, P., Kreipe, H. H., Pfeifer, G. P., Schlegelberger, B., and Dammann, R. (2003) Frequent epigenetic inactivation of the RASSF1A gene in hepatocellular carcinoma. *Oncogene* 22, 1866-1871

43. Lee, S., Lee, H. J., Kim, J. H., Lee, H. S., Jang, J. J., and Kang, G. H. (2003) Aberrant CpG island hypermethylation along multistep hepatocarcinogenesis. *Am J Pathol* 163, 1371-1378

44. Liu, L., Xie, R., Yang, C., and McKeehan, W. L. (2009) Dual function microtubule- and mitochondria-associated proteins mediate mitotic cell death. *Cell Oncol* 31, 393-405

45. Kuznetsov, S. A., and Gelfand, V. I. (1987) 18 kDa microtubule-associated protein: identification as a new light chain (LC-3) of microtubule-associated protein 1 (MAP-1). *FEBS Lett* 212, 145-148

46. Mann, S. S., and Hammarback, J. A. (1994) Molecular characterization of light chain 3. A microtubule binding subunit of MAP1A and MAP1B. *J Biol Chem* 269, 11492-11497

47. Xie, R., Nguyen, S., McKeehan, K., Wang, F., McKeehan, W. L., and Liu, L. (2011) Microtubule-associated protein 1S (MAP1S) bridges autophagic components with microtubules and mitochondria to affect autophagosomal biogenesis and degradation. *J Biol Chem* 286, 10367-10377

48. Liang, J., Shao, S. H., Xu, Z. X., Hennessy, B., Ding, Z., Larrea, M., Kondo, S., Dumont, D. J., Gutterman, J. U., Walker, C. L., Slingerland, J. M., and Mills, G. B. (2007) The energy sensing LKB1-AMPK pathway regulates p27(kip1) phosphorylation mediating the decision to enter autophagy or apoptosis. *Nat Cell Biol* 9, 218-224

49. Li, W., Zou, J., Yue, F., Song, K., Chen, Q., McKeehan, W. L., Wang, F., Xu, G., Huang, H., Yi, J., and Liu, L. (2016) Defects in MAP1S-mediated autophagy cause reduction in mouse lifespans especially when fibronectin is overexpressed. *Aging Cell* 15, 370-379

50. Jiang, X., Zhong, W., Huang, H., He, H., Jiang, F., Chen, Y., Yue, F., Zou, J., Li, X., He, Y., You, P., Yang, W., Lai, Y., Wang, F., and Liu, L. (2015) Autophagy defects suggested by low levels of autophagy activator MAP1S and high levels of autophagy inhibitor LRPPRC predict poor prognosis of prostate cancer patients. *Mol Carcinog* 54, 1194-1204

51. Xu, G., Jiang, Y., Xiao, Y., Liu, X. D., Yue, F., Li, W., Li, X., He, Y., Jiang,

X., Huang, H., Chen, Q., Jonasch, E., and Liu, L. (2016) Fast clearance of lipid droplets through MAP1S-activated autophagy suppresses clear cell renal cell carcinomas and promotes patient survival. *Oncotarget* 7, 6255-6265

52. Dallol, A., Agathanggelou, A., Fenton, S. L., Ahmed-Choudhury, J., Hesson, L., Vos, M. D., Clark, G. J., Downward, J., Maher, E. R., and Latif, F. (2004) RASSF1A interacts with microtubule-associated proteins and modulates microtubule dynamics. *Cancer Res* 64, 4112-4116

53. Liu, L., Amy, V., Liu, G., and McKeehan, W. L. (2002) Novel complex integrating mitochondria and the microtubular cytoskeleton with chromosome remodeling and tumor suppressor RASSF1 deduced by in silico homology analysis, interaction cloning in yeast, and colocalization in cultured cells. *In Vitro Cell Dev Biol Anim* 38, 582-594

54. Liu, L., Vo, A., and McKeehan, W. L. (2005) Specificity of the methylation-suppressed A isoform of candidate tumor suppressor RASSF1 for microtubule hyperstabilization is determined by cell death inducer C19ORF5. *Cancer Res* 65, 1830-1838

55. Wang, Q. J., Ding, Y., Kohtz, D. S., Mizushima, N., Cristea, I. M., Rout, M. P., Chait, B. T., Zhong, Y., Heintz, N., and Yue, Z. (2006) Induction of autophagy in axonal dystrophy and degeneration. *J Neurosci* 26, 8057-8068

56. Tommasi, S., Dammann, R., Zhang, Z., Wang, Y., Liu, L., Tsark, W. M.,

Wilczynski, S. P., Li, J., You, M., and Pfeifer, G. P. (2005) Tumor susceptibility of Rassf1a knockout mice. *Cancer Res* 65, 92-98

57. Yue, F., Li, W., Zou, J., Jiang, X., Xu, G., Huang, H., and Liu, L. (2017) Spermidine Prolongs Lifespan and Prevents Liver Fibrosis and Hepatocellular Carcinoma by Activating MAP1S-Mediated Autophagy. *Cancer Res* 77, 2938-2951

58. Czaja, M. J., Ding, W. X., Donohue, T. M., Jr., Friedman, S. L., Kim, J. S., Komatsu, M., Lemasters, J. J., Lemoine, A., Lin, J. D., Ou, J. H., Perlmutter, D. H., Randall, G., Ray, R. B., Tsung, A., and Yin, X. M. (2013) Functions of autophagy in normal and diseased liver. *Autophagy* 9, 1131-1158

59. Kirschke, H., Langner, J., Wiederanders, B., Ansorge, S., and Bohley, P. (1977) Cathepsin L. A new proteinase from rat-liver lysosomes. *Eur J Biochem* 74, 293-301

60. Thoen, L. F., Guimaraes, E. L., Dolle, L., Mannaerts, I., Najimi, M., Sokal, E., and van Grunsven, L. A. (2011) A role for autophagy during hepatic stellate cell activation. *J Hepatol* 55, 1353-1360

61. Bataller, R., and Brenner, D. A. (2005) Liver fibrosis. *J Clin Invest* 115, 209-218

62. Singh, S., Singh, P. P., Roberts, L. R., and Sanchez, W. (2014) Chemopreventive strategies in hepatocellular carcinoma. *Nat Rev Gastroenterol Hepatol* 11, 45-54

63. Schworer, C. M., Shiffer, K. A., and Mortimore, G. E. (1981) Quantitative

relationship between autophagy and proteolysis during graded amino acid deprivation in perfused rat liver. *J Biol Chem* 256, 7652-7658

64. Mortimore, G. E., Hutson, N. J., and Surmacz, C. A. (1983) Quantitative correlation between proteolysis and macro- and microautophagy in mouse hepatocytes during starvation and refeeding. *Proc Natl Acad Sci U S A* 80, 2179-2183

65. Kim, I., and Lemasters, J. J. (2011) Mitochondrial degradation by autophagy (mitophagy) in GFP-LC3 transgenic hepatocytes during nutrient deprivation. *Am J Physiol Cell Physiol* 300, C308-317

66. Lemasters, J. J. (2005) Selective mitochondrial autophagy, or mitophagy, as a targeted defense against oxidative stress, mitochondrial dysfunction, and aging. *Rejuvenation Res* 8, 3-5

67. Ezaki, J., Matsumoto, N., Takeda-Ezaki, M., Komatsu, M., Takahashi, K., Hiraoka, Y., Taka, H., Fujimura, T., Takehana, K., Yoshida, M., Iwata, J., Tanida, I., Furuya, N., Zheng, D. M., Tada, N., Tanaka, K., Kominami, E., and Ueno, T. (2011) Liver autophagy contributes to the maintenance of blood glucose and amino acid levels. *Autophagy* 7, 727-736

68. Singh, R., Kaushik, S., Wang, Y., Xiang, Y., Novak, I., Komatsu, M., Tanaka, K., Cuervo, A. M., and Czaja, M. J. (2009) Autophagy regulates lipid metabolism. *Nature* 458, 1131-1135

69. Lee, H. K., Lund, J. M., Ramanathan, B., Mizushima, N., and Iwasaki, A. (2007) Autophagy-dependent viral recognition by plasmacytoid dendritic

cells. *Science* 315, 1398-1401

70. Seki, E., and Brenner, D. A. (2008) Toll-like receptors and adaptor molecules in liver disease: update. *Hepatology* 48, 322-335

71. Knodler, L. A., and Celli, J. (2011) Eating the strangers within: host control of intracellular bacteria via xenophagy. *Cell Microbiol* 13, 1319-1327

72. English, L., Chemali, M., Duron, J., Rondeau, C., Laplante, A., Gingras, D., Alexander, D., Leib, D., Norbury, C., Lippe, R., and Desjardins, M. (2009) Autophagy enhances the presentation of endogenous viral antigens on MHC class I molecules during HSV-1 infection. *Nat Immunol* 10, 480-487

73. Lee, H. K., Mattei, L. M., Steinberg, B. E., Alberts, P., Lee, Y. H., Chervonsky, A., Mizushima, N., Grinstein, S., and Iwasaki, A. (2010) In vivo requirement for Atg5 in antigen presentation by dendritic cells. *Immunity* 32, 227-239

74. Nimmerjahn, F., Milosevic, S., Behrends, U., Jaffee, E. M., Pardoll, D. M., Bornkamm, G. W., and Mautner, J. (2003) Major histocompatibility complex class II-restricted presentation of a cytosolic antigen by autophagy. *Eur J Immunol* 33, 1250-1259

75. Paludan, C., Schmid, D., Landthaler, M., Vockerodt, M., Kube, D., Tuschl, T., and Munz, C. (2005) Endogenous MHC class II processing of a viral nuclear antigen after autophagy. *Science* 307, 593-596

76. Schmid, D., Pypaert, M., and Munz, C. (2007) Antigen-loading compartments for major histocompatibility complex class II molecules

continuously receive input from autophagosomes. *Immunity* 26, 79-92

77. Liu, L., McKeehan, W. L., Wang, F., and Xie, R. (2012) MAP1S enhances autophagy to suppress tumorigenesis. *Autophagy* 8, 278-280

78. Fariss, M. W., Chan, C. B., Patel, M., Van Houten, B., and Orrenius, S. (2005) Role of mitochondria in toxic oxidative stress. *Mol Interv* 5, 94-111

79. Jin, S. (2006) Autophagy, mitochondrial quality control, and oncogenesis. *Autophagy* 2, 80-84

80. Tu, B. P., and Weissman, J. S. (2004) Oxidative protein folding in eukaryotes: mechanisms and consequences. *J Cell Biol* 164, 341-346

81. D'Angiolella, V., Santarpia, C., and Grieco, D. (2007) Oxidative stress overrides the spindle checkpoint. *Cell Cycle* 6, 576-579

82. Sallmyr, A., Fan, J., and Rassool, F. V. (2008) Genomic instability in myeloid malignancies: increased reactive oxygen species (ROS), DNA double strand breaks (DSBs) and error-prone repair. *Cancer Lett* 270, 1-9

83. Liu, L., Trimarchi, J. R., Smith, P. J., and Keefe, D. L. (2002) Mitochondrial dysfunction leads to telomere attrition and genomic instability. *Aging Cell* 1, 40-46

84. Mishra, P. K., Raghuram, G. V., Panwar, H., Jain, D., Pandey, H., and Maudar, K. K. (2009) Mitochondrial oxidative stress elicits chromosomal instability after exposure to isocyanates in human kidney epithelial cells. *Free Radic Res* 43, 718-728

85. McClintock, B. (1942) The Fusion of Broken Ends of Chromosomes

Following Nuclear Fusion. *Proc Natl Acad Sci U S A* 28, 458-463

86. Gisselsson, D., Pettersson, L., Hoglund, M., Heidenblad, M., Gorunova, L., Wiegant, J., Mertens, F., Dal Cin, P., Mitelman, F., and Mandahl, N. (2000) Chromosomal breakage-fusion-bridge events cause genetic intratumor heterogeneity. *Proc Natl Acad Sci U S A* 97, 5357-5362

87. Heindryckx, F., Colle, I., and Van Vlierberghe, H. (2009) Experimental mouse models for hepatocellular carcinoma research. *Int J Exp Pathol* 90, 367-386

88. Kuo, L. J., and Yang, L. X. (2008) Gamma-H2AX - a novel biomarker for DNA double-strand breaks. *In Vivo* 22, 305-309

89. Fink, S. L., and Cookson, B. T. (2005) Apoptosis, pyroptosis, and necrosis: mechanistic description of dead and dying eukaryotic cells. *Infect Immun* 73, 1907-1916

90. Suzuki, T., Franchi, L., Toma, C., Ashida, H., Ogawa, M., Yoshikawa, Y., Mimuro, H., Inohara, N., Sasakawa, C., and Nunez, G. (2007) Differential regulation of caspase-1 activation, pyroptosis, and autophagy via Ipaf and ASC in Shigella-infected macrophages. *PLoS Pathog* 3, e111

91. Hornung, V., Bauernfeind, F., Halle, A., Samstad, E. O., Kono, H., Rock, K. L., Fitzgerald, K. A., and Latz, E. (2008) Silica crystals and aluminum salts activate the NALP3 inflammasome through phagosomal destabilization. *Nat Immunol* 9, 847-856

92. Lamkanfi, M., and Dixit, V. M. (2014) Mechanisms and functions of

inflammasomes. *Cell* 157, 1013-1022

93. Ryter, S. W., Mizumura, K., and Choi, A. M. (2014) The impact of autophagy on cell death modalities. *Int J Cell Biol* 2014, 502676

94. Yu, J., Nagasu, H., Murakami, T., Hoang, H., Broderick, L., Hoffman, H. M., and Horng, T. (2014) Inflammasome activation leads to Caspase-1-dependent mitochondrial damage and block of mitophagy. *Proc Natl Acad Sci U S A* 111, 15514-15519

95. Terlizzi, M., Casolaro, V., Pinto, A., and Sorrentino, R. (2014) Inflammasome: cancer's friend or foe? *Pharmacol Ther* 143, 24-33

96. Doitsh, G., Galloway, N. L., Geng, X., Yang, Z., Monroe, K. M., Zepeda, O., Hunt, P. W., Hatano, H., Sowinski, S., Munoz-Arias, I., and Greene, W. C. (2014) Cell death by pyroptosis drives CD4 T-cell depletion in HIV-1 infection. *Nature* 505, 509-514

97. Pankiv, S., Clausen, T. H., Lamark, T., Brech, A., Bruun, J. A., Outzen, H., Overvatn, A., Bjorkoy, G., and Johansen, T. (2007) p62/SQSTM1 binds directly to Atg8/LC3 to facilitate degradation of ubiquitinated protein aggregates by autophagy. *J Biol Chem* 282, 24131-24145

98. Wooten, M. W., Geetha, T., Babu, J. R., Seibenhener, M. L., Peng, J., Cox, N., Diaz-Meco, M. T., and Moscat, J. (2008) Essential role of sequestosome 1/p62 in regulating accumulation of Lys63-ubiquitinated proteins. *J Biol Chem* 283, 6783-6789

99. Thurston, T. L., Ryzhakov, G., Bloor, S., von Muhlinen, N., and Randow,

F. (2009) The TBK1 adaptor and autophagy receptor NDP52 restricts the proliferation of ubiquitin-coated bacteria. *Nat Immunol* 10, 1215-1221

100. Novak, I., Kirkin, V., McEwan, D. G., Zhang, J., Wild, P., Rozenknop, A., Rogov, V., Lohr, F., Popovic, D., Occhipinti, A., Reichert, A. S., Terzic, J., Dotsch, V., Ney, P. A., and Dikic, I. (2010) Nix is a selective autophagy receptor for mitochondrial clearance. *EMBO Rep* 11, 45-51

101. Waters, S., Marchbank, K., Solomon, E., Whitehouse, C., and Gautel, M. (2009) Interactions with LC3 and polyubiquitin chains link nbr1 to autophagic protein turnover. *FEBS Lett* 583, 1846-1852

102. Xie, R., Nguyen, S., McKeehan, W. L., and Liu, L. (2010) Acetylated microtubules are required for fusion of autophagosomes with lysosomes. *BMC Cell Biol* 11, 89

103. Fass, E., Shvets, E., Degani, I., Hirschberg, K., and Elazar, Z. (2006) Microtubules support production of starvation-induced autophagosomes but not their targeting and fusion with lysosomes. *J Biol Chem* 281, 36303-36316

104. Kochl, R., Hu, X. W., Chan, E. Y., and Tooze, S. A. (2006) Microtubules facilitate autophagosome formation and fusion of autophagosomes with endosomes. *Traffic* 7, 129-145

105. Yue, F., Li, W., Zou, J., Chen, Q., Xu, G., Huang, H., Xu, Z., Zhang, S., Gallinari, P., Wang, F., McKeehan, W. L., and Liu, L. (2015) Blocking the association of HDAC4 with MAP1S accelerates autophagy clearance of

mutant Huntingtin. *Aging (Albany NY)* 7, 839-853

106. Hubbert, C., Guardiola, A., Shao, R., Kawaguchi, Y., Ito, A., Nixon, A., Yoshida, M., Wang, X. F., and Yao, T. P. (2002) HDAC6 is a microtubule-associated deacetylase. *Nature* 417, 455-458

107. Behrends, C., Sowa, M. E., Gygi, S. P., and Harper, J. W. (2010) Network organization of the human autophagy system. *Nature* 466, 68-76

108. Downing, K. H. (2000) Structural basis for the interaction of tubulin with proteins and drugs that affect microtubule dynamics. *Annu Rev Cell Dev Biol* 16, 89-111

109. Nogales, E. (2001) Structural insight into microtubule function. *Annu Rev Biophys Biomol Struct* 30, 397-420

110. Vale, R. D. (2003) The molecular motor toolbox for intracellular transport. *Cell* 112, 467-480

111. Collot, M., Louvard, D., and Singer, S. J. (1984) Lysosomes are associated with microtubules and not with intermediate filaments in cultured fibroblasts. *Proc Natl Acad Sci U S A* 81, 788-792

112. Matteoni, R., and Kreis, T. E. (1987) Translocation and clustering of endosomes and lysosomes depends on microtubules. *J Cell Biol* 105, 1253-1265

113. Donninger, H., Vos, M. D., and Clark, G. J. (2007) The RASSF1A tumor suppressor. *J Cell Sci* 120, 3163-3172

114. Soppina, V., Herbstman, J. F., Skiniotis, G., and Verhey, K. J. (2012)

Luminal localization of alpha-tubulin K40 acetylation by cryo-EM analysis of fab-labeled microtubules. *PLoS One* 7, e48204

115. Chang, Y. Y., Juhasz, G., Goraksha-Hicks, P., Arsham, A. M., Mallin, D. R., Muller, L. K., and Neufeld, T. P. (2009) Nutrient-dependent regulation of autophagy through the target of rapamycin pathway. *Biochem Soc Trans* 37, 232-236

116. Jung, C. H., Ro, S. H., Cao, J., Otto, N. M., and Kim, D. H. (2010) mTOR regulation of autophagy. *FEBS Lett* 584, 1287-1295

117. Inoki, K., Li, Y., Zhu, T., Wu, J., and Guan, K. L. (2002) TSC2 is phosphorylated and inhibited by Akt and suppresses mTOR signalling. *Nat Cell Biol* 4, 648-657

118. Manning, B. D., Tee, A. R., Logsdon, M. N., Blenis, J., and Cantley, L. C. (2002) Identification of the tuberous sclerosis complex-2 tumor suppressor gene product tuberin as a target of the phosphoinositide 3-kinase/akt pathway. *Mol Cell* 10, 151-162

119. Menon, S., Dibble, C. C., Talbott, G., Hoxhaj, G., Valvezan, A. J., Takahashi, H., Cantley, L. C., and Manning, B. D. (2014) Spatial control of the TSC complex integrates insulin and nutrient regulation of mTORC1 at the lysosome. *Cell* 156, 771-785

120. Inoki, K., Li, Y., Xu, T., and Guan, K. L. (2003) Rheb GTPase is a direct target of TSC2 GAP activity and regulates mTOR signaling. *Genes Dev* 17, 1829-1834

121. Tee, A. R., Manning, B. D., Roux, P. P., Cantley, L. C., and Blenis, J. (2003) Tuberous sclerosis complex gene products, Tuberin and Hamartin, control mTOR signaling by acting as a GTPase-activating protein complex toward Rheb. *Curr Biol* 13, 1259-1268

122. Funakoshi, T., Matsuura, A., Noda, T., and Ohsumi, Y. (1997) Analyses of APG13 gene involved in autophagy in yeast, Saccharomyces cerevisiae. *Gene* 192, 207-213

123. Kamada, Y., Yoshino, K., Kondo, C., Kawamata, T., Oshiro, N., Yonezawa, K., and Ohsumi, Y. (2010) Tor directly controls the Atg1 kinase complex to regulate autophagy. *Mol Cell Biol* 30, 1049-1058

124. Kamada, Y., Funakoshi, T., Shintani, T., Nagano, K., Ohsumi, M., and Ohsumi, Y. (2000) Tor-mediated induction of autophagy via an Apg1 protein kinase complex. *J Cell Biol* 150, 1507-1513

125. Kim, J., Kundu, M., Viollet, B., and Guan, K. L. (2011) AMPK and mTOR regulate autophagy through direct phosphorylation of Ulk1. *Nat Cell Biol* 13, 132-141

126. Vairo, G., Soos, T. J., Upton, T. M., Zalvide, J., DeCaprio, J. A., Ewen, M. E., Koff, A., and Adams, J. M. (2000) Bcl-2 retards cell cycle entry through p27(Kip1), pRB relative p130, and altered E2F regulation. *Mol Cell Biol* 20, 4745-4753

127. Zhang, G., Park, M. A., Mitchell, C., Walker, T., Hamed, H., Studer, E., Graf, M., Rahmani, M., Gupta, S., Hylemon, P. B., Fisher, P. B., Grant, S.,

and Dent, P. (2008) Multiple cyclin kinase inhibitors promote bile acid-induced apoptosis and autophagy in primary hepatocytes via p53-CD95-dependent signaling. *J Biol Chem* 283, 24343-24358

128. Guo, C., Zhang, X., and Pfeifer, G. P. (2011) The tumor suppressor RASSF1A prevents dephosphorylation of the mammalian STE20-like kinases MST1 and MST2. *J Biol Chem* 286, 6253-6261

129. Cinar, B., Fang, P. K., Lutchman, M., Di Vizio, D., Adam, R. M., Pavlova, N., Rubin, M. A., Yelick, P. C., and Freeman, M. R. (2007) The pro-apoptotic kinase Mst1 and its caspase cleavage products are direct inhibitors of Akt1. *EMBO J* 26, 4523-4534

130. Yu, F. X., Zhao, B., and Guan, K. L. (2015) Hippo Pathway in Organ Size Control, Tissue Homeostasis, and Cancer. *Cell* 163, 811-828

131. Dong, J., Feldmann, G., Huang, J., Wu, S., Zhang, N., Comerford, S. A., Gayyed, M. F., Anders, R. A., Maitra, A., and Pan, D. (2007) Elucidation of a universal size-control mechanism in Drosophila and mammals. *Cell* 130, 1120-1133

132. Pan, D. (2010) The hippo signaling pathway in development and cancer. *Dev Cell* 19, 491-505

133. Fausti, F., Di Agostino, S., Sacconi, A., Strano, S., and Blandino, G. (2012) Hippo and rassf1a Pathways: A Growing Affair. *Mol Biol Int* 2012, 307628

134. Moroishi, T., Hansen, C. G., and Guan, K. L. (2015) The emerging roles of YAP and TAZ in cancer. *Nat Rev Cancer* 15, 73-79

135. Steinhardt, A. A., Gayyed, M. F., Klein, A. P., Dong, J., Maitra, A., Pan, D., Montgomery, E. A., and Anders, R. A. (2008) Expression of Yes-associated protein in common solid tumors. *Hum Pathol* 39, 1582-1589

136. Maejima, Y., Kyoi, S., Zhai, P., Liu, T., Li, H., Ivessa, A., Sciarretta, S., Del Re, D. P., Zablocki, D. K., Hsu, C. P., Lim, D. S., Isobe, M., and Sadoshima, J. (2013) Mst1 inhibits autophagy by promoting the interaction between Beclin1 and Bcl-2. *Nat Med* 19, 1478-1488

137. Tooze, S. A., and Yoshimori, T. (2010) The origin of the autophagosomal membrane. *Nat Cell Biol* 12, 831-835

138. Qu, Z., Jiang, Y., Li, H., Yu, D. C., and Ding, Y. T. (2015) Detecting abnormal methylation of tumor suppressor genes GSTP1, P16, RIZ1, and RASSF1A in hepatocellular carcinoma and its clinical significance. *Oncol Lett* 10, 2553-2558

139. Yin, X. M., Ding, W. X., and Gao, W. (2008) Autophagy in the liver. *Hepatology* 47, 1773-1785

140. O'Sullivan, T. E., Geary, C. D., Weizman, O. E., Geiger, T. L., Rapp, M., Overholtzer, M., Sun, J.C. (2016) Atg5 is essential for the development and survival of innate lymphocytes. *Cell Rep* 15, 1910-1919